DEPARTMENT OF THE INTERIOR
U.S. GEOLOGICAL SURVEY

Mineralogy And Geochemistry Of Co-Rich Ferromanganese Crusts And Substrate Rocks From Karin Ridge And Johnston Island, *Farnella* Cruise F7-86-HW

by

James R. Hein[1], Herbert Kirschenbaum[2], William C. Schwab[3], Akira Usui[4], Joseph E. Taggart[5], Kathleen C. Stewart[5], Alicé S. Davis[1], Shigeru Terashima[4], Paula J. Quinterno[1], Renee L. Olson[1], LedaBeth G. Pickthorn[1], Marjorie S. Schulz[1], and Charles L. Morgan[6]

Open File Report 90-298

1 U.S. Geological Survey, Menlo Park, CA
2 U.S. Geological Survey, Reston, VA
3 U.S. Geological Survey, Woods Hole, MA
4 Geological Survey of Japan, Tsukuba
5 U.S. Geological Survey, Denver, CO
6 Marine Minerals Technology Center, Honolulu, HI

INTRODUCTION

This report is an extension of Open File Report 87-663 (Hein et al., 1987a), which presented maps of camera and dredge stations, lithologic descriptions, bathymetry, seismic-reflection profiles, bottom photographs, chemical analyses of representative splits of homogenized dredge hauls (substrates plus crusts), and a crew list for Farnella cruise F7-86-HW. Here we present detailed chemical (major, minor, Pt-group, and rare earth elements) and mineralogical analyses of bulk crusts, subsamples of crusts, and substrate rocks collected during the same cruise. The chemical analyses of crusts are treated statistically using correlation coefficients and Q-mode factor analysis. Transmitted- and reflected-light petrography of standard thin sections and doubly polished thin sections is presented. Nannofossil ages of sediments and sedimentary rocks and radiometric ages of volcanic rocks are also included. Additional radiometric ages and more extensive volcanic rock petrography and geochemistry will be presented elsewhere.

Two submarine volcanic ridges, Karin Ridge and south Johnston Island ridge (hereafter referred to as SOJIR), within the U.S. Johnston Island Exclusive Economic Zone (EEZ) were sampled during cruise F7-86-HW (Fig. 1; Table 1). Thirty dredge attempts resulted in 29 recoveries of samples and one lost dredge bag. About 8600 kg of rocks and crusts were recovered (Table 1).

SUBSTRATE ROCKS

Substrate rock types in decreasing order of abundance are breccia, basalt, volcaniclastic mudstone-siltstone-sandstone, limestone, phosphorite, siltstone-tuff, and ironstone. As many as four rock types were recovered within single dredge hauls. Volcanic breccia consists predominantly of basalt clasts in various kinds of cement, or with a matrix composed of altered fine-grained volcanic debris or carbonate sediment. Limestones include weakly indurated foraminiferal sand, bioclastic siltstone and sandstone, and framework reefal limestone. Limestones are of Paleogene age, predominantly Eocene and Oligocene (Table 2). Carbonate sediments and mudstones are generally of Neogene age, Miocene, Pliocene, and Pleistocene (Table 2). Basalt is massive to highly vesicular and amygdaloidal, and is primarily of differentiated alkalic composition. A preliminary whole-rock, conventional K-Ar age of 82.4 ± 2.1 MA was obtained for

one of the least altered Hawaiites from Karin Ridge and should be considered a minimum age. Preliminary results of $^{40}Ar/^{39}Ar$ incremental heating experiments of mugearites from SOJIR yielded slightly discordant ages of about 71 MA.

X-ray Diffraction Mineralogy And Petrography

The various types of limestone are composed of calcite and, when partly phosphatized, carbonate fluorapatite (Table 3). Most of the Paleogene limestone is bioclastic and composed of recrystallized fragments of pelecypods, gastropods, echinoids, calcareous algae, foraminifers, and many unidentifiable grains, all in calcite cement. Coarse-grained mosaic calcite cements some breccias (e.g. CD20-2, CD24-2), and drusy- and dog-tooth spar calcite line vugs in breccia. Calcite is also mixed with other minerals in mudstone and in mud infilling burrows and borings in the rocks. Dolomite has not been previously reported to occur in rocks from environments like those sampled here, but we may have found it as the dominant mineral in two samples of mud (Table 3); however, the X-ray reflections can also be assigned to kutnahorite, which may be a more likely mineral to occur in these rocks.

Phosphorite is composed of carbonate fluorapatite that, in most samples, completely replaced limestone. Foraminiferal sand is the most common carbonate replaced by carbonate fluorapatite and ghosts of foraminifera are commonly present. Carbonate fluorapatite also cements the fine-grained clastic rocks and breccia, infills fractures, and infills vesicles in basalt. Some phosphorite contains minor amounts of volcanic rock fragments, and all gradations exist from grain-supported phosphorite-cemented breccia to phosphorite.

Primary volcanogenic minerals that occur in basalt, fine-grained clastic rocks, and breccia include plagioclase, pyroxene, magnetite, and amphibole. Most of the volcanic rocks and volcaniclastic rocks have altered to phillipsite, smectite, goethite, and lesser amounts of clinoptilolite, chlorite, mixed-layer clay minerals, and anatase. Nearly all volcanic rock fragments in clastic rocks and hyaloclastites are altered to goethite. Phillipsite is a common cement in the clastic rocks, and is only exceeded as a cement by phosphorite. Phillipsite forms blocky or tabular radially arranged crystals as cement or forms an acicular rim cement. Clinoptilolite is the predominant mineral in only one sample (CD7-9C), a mudstone, and probably was produced from the reconstitution of the alteration products of volcanic debris with the addition of silica. Smectite is commonly a

rim cement on volcanic rock clasts, which may by followed by todorokite cement. When more than one cement is present, the order of formation is smectite-phillipsite-todorokite or smectite-phosphorite. Basalt is generally differentiated alkalic and some are highly altered. Basalt ranges from highly vesicular to massive and is most commonly plagioclase phyric. Hornblende occurs in some samples. A more detailed description of basalts is given in the Chemistry Section.

Quartz is most abundant in the mud that fills animal burrows and borings and must have been either preferentially concentrated by the organisms or is of secondary origin. If primary, it was transported by eolian processes, as there is no local source for quartz (Hein et al., 1985a).

Goethite is the sole mineral in bedded and banded ironstone, and occurs with other minerals where the ironstone occurs as clasts in breccia. Apatite occurs with the goethite in some samples as a vug infilling or bedding-parallel lenses, and may by replaced by the goethite. We suspect that the ironstones are hydrothermally replaced volcanogenic rocks, although relict volcanic textures are not present in the most highly developed examples (pure hydrated iron oxide).

Laminated barite and smectite compose a nodule that grew within mudstone (CD5-6C). The barite is uniformly very fine grained with the laminae being defined by variable, but generally decreasing upward, concentrations of smectite.

Chemistry

Sedimentary Rocks

The most P_2O_5 rich sedimentary rocks have CaO/P_2O_5 ratios that range between 1.6 and 1.7, whereas the theoretical chemical compositions for carbonate fluorapatites range between 1.5 and 1.6 (Manheim and Gulbrandsen, 1979). The excess Ca over P in our samples is probably due to Ca associated with plagioclase in the basalt clasts and phillipsite cement in the breccias and to relict calcite in the phosphatized limestone. Some of the phosphorites are very pure, consisting of over 85% carbonate fluorapatite (e.g. CD1-15B and CD2-19D, Table 4).

Sample BMDS3-B is composed of nearly pure phillipsite, with perhaps a trace of smectite (Table 4). The Si/Al ratio of this sample

is 2.6, within the range of other marine phillipsites (2.3-2.8), and greater than the ratio for phillipsite in mafic igneous rocks (1.3-2.4) (Kastner, 1979). In fact, seven out of the nine samples with phillipsite as the sole major mineral (Tables 3, 4) have Si/Al ratios of 2.3-2.8. The one sample that is predominantly clinoptilolite has an Si/Al ratio of 3.3, clearly below that (4.2-5.2) of other marine clinoptilolites (Kastner, 1979); the presence of smectite causes the decrease in the ratio.

Ironstones range from nearly pure hydrous iron oxides (>90% $Fe_2O_3 \cdot nH_2O$, CD1-16B) to carbonate fluorapatite-rich ironstones (CD1-6B, CD28-2C). Compositional gradations exist between altered breccia (21% Fe_2O_3, CD1-14; 31% Fe_2O_3, CD15-2D) and ironstone, and between ferruginous phosphorite (CD28-1F) and ironstone (Table 4). Some breccias could also be classified as ironstones as they contain substantial amounts of Fe (>15%), for example CD15-2D and CD1-14B.

Most of the basalt and basalt clasts in breccia are altered. Alteration is best characterized by increases in ferric Fe and water and decreases in ferrous Fe and K_2O contents (Table 4). Increase in ferric Fe is especially prominent in some breccias and hyaloclastites, where glassy volcanic debris essentially altered completely to (or was replaced by) Fe oxide. The volcaniclastic mudstones, siltstones, and hyaloclastites have compositions comparable to those of the altered basalts.

Volcanic Rocks

Relatively fresh volcanic rocks from Karin Ridge are predominantly differentiated alkalic basalt (Table 5). Two samples plot at the boundary separating tholeiitic from alkalic basalt (MacDonald and Katsura, 1964) on the alkali versus silica diagram and could be considered transitional between alkalic and tholeiitic basalt. Differentiated compositions include hawaiite and benmoreite (Table 5). Hawaiite and benmoreite are either sparsely or highly plagioclase-phyric, with phenocrysts in a groundmass of trachytic plagioclase microlites and iron oxides. The transitional basalts are commonly highly plagioclase-phyric with centimeter-size plagioclase phenocrysts in a groundmass of subtrachytic or seriate plagioclase microlites, granular clinopyroxene and iron oxides, and variable amounts of clay minerals. Other basalt samples are either aphyric or sparsely to moderately plagioclase-phyric with plagioclase phenocrysts accompanied by variable amounts of olivine and clinopyroxene. The olivine is typically replaced by iddingsite and

clay minerals, but unaltered cores of some phenocrysts still persist and are magnesian olivine with Fo 86 to Fo 90. The least differentiated sample (MgO ≈5.6%) is a highly vesicular ankaramite with optically zoned clinopyroxene phenocrysts in a groundmass of euhedral to subhedral clinopyroxene and altered glass. All of the rocks are somewhat altered, with the hawaiite and benmoreite the least altered and the ankaramite the most altered. The clinopyroxene is unaltered in all samples and ranges from augite to salite in composition and is typically high in TiO_2 (≈3%) and Al_2O_3 (to 8%).

Relatively fresh volcanic rocks from SOJIR are also largely differentiated alkalic basalt, but also include one transitional and some strongly alkalic compositions, such as basanite and nephelinite. Differentiated compositions include hawaiite and mugearite (Table 5). The strongly alkalic samples are moderately to highly vesicular ankaramite with compositionally zoned clinopyroxene phenocrysts in an altered glass matrix. The clinopyroxene phenocrysts are Ti-rich augite and salite and some have greenish cores that are acmitic ferrosalite in composition. Alkalic basalt is either highly vesicular and aphyric or sparsely to non-vesicular and porphyritic with plagioclase, olivine, and variable amounts of clinopyroxene phenocrysts. The groundmass in both groups consists of plagioclase microlites accompanied by variable amounts of granular clinopyroxene, iron oxides, and clay minerals, replacing olivine and glass. Two of the hawaiite samples have amphibole phenocrysts, accompanied by variable amounts of clinopyroxene microphenocrysts in a groundmass of plagioclase, clinopyroxene, iron oxides, and traces of apatite. Mugearite is sparsely vesicular and aphyric with a groundmass of trachytic plagioclase and abundant iron oxides. Similar to Karin Ridge samples, hawaiite and mugearite are the least altered and the strongly alkalic rocks are the most altered.

FERROMANGANESE CRUSTS

Crusts vary in thickness from a patina to 160 mm. Dredge haul CD29 has the thickest Co-rich crusts known and the thickest crust average (75 mm) known to the authors (Table 1). All thicker crusts are composed of two or more layers, eight layers being the maximum noted. Layers may be laminated, massive, or composed of crystallites oriented perpendicular to crust-growth layers; they may

contain columnar structures, abundant fractures, abundant phosphorite veins, or may be reddish-brown and minutely fractured. Phosphorite laminae occur in some crusts (as many as five laminae), and separate the crust from the substrate in other samples. Based on the Co, Mn, and P contents and the equations of Puteanus and Halbach (1988), the growth rates of bulk crusts varied from 1.6 to 10.0 mm/m.y. The average growth rate was 3.8 mm/m.y., somewhat faster than for thinner crusts from other areas. The growth rates of individual layers within crusts varied from 1.5 to 64 mm/m.y. Growth rates of about 1 to 10 mm/m.y. are common for hydrogenetic crusts (Hein et al., 1987b, 1990a); faster growth rates may indicate a hydrothermal or detrital input (Hein et al., 1990b). The two thickest crusts analyzed, CD29-2 (110 mm) and CD29-7A (138 mm), began growing about 22 m.y. ago and 23 m.y. ago, respectively, based on the growth rates of individual layers and the thickness of each layer.

The surface textures of crusts are dominantly smooth or botryoidal. Smooth surface textures are also flat, finely granular, or bulbous. Botryoidal textures consist of large to small botryoids that were partly smoothed by current action; modified botryoids that were eroded or dissolved at their base forming mushroom-like forms; botryoids that merged to form a rippled surface; and other modifications of the botryoidal surface. A complete gradation exists from unmodified botryoidal surfaces to smooth surfaces.

Great care was taken in sampling crusts for chemical and mineralogical analyses. All contamination from recent sediments was removed, which was especially critical in a porous layer that commonly separates layers one and three in thicker crusts. Also, special attention was paid to obtaining a clean separation of the lower crust layers from the substrate. Any minerals or elements determined to exist in the various crust layers were incorporated into those layers during deposition or diagenesis and are not due to sampling procedures or postdepositional infiltration of sediment. Finally, all encrusting organisms and other debris were cleaned from the crust surfaces before sampling. Bulk always refers to the entire crust thickness, whether composed of layers or not.

X-ray Diffraction Mineralogy

All bulk crusts are composed of over 90% δ–MnO_2 (vernadite), which has only two X-ray reflections at about 2.42Å and 1.41Å (Table 6). X-ray amorphous Fe oxyhydroxide epitaxially intergrown

with δ-MnO_2 is also a dominant phase. This Fe phase crystallized to geothite in the inner part of some crusts (CD2-38, CD16-1, Table 6). Most crust and nodule layers are also predominantly δ-MnO_2, but some contain up to 36% apatite. Only the inner layers contain apatite, although there may not necessarily be a continuous increase of apatite toward the substrate in the lower parts of the crusts (see for example, CD2-8, Table 6). Rarely, todorokite and birnessite occur in the innermost crust layers and in the underside crusts (crusts that occur on the opposite side of the substrate rock). Generally, clastic minerals are also most abundant in the inner layers. Quartz and plagioclase are rarely greater than 1% and 2%, respectively, in bulk crusts. However, some inner crust layers contain up to 6% plagioclase and 3% quartz. The quartz and some of the plagioclase are of eolian origin, carried by the trade winds from Asia. There is no local or regional source for quartz in the central Pacific. The remainder of the plagioclase and the phillipsite, K-feldspar, and calcite are reworked from local outcrops and incorporated into the crusts during precipitation of the Fe-Mn oxyhydroxides. On the average, the amount of phosphorite and clastic debris is about 2% greater in bulk crusts from southern Karin Ridge (dredges 28, 29, and 30) than they are in crusts from both central Karin Ridge and SOJIR.

The todorokite that occurs in several crusts may have formed under different redox conditions than the more oxidized Mn phase, δ–MnO_2 (such as in samples CD2-37B and CD6-22B), or from diagenesis or hydrothermal input (perhaps in samples CD1-17C, CD2-38F, and CD6-3C). The kutnahorite probably formed by substitution of some of the Ca in calcite by Mn in a low oxygen environment.

An Fe-Mn oxide fracture fill (CD16-6A) contains substantial todorokite as well as δ-MnO_2 and probably formed by diagenetic or hydrothermal processes; the chemical composition favors a diagenetic origin (see next section). A Mn oxide stratabound layer (CD26-7C) contains δ-MnO_2, todorokite, and birnessite. The mineralogy, occurrence, and chemical composition support a hydrothermal origin. Both of these uncommon deposit types have been partly phosphatized.

Chemistry

General

Chemical analyses for 212 samples and subsamples of crusts and nodules analyzed by the U.S. Geological Survey and 35 samples analyzed by the Geological Survey of Japan (GSJ) are listed in Tables 7 and 8, respectively. The mean composition of 97 bulk crusts for Fe and Mn is 13.7% and 19.2% respectively, yielding a Mn/Fe ratio of 1.40 (Tables 7, 9); this ratio is somewhat lower than the average ratio for the entire central Pacific region (1.46), and both Fe and especially Mn are lower than their regional averages of 15.7% and 23.0%, respectively (Hein et al., 1987b, 1990a). Most of the other metals are also below the central Pacific regional average (Table 10). The mean contents of the economically important metals Co (0.58%), Ni (0.35%), and Pt (0.17 ppm) are especially low compared to their regional averages of 0.79%, 0.47%, and 0.24 ppm, respectively.

All of the metals analyzed by XRF by the GSJ for 8 bulk crusts are greater than the values determined by ICP by the USGS (Tables 7, 8, 9, 10). The XRF values are close to the regional average, except for Co, which is lower (Table 10). A major difference between the USGS and GSJ data is the loss on ignition (represents predominantly H_2O^+ and H_2O^-) with mean values of 33.51 and 10.64, respectively. The higher LOI (water contents) accounts for the relatively lower metal values in the USGS data set. The difference in water contents is due to different drying tecniques; the GSJ dried samples at 105° C and the USGS analyzed air dried samples. Normalization of the USGS data to 0% H_2O^- will yield values similar to those produced by the GSJ. LOI determined by the USGS for central Pacific crusts generally ranges from about 20% to 35%, with means commonly near 25% to 30% (see for example, Hein et al., 1988).

Layers

It has been well established that Co content in general decreases in abundance from the surface of crusts to the substrates (Halbach et al., 1982; Hein et al., 1985b). This relation can also be demonstrated here (Table 10), where Co increases with decreasing crust thickness and Co is greater in outer layers relative to inner layers of the crusts. Other elements also vary with depth in the crusts. Thinner crusts are chemically equivalent to the outer parts of thicker crusts (Tables 7, 10); it is the inner, older parts of thick crusts that are missing in thinner crusts, because they were eroded prior to deposition of the younger crust layers. It is very rare to find crusts consisting solely

of the older growth layers without the more Co-rich younger layers. Only one dredge from the hundreds we have taken in the central Pacific has recovered such crusts (Hein, unpublished data), and these crusts exist only because the outer layers were removed by a turbidity current flow. More typically, thinner crusts exist because the earlier-formed crusts were destroyed by gravity flows and accretion had to begin again (Hein et al., 1985a, 1988). Some of these older reworked crusts provided nuclei for growth of nodules and clasts for breccias. The composition of nodule nuclei composed of Fe-Mn oxyhydroxides is the same as the composition of the older generation of crusts and may have formed at the same time as the older crust generation or were acquired as nuclei after the fragmentation of crusts (Table 7).

Clastic debris is more abundant in inner crust layers than in outer layers as indicated by mean Al contents (Table 10). However, thin bulk crusts have higher mean Al contents than thick bulk crusts. Crusts with very high Co (very slow growth rates) have the lowest Al contents.

In detail, the metal concentrations vary widely among the layers of individual crusts and among different crusts. Even though in general Co, Ni, Mn, and other metals are enriched in outer layers and Fe, Pt, Cu, and P in inner layers, any individual layer, regardless of position, may be enriched in one or more of the metals.

Variations With Geographic Location

Bulk crusts from central Karin Ridge, southern Karin Ridge, and SOJIR also show compositional variations (Table 10). SOJIR crusts are highest in Mn, Mn/Fe, and Cu. Central Karin Ridge crusts are highest in Fe, Al, and Co and lowest in Mn, Mn/Fe, P, Cu, Ni, and Pt. Southern Karin Ridge crusts are highest in P and Pt and lowest in Fe and Co. However, Co, Ni, and Cu vary little among the areas. The greatest detrital input (Al, Si, Ti) is to central Karin Ridge crusts, and the greatest biological input (P, Ca, Ba) is to southern Karin Ridge crusts.

Samples With Atypical Compositions

Some crusts display atypical chemical compositions. Three of the four crusts with Co >1% are from crusts that grew on the underside of the substrate rocks, where seawater penetrated along a fracture or the lower surface was exposed along an overhanging outcrop or by

reworking of talus debris. It is generally true that crusts from the sides and undersides of substrate rocks are richer in Mn and Co and texturally are very porous and granular.

The inner part of one crust (CD1-17C, Table 7) also shows an uncommon composition. The very low concentrations of Fe, Mn, Co, H_2O^-, As, and Zn are the result of impregnation of the lower part of the crust by not only the typical large amounts of carbonate fluorapatite, but also probably by barite (2.85% Ba) and todorokite (table 6). Interestingly, both Ni (0.75%) and Cu (0.26%) are anomalously enriched in this layer and may be associated in part with the large biogenic (apatite-barite) component.

Three ferromanganese nodules (JOD4-2-I,II,III) have anomalously high Cu (average 0.22%) concentrations and low Mn/Fe ratios (Table 7). This concentration of Cu can be explained by one of two mechanisms. The nodules perhaps grew by both hydrogenetic and diagenetic processes, thereby preferentially concentrating Cu relative to the other metals of predominantly hydrogenetic origin. Abyssal nodules form in this way and Cu is associated with the Mn phase. However, seamount nodules typically do not form by diagenetic processes and are not compositionally like abyssal nodules, but rather reflect the same hydrogenetic composition as adjacent crusts. In crusts, the Cu is associated with the Fe phase, or with several different phases, and thus Cu in these nodules probably reflects their relatively greater Fe contents.

Two atypical deposits, a Fe-Mn oxyhydroxide vein (CD16-6A) and a Mn oxyhydroxide stratabound layer (CD26-7C), also have uncommon compositions that are typical of diagenetic and hydrothermal processes. The vein is significantly depleted in Fe, Mn, H_2O^-, LOI, Co, Mo, and As, and enriched in Ca, Al, P, CO_2, Ba, Ni, Y, Cr, and Zn relative to the average crust. Ni (0.77%) is especially high and Fe (6.6%) especially low; Mn/Fe is also high (2.23). The generally moderate metal enrichments and the high Mn/Fe ratio indicate a diagenetic origin. The stratabound layer is depleted in Mn, Ti, and Ni; strongly depleted in Fe, H_2O^-, LOI, Co, Mo, Ce, As, and Pb; and enriched in Ca, K, Al, P, CO_2, Ba, Cu, Y, and Cr relative to the average crust. The very high Mn/Fe (7.63) ratio and generally low metal and Ce contents indicate a strong hydrothermal component to the layer.

Rare Earth Elements (REEs)

Forty-two samples, 14 bulk crusts and 28 layers, were analyzed for REEs (Table 11). For bulk crusts, ΣREEs range from 0.11% to 0.24% and averages 0.18%. The highest ΣREEs is for the innermost layer (22-50 mm) in crust CD24-1, 0.33%. The lowest ΣREEs is for bulk crust CD1-17E, which is the only crust with a negative Ce anomaly; these REE characteristics and the relatively high Ba and low Fe contents suggest a high biogenic component or a diagenetic influence in the formation of this crust.

Chondrite-normalized REE patterns (Haskin et al., 1968) are shown in Figures 2-13. Different REEs are enriched from about 70 to 3000 times over chondrites (Fig. 2). The chondrite-normalized patterns are typical of Fe-Mn oxyhydroxide crusts and nodules (Piper, 1974; Elderfield et al., 1981; Aplin, 1984; Hein et al., 1988) with heavy REE (HREE) depletion, nearly flat HREE pattern, positive Ce anomaly, and small positive Gd anomaly (the occurrence of Gd* has been reported only for crusts; Hein et al., 1988). Rarely do the samples analyzed here deviate from this characteristic chondrite-normalized pattern (Figs. 3-13). These characteristics of the REE patterns of crusts have some aspects in common with seawater (Gd anomaly; also in some samples a small negative Tb anomaly, Hein et al., 1988) and others opposite to those of seawater (HREE depletion, positive Ce anomaly). This variation in characteristics relative to seawater indicates that the REEs were scavenged by several different phases within the crusts, predominantly Fe and Mn oxyhydroxides, but also phosphorite, barite, zeolites, and others.

Unlike the other REEs, soluble Ce^{+3} is oxidized to insoluble Ce^{+4} at the Fe-Mn surface and fixed in Fe, Mn, and other phases, thus creating a large positive Ce anomaly on both shale- and chondrite-normalized plots. The Ce anomaly, Ce* (normalized Ce/La+Pr), ranges from 0.20 to 1.75 for all samples analyzed here, and averages 0.88 for 14 bulk crusts. Only one sample (CD1-17E) has a negative Ce anomaly (Ce* <0.5) (Table 11; Fig. 3); the others have the positive Ce anomaly typical of marine diagenetic and hydrogenetic Fe-Mn oxyhydroxides, although two crust layers (CD2-8A, CD2-38A) have only very small positive anomalies (0.57 and 0.56, respectively).

The Gd anomaly was first discovered to occur in seawater by DeBaar et al. (1985) and in marine ferromanganese deposits by Hein et al. (1988). DeBaar et al. (1985) attributed the Gd/Tb fractionation

in seawater to anomalous properties associated with the shift from an exactly half-filled 4f electron shell.

The HREE depletion results from the formation of more stable complexes by the HREEs in seawater than by the light REEs (LREEs), and consequently, the HREEs are more difficult to fix in the crusts than the LREEs.

The REE compositions and chondrite-normalized patterns change with depth in the crusts. With one exception (JTD9-2, Fig. 4), the highest ΣREEs occurs at the base of the crusts, the innermost interval (Table 11; Figs. 5, 6, 8, 10, 11, 12, 13). In general, ΣREEs increase with increasing depth in the crusts, toward the substrates. The Ce* also shows a general increase toward the substrate, with the largest anomaly being either the innermost layer or the second layer out from the substrate. Even though P content is generally higher in the inner layers, the highest ΣREE layer does not generally correspond to the richest P layer (for example, CD2-38, Fig. 6; CD13-8, Fig. 8; CD21-7, Fig.10; CD29-2, Fig. 12). This indicates that carbonate fluorapatite is not the dominant host for the REEs.

ΣLREEs shows the same pattern of distribution within individual crusts as the ΣREE, because both are dominated by the high Ce contents. However, ΣHREEs shows a trend opposite to that of the ΣLREEs, and invariably has its highest concentration in the outermost crust layer. ΣHREEs generally decreases toward the substrate. In some samples, ΣHREEs show an increase in the innermost layer relative to middle layers (for example, CD2-8 and CD21-7). These REE distributions with depth in the crusts are not related to Mn/Fe, detrital mineral content, or apatite content. Rather, they are probably related primarily to growth rates (slower in the outer layers) and to the non-carbonate fluorapatite biogenic components.

Interelement Relationships: Correlation Coefficient Matrix

Fifteen correlation coefficient matrices were calculated, one on the total data set and 14 on various subsets of data. Nine of these 15 matrices are presented here: All bulk crusts, Table 12; all bulk crusts ≤20 mm thick, Table 13; all bulk crusts ≥20 mm thick, Table 14; layers from sample CD2-8, Table 15; layers from sample CD2-38, Table 16; all bulk crusts with REE analyses, including selected major elements, Table 17; REEs and selected major elements from layers of CD2-8, Table 18; REEs and selected major elements from layers of

CD2-38, Table 19; and the innermost 5 mm of crusts, including selected elements and element ratios from the underlying substrate rock, Table 20.

Bulk Crusts

For the 97 bulk crusts, statistically significant strong to moderate positive correlations are found among the following elements: **Fe**: As; **Mn**: Ni, Mn/Fe, Cd, Mo; **Si**: Al, Fe, Cr; **Mg**: Cd, Co, Ni; **K**: Al; **Ca**: P, CO_2; **Al**: K, Cr, Si; **P**: Ca, CO_2; **Ba**: Ce, Zn; **Co**: Cd, Mg; **Cu**: Zn; **Mo**: Sr, Mn, Mn/Fe, V; **Ni**: Mn/Fe, Cd, Mn, Mg, Co; **Sr**: Mo, V, Ce; **V**: Pb, Sr, Mo; **Ce**: Ba, Sr; **Cd**: Ni, Mn, Mn/Fe, Co, Mg; **Zn**: Ba, Cu, Pt; **Pt**: crust thickness, Zn; **crust thickness**: Ca, P, Pt (Table 12). Many statistically significant weak correlations also exist among the various elements. All of the elements are associated with one or more mineral phases within the crusts. We interpret the correlations in Table 12 to indicate the following phases and their associated elements: δ-MnO_2 phase: Mn, Ni, Cd, Mo, Co, Zn, Mg, Sr; Fe-oxyhydroxide phase: Fe, As; aluminosilicate component: Si, Al, Cr, Fe, K, Ti, ± Na; carbonate fluorapatite component: Ca, P, CO_2, Ba, Ce, ± Pt, Sr, Zn; residual biogenic component: Ba, Cu, Zn, Mo, V, Ce, ± Sr, P, Rh. In addition, the apatite component varies directly, and the aluminosilicate component varies inversely, with crust thickness. Elements of the δ-MnO_2 phase have a negative correlation with elements of the aluminosilicate phase and the Fe oxyhydroxide phase. These interelement associations are similar to those determined for other areas of the central Pacific, although regional differences do occur (Hein et al., 1990a).

The correlations change somewhat when only thin (≤5 mm) bulk crusts are considered. These thin crusts have fewer interelement correlations and contain little P and no detectable carbonate fluorapatite. P has a positive correlation with Fe as do As, Pb, and V. Fe is not included in the aluminosilicate phase nor Co with the Mn phase. Cu correlates positively with the manganophile elements Ni, Cd, and the Mn/Fe ratio. Ca has no positive or negative correlations. When all bulk crusts ≤20 mm are considered (Table 13), the correlations are more similar to those for all bulk crusts, but with some differences. The correlation of elements (Ca, P, CO_2) in the carbonate fluorapatite phase are weak rather than strong as in the data set containing thicker crusts. Mn has a weak positive correlation with Ca, V, and Pb; Cu has moderate positive correlations

with K and Ti; Pd a strong positive correlation with Ca; and Pt a strong positive correlation with Rh, as is found in many other areas of the central Pacific. Element correlations for thick bulk crusts (≥20 mm) are very similar to those for all bulk crusts considered together, but again with some minor differences (Table 14). There are generally fewer strong correlations with the thick crusts. Fe is more strongly associated with the aluminosilicate phase; Mg is positively correlated with Ti and K, and Cu with Pt as well as Zn. These variations in element associations with bulk crusts of different thicknesses indicate that: 1. minor diagenesis probably redistributed some elements, 2. growth rates effect element associations, and 3. P is associated with apatite only in thick crusts, suggesting at least two mechanisms of incorporation of P into crusts. The significance of the P, Ca, and CO_2 correlations increases with increasing crust thickness.

Layers

Four correlation coefficient matrices were constructed to determine interelement association among layers within individual crusts. Two crusts with 5 layers each (Tables 15, 16) and 2 crusts (CD2-15, CD29-2) with 4 layers each (not presented) were studied. In general, the number of correlations decreases markedly from that of bulk crusts. However, many of the strong and moderate interelement correlations in the complete data set for bulk crusts occur for the elements in the layers of crust CD2-38 (Table 16). The most striking difference is with the platinum group elements, where Pd is positively correlated with Ni, Na, and K; and Pt is positively correlated with Rh and Cu for crust CD2-38. In contrast, element associations for layers in crust CD2-8 are few, and contrast with those from bulk crusts (Table 15). The strongest and most striking correlations again are with the platinum group elements, where positive correlations occur: **Pd**: Mg, Ni, Mn/Fe; **Pt**: Rh, Zn, Ba; **Rh**: Zn, Cu, Pt. The paucity of correlations of elements among crust layers is partly due to the high zero correlation for 5 points at the 95% confidence level, |0.883| and partly due to the smaller compositional variability among the layers (especially for sample CD2-8) compared to bulk crusts..

Rare Earth Elements

Correlations among REEs and selected major elements were determined for all bulk crusts for which REE analyses are available (n=14; Table 17), for layers in crust CD2-8 (Table 18), and for layers in crust CD2-38 (Table 19). Ce is unique among the REEs and does not have a positive correlation with any of the other REEs, although for bulk crusts it has a negative correlation with Er, Tm, Yb, and Lu. Ce, being the most abundant REE, has a positive correlation with ΣREEs, as well as with water depth of bulk crusts and Ba in CD2-8 and CD2-38. Correlations with La, Pr, and Nd generally decrease in significance with increasing atomic number of the REEs. Lu and Yb show the opposite trend. Each element from Sm through Tm shows a decrease in the significance of its correlations moving in both directions to REEs with higher and lower atomic numbers; this results in a V-shaped pattern centered on each element.

For bulk crusts, positive correlations occur between: **Fe**: Pr through Dy; **Si**: Pr through Tm; **Ni**: Pr through Tb; and negative correlations occur between: **Ca**: Pr through Ho; **P**: Pr through Dy. This clearly shows that carbonate fluorapatite is not a major host for most of the REEs in bulk crusts; instead Fe, Mn, and aluminosilicate phases host most of the REEs.

For layers in CD2-8, with low average P content, positive correlations exist for: **P**: La through Gd; **Co**: Tb through Lu; and negative correlations for: **Cu**: each REE except Ce; **Pt**: Gd through Lu; **Al**: La through Sm (Table 18). These, and other correlations suggest an association of Ce, Ba, Cu, and Pt with a residual biogenic phase, and the other REEs must be distributed among a number of phases because no strong correlations exist except with Co and P (not as apatite).

For layers in CD2-28, with high average P content, positive correlations exist for: **Fe**: Sm through Dy; and negative correlations for: **Cu**: Pr through Ho; **Pt**: Pr, Nd (Table 19). Again, when P, Ca, and CO_2 are abundant in the lower layers of the crust in the form of apatite, no correlations exist with the REEs.

Substrate-Crust Element Correlations

It has been assumed that the composition of substrate rocks does not influence the composition of crusts. This assumption was based on the observation that crust chemistry was similar for crusts within

single dredges regardless of the substrate rock type. However, this assumption has not been tested. In order to test it, we sampled the lowermost 5 mm of 24 crusts (Table 7) and the adjacent substrate rock (Table 4), most commonly about 10 mm below the contact. Great care was taken to assure no contamination of one by the other. Only one strong correlation is noted between elements in the crust and elements in the substrate, Mg/Al* with Y (an * denotes substrate elements and ratios). However, a number of moderate and weak correlations exist (Table 20). Most of these correlations are with the elements that represent carbonate fluorapatite, Ca, P, CO_2, and with other generally mobile elements, As, Fe, Na, Ba, Y, H_2O^-, H_2O^+, Sr, Mn, Co, Cu; however, some relatively immobile elements are also included, Ti, Si. If the substrate and the inner layers of the crusts were phosphatized during the same event(s), a correlation between the two would be expected. Si*, Al*, Na*, K*, and Ti* all have negative correlations with carbonate fluorapatite (Ca, P, CO_2). Many of the correlations dealing with the very mobile elements may indicate transport and exchange between the crust and the substrate. **Ti*** with Ti, Fe; **Mg*** with Fe; **Si*** with Fe, Ti; and **Al*** with Fe, Ti probably represent titanomagnetite, ferromagnesian minerals, and plagioclase that are common components of the volcanogenic substrates and are also commonly present as clastic minerals in the crusts. Overall, the correlations indicate that substrate rocks do not contribute greatly to crust chemistry, but may have partly exchanged some of the most mobile elements with the crusts; exchange probably occurs in both directions, as both crusts and most substrates are very porous and water saturated. Substrate rocks have been the major contributor of the minor detrital phases (except quartz) to the crusts.

Grouping of Elements: Q-mode Factor Analysis

Q-mode factor analysis was completed for the 95 bulk crusts and 9 subsets of the data. Each variable percentage was scaled to the percent of the maximum value before samples were row normalized and cosine theta coefficients calculated. The factors presented here were derived from orthogonal rotations of the principal component eigenvectors using the Varimax method (Klovan and Imbrie, 1971). All communalities are ≥ 0.95.

The groups of elements determined by Q-mode can be assigned to essentially the same crust phases as determined from analysis of the correlation coefficient matrices. Some differences do occur, such as

the Fe phase is not distinguished for some data subsets or may be included as part of the δ-MnO_2 factor in others. More specific differences regarding the placement of individual elements in different phases are also noted.

The 4 factors determined for 95 bulk crusts are interpreted to be aluminosilicate, carbonate fluorapatite, δ-MnO_2, and Fe oxyhydroxide phases (Fig. 14), the same as those determined from correlation coefficients, except for the lack of a residual biogenic phase. The four phases include the same elements as those determined by correlation coefficients plus Y and As for the aluminosilicate phase; Mo for the carbonate fluorapatite phase; Na, V, As, and Pb for the δ-MnO_2 phase; and, Ce and Pb for the Fe oxyhydroxide phase.

The 4 factors determined for bulk crusts $\leq$20 mm thick (low average P content) are interpreted to be Fe oxyhydroxide phase, aluminosilicate phase, δ-MnO_2 phase, and residual biogenic phase, the same as those determined from correlation coefficients, except for the lack of a carbonate fluorapatite phase (Fig. 15). The Fe oxyhydroxide factor includes more than just As and Y as indicated by positive correlations, but also includes Mo, V, and Pb. Pb and Mo commonly have positive correlations with Mn, not Fe. Another difference is the inclusion of Cu with the δ-MnO_2 phase. The residual biogenic and aluminosilicate phases are essentially the same.

The 4 factors for bulk crusts $\geq$20 mm thick (high average P content) are interpreted to be aluminosilicate, carbonate fluorapatite, δ-MnO_2, and Fe oxyhydroxide phases, which are the same as those determined from correlation coefficients, except for a residual biogenic phase (Fig. 16). Two other differences include As with the δ-MnO_2 phase as well as the Fe phase, and Mo with the Fe phase as well as the δ-MnO_2 phase.

The 3 factors for crust CD2-8 (low average P content) are interpreted to be residual biogenic, Fe oxyhydroxide plus δ-MnO_2 phase, and aluminosilicate phase (Fig. 17). The correlation matrix shows few significant correlations, although one of them is Fe negatively correlated with Mn. The residual biogenic phases are the same and contain Pt, Rh, Ba, Cu, Ce, Sr. The Q-mode aluminosilicate factor contains Pd as one of the elements, which is reasonable because Pd is not enriched in crusts over its lithospheric average and has a similar concentration in crusts as in central Pacific substrate rocks (Hein et al., 1988). Q-mode also places Cu, Ni, and Cd in the aluminosilicate factor.

The 3 factors for crust CD29-2 (high average P content) are interpreted to be aluminosilicate, carbonate fluorapatite, and δ-MnO_2 (Fig. 18). The correlation matrix shows very few correlations, so it is difficult to compare the results. The interesting associations with the Q-mode groupings is Cd and Cu with the aluminosilicate phase, Pt and Rh with the carbonate fluorapatite phase, and As, Cr, and Pd with the δ–MnO_2 phase.

RESOURCE CONSIDERATIONS

The United States Johnston Island EEZ has long been considered to have a high potential for Co-rich Fe-Mn crusts, and is consistently rated as one of the top 5 Pacific EEZs. The Marshall Islands EEZ and the Johnston Island EEZ have been the most extensively surveyed areas for potential crust resources (Hein et al., 1990a).

The average Co (0.79%) and Ni (0.48%) contents of crusts are high in the Johnston Island EEZ, but are as high or higher in other EEZs: Marshall Islands, Howland-Baker Islands, Kingman-Palmyra Islands, and Tuvalu Islands (Hein et al., 1990a). The grades determined here for Karin Ridge and SOJIR (Co = 0.56%; Ni = 0.35%) are much lower than the average for the Johnston Island EEZ. The commonly cited cut off grade for potential economic development is 0.8% Co.

Several areas in the Johnston Island EEZ have remarkably thick crusts (large tonnage), including the two areas studied here. However, surveys have not been extensive enough to delineate the extent of these areas of thick crusts. Because the mining of crusts from the rugged flanks and summit of seamounts and ridges will be a difficult endeavor, crust thickness (tonnage) may turn out to be a more important factor in economic and site selection considerations than grade. For the Karin Ridge and SOJIR data presented here, there exists a very weak negative correlation between grade (Co) and tonnage (thickness), but a moderate positive correlation between Pt and tonnage. Thus, tonnage has an inverse relationship with Co content, no relationship with Ni content, and a direct relationship with Pt content.

The area of southern Karin Ridge has the thickest crusts, which were dredged from a relatively flat summit plateau. This area warrants further detailed surveys, and has been proposed for such work in April 1991. Without detailed, site specific surveys, it is difficult to assess the long term economic potential of the Johnston Island, or any of the other EEZs. Identification of areas with

favorable grade, tonnage, and seafloor characteristics will also have to correspond with the appropriate world markets and metals prices before mining can be accomplished. The technological problems of mining can be solved if the other factors are favorable.

ACKNOWLEDGMENTS

We thank Captain John Cannan and the crew of the R.V. *Farnella* for excellent support. This multipurpose cruise was also funded by the U.S. Bureau of Mines, Nuclear Defense Agency, National Oceanographic and Atmospheric Administration, and the Geological Survey of Japan. We thank the shipboard scientific crew from the Bureau of Mines and the U.S. Geological Survey for completing a highly successful cruise. Marlene Noble, U.S. Geological Survey helped with the Q-mode factor analysis, and Randolph Koski, kindly reviewed this report. The following U.S. Geological Survey analysts provided chemical data: P. Aruscavage, A. Bartel, E. Bell, L. Espos, P. Hageman, M. Kavulak, H. Kirschenbaum, J.W. Marinenko, R. Moore, S. Pribble, C.L. Prosser, N. Rait, D. Siems, H. Smith, K. Stewart, J. Taggart. S. Terashima was analyst for the Japanese Geological Survey chemical data.

REFERENCES

Aplin, A.C., 1984, Rare earth element geochemistry of central Pacific ferromanganese encrustations: Earth and Planetary Science Letters, v. 71, p. 13-22.

Cook, H.E., Johnson, P.D., Matti, J.C., and Zemmels, I., 1975, Methods of sample preparation and X-ray diffraction data analysis (X-ray mineralogy laboratory, Deep Sea Drilling Project, University of California Riverside): in Hays, D.E., Frakes. L.A., et al., Initial Reports of the Deep Sea Drilling Project, U.S. Government Printing Office, Washington, D.C., v. 28, p. 999-1007.

DeBaar, H.J.W., Brewer, P.G., and Bacon, M.P., 1985, Anomalies in rare earth distributions in seawater: Gd and Tb: Geochimica et Cosmochimica Acta, v. 49, p. 1961-1969.

Elderfield, H., Hawkesworth, C.J., Greaves, M.J., and Calvert, S.E., 1981, Rare earth element geochemistry of oceanic ferromanganese nodules and associated sediments: Geochimica et Cosmochimica Acta, v. 45, p. 513-528.

Halbach, P., Manheim, F.T., and Otten, P., 1982, Co-rich ferromanganese deposits in the marginal seamount regions of the central Pacific basin - results of the Midpac '81: Erzmetall, v. 35, p. 447-453.

Haskin, L.A., Haskin, M.A., Frey, F.A., and Wildeman, T.R., 1968, Relative and absolute terrestrial abundances of the rare earths: in Ahrens, L.H. (ed.), Origin and Distribution of the Elements, 1, Pergamon, Oxford, p. 889-911.

Hein, J.R., Manheim, F.T., Schwab, W.C., and Davis, A.S., 1985a, Ferromanganese crusts from Necker Ridge, Horizon Guyot, and S.P. Lee Guyot: Geological considerations: Marine Geology, v. 69, p. 25-54.

Hein, J.R., Manheim, F.T., Schwab, W.C., Davis, A.S., Daniel, C.L., Bouse, R.M., Morgenson, L.A., Sliney, R.E., Clague, D.A., Tate, G.B., and Cacchione, D.A., 1985b, Geological and geochemical data for seamounts and associated ferromanganese crusts in and near the Hawaiian, Johnston Island, and Palmyra Island Exclusive Economic Zones: U.S. Geological Survey Open-File Report 85-292, 129 p.

Hein, J.R., Schwab, W.C., Foot, D.G., Masuda, Y., Usui, A., Davis, A.S., Fleishman, C.L., Barna, D.L., Pickthorn, L.B., Larson, D.A., Ruzzi, P., Benninger, L.M., and Gein, L.M., 1987a, Farnella cruise F7-86-HW, cobalt-rich ferromanganese crust data report for Karin Ridge and Johnston Island, central Pacific: U.S. Geological Survey Open-File Report 87-663, 34 p.

Hein, J.R., Morgenson, L.A., Clague, D.A., and Koski, R.A., 1987b, Cobalt-rich ferromanganese crusts from the Exclusive Economic Zone of the United States and nodules from the oceanic Pacific: in Scholl, D.W., Grantz, A. and Vedder, J.G. (eds.), Geology and Resource Potential of the Continental Margin of Western North America and Adjacent Ocean Basins-Beaufort Sea to Baja California. Circum-Pacific Council for Energy and Mineral Resources, Earth Science Series, Houston, Texas, v. 6, p. 753-771.

Hein, J.R., Schwab, W.C. and Davis, A.S., 1988, Cobalt and platinum-rich ferromanganese crusts and associated substrate rocks from the Marshall Islands: Marine Geology, v. 78, p. 255-283.

Hein, J.R., Schulz, M.S., and Gein, L.M., 1990a, Central Pacific cobalt-rich ferromanganese crusts: Historical perspective and regional variability: in Keating, B. and Bolton, B. (eds), Geology and Offshore Mineral Resources of the Central Pacific Region, Circum-Pacific Council for Energy and Mineral Resources, Earth Science Series, Houston, Texas, in press.

Hein, J.R., Schulz, M.S. and Kang, J.K., 1990b, Insular and submarine ferromanganese mineralization of the Tonga-Lau Region: Marine Mining (in press, v. 9, no. 3).

Kastner, M., 1979, Zeolites: in Burns, R.G. (ed.), Marine Minerals, Mineralogical Society of America Short Course Notes, v. 6, p. 111-122.

Klovan, J.E. and Imbrie, J., 1971, An algorithm and FORTRAN-IV program for large-scale Q-mode factor analysis and calculation of factor scores: Mathematical Geology, v. 3, p. 61-77.

MacDonald, G.A. and Katsura, T., 1964, Chemical composition of Hawaiian lavas: Journal of Petrology, v. 5, p. 82-133.

MacKenzie, W.S., Donaldson, C.H., and Guilford, C, 1982, Atlas of igneous rocks and their textures: John Wiley and Sons, New York, 148 p.

Manheim, F.T. and Gulbrandsen, R.A., 1979, Marine Phosphorites: in Burns, R.G. (ed.), Marine Minerals, Mineralogical Society of America Short Course Notes, v. 6, p. 151-173.

Piper, D.Z., 1974, Rare earth elements in ferromanganese nodules and other marine phases: Geochimica et Cosmochimica Acta, v. 38, p. 1007-1022.

Puteanus, D., and Halbach, P., 1988, Correlation of Co concentration and growth rate: a method for age determination of ferromanganese crusts: Chemical Geology, v. 69, p. 73-85.

Table 1. Summary of ferromanganese crusts recovered from south Johnston Island ridge and Karin Ridge, R/V *Farnella* cruise F7-86-HW.

Dredge Number	Water Depth[1]	Water Depth[2]	Total Recovery (kg)	Crust Recovery (kg)	Percent Crust	Maximum Thickness (mm)	Average Thickness (mm)	Dominant Substrate	Location
CD1	2255(?)-2200	?	725	70	10	50	10	Basalt, Limestone	KE
CD2	2900-2650	?	500	100	20	110	50	Volcanic breccia	J
BMDS3	2700-2340	2460-2340	20	10	50	25?	10?	Basalt?	J
JOD4	3175-3200*	3175-2430	70	35	50	30	20	Volcanic breccia	J
CD5	2750-2350	2750	200	40	20	100	45	Mudstone	J
CD6	2300-2150	2240-2150	365	40	11	60	28	Volcanic breccia, basalt, mudstone	KW
CD7	3100-1990	2340-2120	270	35	13	72	35	Mudstone, basalt, volcanic breccia	KW
CD8	2675-1685	1910-1850	30	10	33	70	40	Basalt	KW
JTD9	2980-2600	2910-2260	450	100	22	70	40+	Mudstone, basalt	KW
JOD10	2830-2160	2830-2160	20	5	25	50	30	Volcanic breccia, basalt	KW
CD11	2530-2240	2530-2240	300	50	17	30	15	Volcanic breccia	KE
CD12	2550-2110	2280-2100	400	70	18	~50	~25	Volcanic breccia	KE
CD13	2310-2140	2310-2140	500	140	28	70	40	Tuff, siltstone	J
CD14	2370-2340	2370-2340	545	60	9	60	25	Basalt, volcanic breccia, tuff	J
CD15	2350-2250	2350-2250	115	25	22	60	20	Mudstone, basalt	J
CD16	2650-2520	2540-2520	455	150	33	120	65	Volcanic breccia	J
CD17	2620-2600	2620-2315	775	125	16	70	30	Basalt, volcanic breccia	J
CD18	2560-2420	2560-2420	130	40	31	60	40	Volcanic breccia, basalt	J
CD19	2880-2530	2530-2430	25	10	40	25	10	Limestone	J
CD20	2340-2100	2280-2070	70	5	7	15	2	Volcanic breccia	J
CD21	2775-2350	2775-2370	570	180	32	130	45	Volcanic breccia, basalt	J
CD22	2630-2320	2430-2340	12	3	25	60	45	Basalt	J
CD23	2740-2340	2370-2340	230	50	22	60	30	Volcanic breccia	J
CD24	2380-2290	2380-2290	155	30	19	65	40	Volcanic breccia	J
CD25	2450-2320	2450-2320	550	115	21	90	45	Basalt	J
CD26	2440-2220	2350-2220	600	90	15	65	30	Basalt	J
CD27	Lost Dredge Bag		-	-	-	-	-	-	-
CD28	2210-1950	2210-2070	40	22	55	95	45	Basalt	KS
CD29	2400-1950	2390-2290, 2120-1970	295	193	65	160	75	Volcanic breccia, basalt	KS
CD30	2000-1920	1950-1920	220	30	14	70	15	Basalt, volcanic breccia	KS
Total	-	-	8637	1833	26 (ave.)	-	-	-	-

* Went up and over a hill

J = south Johnston Island ridge
KE = east-central Karin Ridge
KW = west-central Karin Ridge
KS = south Karin Ridge

CD = USGS circular chain-bag dredge
BMDS = Bureau of Mines dredge sled
JOD = Japanese oval dredge
JTD = Japanese toothed dredge

[1]Water depth of dredge on and off bottom, as determined by 3.5 and 12 kHz seismic recorders and satellite navigation.
[2]Depth interval samples were probably recovered from, as determined by 3.5 and 12 kHz seismic recorders at the times of high tensiometer readings on the wire.

Table 2. Calcareous nannofossils and ages of sediment and sedimentary rocks.

Sample No.	Sample Type	Nannofossils	Age	Comments
CD1-8	Reefal limestone	*Zygrhablithus?*, *Fasciculithus?*, *Ceratolithus cristatus* (Pleistocene)	Indeterminate	Either Pleistocene with reworked early Tertiary or early Tertiary with Pleistocene contamination.
CD1-9	Reefal limestone	*Fasciculithus* sp., *Cyclicargolithus abisectus*	early Tertiary	Questionable age date.
CD1-9	Mud infilling from vugs	*Ceratolithus cristatus*, *C. simplex*, *C. telesmus* (Pleistocene); *Gephyrocapsa* spp. (late Pliocene to present); *Discoaster* spp. (pre-Pleistocene); *Coccolithus eopelagicus?* (Eocene-Oligocene); *Cyclicargolithus abisectus* (Oligocene); *Dictyococcites bisectus* (Eocene-Oligocene); *Fasciculithus* sp. (Paleocene), *Helicosphaera* sp., *Rhabdosphaera* sp.	Indeterminate	Nannofossils of mixed ages.
CD1-10B	Reefal limestone, partially phosphatized	*Fasciculithus* sp., *Sphenolithus* sp. aff. *S. pseudoradians*, *Zygrhablithus* sp.	Eocene	Questionable age date.
CD1-12	Bioclastic limestone, partially phosphatized	-	Indeterminate	Barren.
CD2-30	Limestone	*Chiasmolithus* sp. *Coccolithus pelagicus* group, *Sphenolithus* sp.	Paleogene	Questionable age date; nannofossils replaced with apatite.
CD5-13	Mudstone	-	Indeterminate	Barren
CD5-14	Bioclastic limestone	*Chiasmolithus* sp., *Coccolithus (eo?)pelagicus*, *Fasciculithus* sp., *Sphenolithus obtusus*	Eocene	Some nannofossils appear to be replaced by another mineral.
CD6-12B	Siltstone and mudstone, partially phosphatized	-	Indeterminate	Barren.
CD13-3	Mud infilling from fractures	-	Indeterminate	Barren.
CD13-13C	Tuffaceous siltstone, with phosphorite cement	-	Indeterminate	One non-diagnostic nannofossil fragment.
CD15-1D	Tuffaceous siltstone	-	Indeterminate	Barren.
CD15-2E	Limestone clast found between Fe-Mn crust layers	-	Indeterminate	Rare non-diagnostic nannofossils.
CD19-1	Phosphorite	-	Indeterminate	A few poorly preserved placoliths replaced by apatite.
CD19-3	Limestone/Phosphorite	*Sphenolithus tribulosus?*, *Zygrhablithus bijugatus*	Oligocene	Questionable age date; sparse, poorly preserved flora; replaced by apatite?
CD29-3	Foram sand	*Discoaster* sp. aff. *D. brouweri*, *D.* sp. aff. *D. exilis*, *D* sp. aff. *D. variabilis*, *D.* spp.; *Gephyrocapsa* sp., *Reticulofenestra* sp.	Miocene	Probably Miocene with minor latest Pliocene to recent contamination; or late Pliocene to recent with considerable Miocene and Pliocene contamination.
CD30-2	White clay	*Discoaster* sp. aff. *D. exilis*, *D. variabilis*, *D.* spp.	Miocene-Pliocene	Probably early Miocene to mid Pliocene; most of the sample is made up of non-birefringent hexagonal crystals (apatite).
CD30-11	Phosphatized mudstone	*Dictyococcites bisectus*, *Discoaster variabilis?*	Indeterminate	Nannofossils are phosphatized, therefore identification is questionable. Ages range from Eocene or Oli ocene to Miocene.

y

Table 3. X-Ray diffraction mineralogy of substrate rocks from cruise F7-86-HW.

Sample	Major[1]	Moderate	Minor/Trace	Lithology
CD1-3B	Plagioclase	Pyroxene, Apatite, Magnetite, Phillipsite	Mixed-layer clays, Illite?	Altered vesicular aphanitic basalt with phosphorite infilled vesicles
CD1-4B	Apatite[2]	Plagioclase	-	Brown phosphorite cemented breccia[3]
CD1-6B	Goethite	Apatite	-	Phosphatic ironstone
CD1-8	Calcite	Apatite	-	Bioclastic limestone, partly phosphatized
CD1-9	Calcite	-	-	Reefal limestone
CD1-10-B	Calcite, Apatite	-	-	Reefal limestone, partly phosphatized
CD1-11B	Plagioclase	Apatite, Smectite, Magnetite	Phillipsite	Pale brown mudstone with Mn speckling, partly phosphatized
CD1-12	Calcite	Apatite	-	Limestone: calcite replaced volcaniclastic sandstone(?), partly phosphatized
CD1-14B	Goethite	Apatite, Smectite	-	Altered, phosphorite cemented breccia
CD1-15B	Apatite	-	-	Phosphorite
CD1-16B	Goethite	-	-	Ironstone
CD1-17F	Apatite	-	-	Phosphorite
CD1-17G	Apatite	-	-	Phosphorite
CD1-19B	Apatite	-	Plagioclase, Quartz	Breccia with white phosphorite cement
CD2-3D	Phillipsite	-	Apatite, Smectite	Altered breccia with white zeolite and phosphorite cement
CD2-8G	Smectite	-	Phillipsite, Anatase	Altered breccia
CD2-19B	Calcite	-	Halite	Foraminifera sand from vug
CD2-19C	Calcian Dolomite or Kutnahorite	Quartz, Todorokite	Plagioclase, Phillipsite	Mud filled fracture
CD2-19D	Apatite	-	-	Phosphorite
CD2-29	Apatite	Mixed-layer clays	-	Phosphatized hyaloclastite
CD2-30	Calcite	-	-	Recrystallized foraminiferal limestone
CD2-37C	Apatite, Phillipsite	-	Smectite	Altered breccia with white zeolite and phosphorite cement
CD2-38G	Apatite	-	Smectite	Phosphorite cemented breccia
CD2-38M	Calcian Dolomite or Kutnahorite	Apatite, Quartz	Phillipsite, Mixed-layer clays, Barite?	Mud infilling from vugs in second layer of Fe-Mn crust
BMDS3-B	Phillipsite	-	Smectite	White sediment between crust and altered basalt substrate
JOD4-1C	Phillipsite	-	Smectite, Apatite	Altered breccia with phosphorite and zeolite cement
CD5-1-IID	Apatite	-	-	Brown phosphorite from fracture in basalt
CD5-2-IIE	Apatite, Calcite	-	-	Pale brown, partly phosphatized bioclastic siltstone
CD5-3D	Apatite	-	-	Brown phosphorite
CD5-6B	Smectite	-	Quartz?	Mudstone
CD5-6C	Barite	Smectite	-	Nodule within mudstone
CD5-11D	Smectite	Apatite	-	Mudstone, partly phosphatized
CD6-3D	Apatite	Plagioclase	Phillipsite	Altered breccia with white phosphorite cement
CD6-4C	Plagioclase	Smectite	Pyroxene	Altered breccia with sparse smectite and Mn oxide cement
CD6-7C	Phillipsite	-	Smectite, Plagioclase	Altered breccia, with zeolite cement
CD6-8C	Phillipsite	-	Plagioclase	Altered breccia, with zeolite cement

Table 3. continued

CD6-10E	Phillipsite	Clinoptilolite, Smectite	-	Bioturbated brown siltstone
CD6-12B	Apatite, Plagioclase	Smectite	-	Siltstone and mudstone with Mn coated borings, smectite and phosphorite? cement
CD6-15B	Plagioclase	Smectite, Goethite, Phillipsite, Clinoptilolite, Calcite	Magnetite ?	Siltstone with Mn coated, mud infilling borings
CD6-15C	Calcite	Plagioclase, Quartz	Mixed-layer clays, Chlorite	Mud infilling borings
CD6-21A	Plagioclase	Pyroxene, Magnetite, Smectite	Apatite	Altered breccia, minor phosphorite cement
CD6-21B	Plagioclase	-	Smectite, Pyroxene	Altered aphanitic basalt, slightly plagioclase phyric
CD6-22C	Phillipsite	Apatite	Plagioclase	Altered breccia with phosphorite and zeolite cement
CD6-23C	Plagioclase	Quartz	Smectite, Apatite	Altered basalt
CD6-24B	Plagioclase	Apatite	Phillipsite	Altered breccia with phosphorite cement
CD6-24C	Apatite, Plagioclase	Quartz, Mixed-layer clays	Chlorite	Partly phosphatized mud infilling of vug in breccia
CD6-25B	Phillipsite	Plagioclase	Smectite	Altered breccia, with zeolite cement
CD7-3B	Plagioclase	Apatite, Smectite, Clinoptilolite, Quartz	-	Partly phosphatized mudstone with many Mn coated, mud infilling borings
CD7-3D	Plagioclase	Apatite, Quartz, Mixed-layer clays	Chlorite	Mud infilling borings
CD7-9C	Clinoptilolite,	Smectite	-	Bioturbated mudstone
CD7-11C	Plagioclase	Apatite, Smectite, Quartz, Clinoptilolite	-	Partly phosphatized mudstone, bioturbated, Mn dendrites
CD7-13B	Plagioclase	Apatite	Smectite	Vesicular basalt, and feldspar phyric basalt, with phosphorite infilled vesicles
CD7-14B	Calcite	Phillipsite	Smectite	Breccia with cream colored mudstone matrix, and calcite cement
CD7-14C	Calcite	-	-	Calcite "dog-tooth spar" in breccia vugs
CD7-15B	Apatite	-	-	Phosphorite
CD7-15C	Plagioclase	-	Smectite	Red clay in phosphorite
CD7-15D	Apatite	-	-	Phosphorite
CD7-16A	Calcite	-	-	Limestone infilled vesicles
CD7-16B	Plagioclase, Calcite	-	Smectite	Pale brown mudstone
CD7-16C	Calcite, Plagioclase	-	Apatite	Altered vesicular basalt with calcite and phosphorite infilled vesicles
CD8-A	Apatite	Plagioclase	-	Breccia with phosphorite cement
JTD9-1B	Phillipsite	-	Apatite	Breccia with zeolite and phosphorite cement
JTD9-1C	Phillipsite	-	Smectite	Zeolite cement
JTD9-2D	Plagioclase	Smectite, Clinoptilolite	-	Siltstone with Mn coated, mud infilling borings
JTD9-2E	Phillipsite	Quartz, Smectite	Plagioclase	Mud infilling borings
JTD9-3BI	Plagioclase	Smectite		Altered, highly vesicular basalt
JTD9-3BII	Phillipsite	-	Smectite	Altered, highly vesicular basalt
JTD9-3BIII	Phillipsite	-	Smectite	Altered, highly vesicular basalt
CD11-2C	Phillipsite	Plagioclase	Smectite	Breccia with pale brown zeolite cement
CD11-2CI	Plagioclase	Pyroxene, Magnetite	Smectite, Chlorite	Highly altered basalt clast in breccia

Table 3. continued

CD11-2CII	Smectite, Plagioclase	-	-	Mudstone clast in breccia
CD11-11C	Phillipsite	-	Plagioclase	Breccia, with zeolite cement
CD11-12B	Phillipsite, Plagioclase	-	Smectite, Quartz?	Breccia, basalt clasts with alteration rims and zeolite cement
CD12-1B	Phillipsite	-	-	Breccia with zeolite cement
CD12-1C	Phillipsite	-	-	Crystals from cement
CD12-2B	Plagioclase	-	-	Basalt with rare plagioclase phenocrysts
CD13-3B	Apatite, Smectite	Plagioclase	-	Tuffaceous siltstone, with phosphorite cement
CD13-6B	Goethite, Apatite	-	-	Phosphatic ironstone
CD13-8F	Apatite	Smectite	-	Hyaloclastite with phosphorite cement
CD13-13C	Apatite, Smectite	-	-	Tuffaceous siltstone, with phosphorite cement
CD13-27-8B	Apatite,Smectite	-	-	Tuffaceous siltstone, with phosphorite cement
CD14-2B	Apatite	-	-	Phosphorite
CD14-2C	Apatite	Magnetite, Plagioclase?	Smectite	Basalt clast embedded in phosphorite layer
CD14-11B	Phillipsite	Apatite, Smectite	Calcite	Partly phosphatized, white mud between Fe-Mn crust and basalt substrate
CD15-1C	Smectite	-	-	Tuffaceous siltstone
CD15-2D	Goethite, Apatite	Plagioclase, Calcite		Altered breccia, with phosphorite cement
CD15-2E	Calcite	-	-	Limestone clast between Fe-Mn crust layers 2 and 3
CD16-5B-1	δ–MnO_2	-	Todorokite, Quartz, Plagioclase	Breccia with Mn oxide cement
CD16-6B	Phillipsite,	Todorokite,Smectite	Apatite	Breccia with highly altered basalt clasts, with zeolite , clay, and Mn-oxide cement
CD19-1A	Apatite	-	-	Phosphorite
CD19-2	Apatite	-	-	Phosphorite clast in breccia
CD20-1	Phillipsite	Smectite	-	Breccia
CD20-2	Calcite	-	Smectite	Breccia with drusy calcite crystals and calcite cement
CD20-2A	Calcite	-	Smectite	Drusy calcite crystals
CD21-7-E	Apatite	-	-	Phosphorite in basalt vesicle
CD26-2B	Plagioclase, Phillipsite	Apatite, Magnetite	Smectite	Breccia with phosphorite cement
CD26-4C	Apatite	Phillipsite	Smectite ?	Breccia with phosphorite cement
CD26-5C	Plagioclase	Pyroxene, Apatite, Magnetite	Mica	Vesicular, trachytic basalt with phosphorite in some vesicles
CD26-7B	Apatite	Phillipsite	Smectite	Breccia with phosphorite cement
CD28-1F	Goethite, Apatite	-	Smectite	Ferruginous phosphorite: altered and replaced hyaloclastite
CD28-2C	Goethite, Apatite	-	-	Phosphatic ironstone
CD29-2F	Apatite	Smectite	Quartz	Phosphatized hyaloclastite
CD30-10E	Plagioclase	Apatite, Magnetite	-	"Wood-grained" phosphatized clast from phosphorite cemented breccia.
CD30-11	Apatite	-	Quartz?, K-feldspar?, Chlorite?, Barite?, Smectite?	Phosphatized mudstone

1. Major: >25%, Moderate: >5% to <25% , Minor: <5%.
2. All apatite is Carbonate Fluorapatite.
3. All breccias are sedimentary volcaniclastic.

Table 4. Chemical composition in weight percent of substrate rocks.

	CD1-3B	CD1-4B	CD1-6B[2]	CD1-10B	CD1-11B	CD1-14B	CD1-15B	CD1-16B[2]	CD1-19B	CD2-3D	CD2-8G[3]	CD2-19D	CD2-37C	CD2-38G
SiO_2	46.30	14.80	5.5	1.36	44.70	29.90	6.40	5.8	13.50	37.00	41.6	4.69	25.70	12.60
Al_2O_3	17.70	5.56	1.1	0.36	17.00	14.00	2.06	0.1	4.51	12.40	12.6	1.44	8.50	2.81
FeO	nd	nd	0.8	nd	0.17	nd	0.17	nd	nd	1.02	<0.02	nd	0.49	nd
Fe_2O_3	4.88[1]	3.42[1]	52.0	0.27[1]	6.84	20.70[1]	1.00	80.5[1]	5.48[1]	12.56	16.8	0.93[1]	7.76	18.00[1]
MgO	0.65	0.95	0.9	0.62	2.68	4.54	0.47	0.7	1.31	1.84	2.9	0.53	1.46	1.24
CaO	7.21	36.20	16.5	53.50	4.87	5.57	48.10	1.3	34.20	7.10	0.5	47.80	23.30	30.80
Na_2O	3.10	1.49	0.6	0.39	2.62	1.23	0.99	0.2	1.49	2.97	1.8	1.01	2.17	0.77
K_2O	4.70	0.85	0.3	0.08	3.17	1.68	0.72	0.1	0.82	3.34	2.5	0.25	2.28	1.16
TiO_2	1.32	0.89	0.1	0.04	1.95	3.45	0.39	0.1	0.86	3.22	4.1	0.06	1.94	0.68
P_2O_5	3.76	21.70	10.6	12.50	2.37	3.66	30.10	1.3	20.50	3.74	0.3	29.80	14.00	18.90
MnO	1.37	1.82	0.3	<0.02	<0.02	0.24	0.04	0.2	3.73	0.48	0.4	0.72	0.37	0.93
LOI	5.43	6.65	10.9	28.10	13.00	14.70	6.28	11.7	8.01	13.30	16.3	7.32	9.91	9.11
Total	96.42	94.33	99.6	97.22	99.37	99.67	96.72	102.0	94.41	98.97	99.8	94.55	97.88	97.00
H_2O+	2.97	2.18	7.88	0.78	3.87	7.51	2.09	10.60	2.42	4.99	5.71	1.98	3.83	4.08
H_2O-	1.98	1.53	0.98	0.23	7.53	6.12	0.61	0.82	2.22	7.07	9.39	1.15	4.20	2.49
CO_2	0.60	3.73	2.16	28.00	0.40	0.58	5.22	0.45	3.60	0.98	0.23	2.34	2.38	3.25
Lithology	Vesicular basalt	Phosphorite cemented breccia	Phospha-tized ironstone	Phospha-tized lime-stone	Mudstone	Phosphorite cemented breccia	Phosphorite	Ironstone	Phosphorite cemented breccia	Phosphorite cemented breccia	Altered breccia	Phosphorite	Phosphorite cemented breccia	Phosphorite cemented breccia

	BMDS3-B	JOD4-1C	CD5-6B	CD6-3D	CD6-4C	CD6-7C	CD6-8C	CD6-10E	CD6-12B	CD6-15B	CD6-21A	CD6-21B	CD6-22C	CD6-23C
SiO_2	51.80	35.70	42.40	15.60	44.70	41.20	40.20	47.70	43.60	46.30	44.50	44.10	39.20	40.30
Al_2O_3	17.50	10.50	12.70	5.35	14.40	15.00	15.60	12.60	11.00	12.40	14.60	15.60	15.50	14.70
FeO	nd	nd	nd	nd	nd	nd	0.43	nd	0.33	nd	0.11	2.52	nd	1.32
Fe_2O_3	1.32[1]	13.4[1]	13.5[1]	6.00[1]	12.9[1]	13.20[1]	13.62	8.86[1]	10.83	9.37[1]	12.98	11.30	16.0[1]	14.63
MgO	0.44	2.92	3.20	0.93	2.58	2.00	1.16	2.43	2.67	2.61	2.98	3.57	1.35	1.70
CaO	0.62	7.62	0.60	35.50	4.20	6.86	4.45	1.84	7.44	2.03	6.03	8.63	5.01	8.96
Na_2O	5.55	2.27	2.04	1.58	2.32	2.66	3.78	2.74	2.50	2.60	2.36	2.39	3.26	2.74
K_2O	6.28	2.50	2.10	0.95	1.91	2.32	2.85	3.76	2.59	3.50	2.07	1.30	2.41	1.38
TiO_2	0.36	2.82	3.93	1.28	3.13	3.33	3.46	1.52	1.82	1.66	3.11	3.94	4.10	4.27
P_2O_5	0.33	4.11	0.25	21.30	0.89	2.47	1.32	0.54	4.19	0.44	1.52	0.60	1.36	3.10
MnO	0.10	2.28	0.40	0.98	1.69	0.60	0.68	2.85	0.15	2.93	0.46	0.43	0.34	0.26
LOI	15.10	13.70	15.60	7.18	11.10	9.90	12.30	14.40	12.50	15.20	9.34	5.35	11.30	6.19
Total	99.40	97.82	96.72	96.65	99.82	99.54	99.85	99.24	99.62	99.04	100.06	99.73	99.83	99.55
H_2O+	7.04	4.82	5.41	2.59	3.67	5.08	6.16	6.65	4.92	6.03	4.71	2.73	5.52	3.08
H_2O-	7.74	7.56	9.23	2.11	6.52	5.16	6.40	7.69	7.13	8.33	5.41	3.21	5.98	3.05
CO_2	0.21	0.84	0.23	3.65	0.33	0.49	0.26	0.51	0.68	0.76	0.27	0.13	0.29	0.42
Lithology	Mud between crust and substrate	Phosphorite cemented breccia	Altered Hyalo-clastite	Phosphorite cemented breccia	Altered breccia	Altered breccia	Altered breccia	Bioturbated siltstone	Siltstone, phospho-rite cement	Siltstone-mudstone, phosphorite cement	Breccia, partly phospha-tized	Altered aphanitic basalt	Breccia with phosphorite cement	Altered basalt

	CD6-24B	CD6-25B	CD7-3B	CD7-9C	CD7-11C	CD7-13B	CD7-14B	JTD9-1B	JTD9-3B	CD11-2C	CD11-11C	CD11-12B	CD12-1B	CD12-2B
SiO_2	19.80	42.30	46.20	49.80	41.00	41.20	29.50	43.10	39.70	48.90	42.40	45.90	45.70	48.30
Al_2O_3	6.92	17.10	12.40	13.30	10.10	16.40	12.60	14.70	14.70	13.50	18.10	16.20	14.20	14.40
FeO	nd	1.20	nd	nd	nd	1.26	0.93	0.73	0.58	0.49	0.76	1.22	0.93	4.48
Fe_2O_3	8.44[1]	8.49	10.10[1]	9.61[1]	12.80[1]	14.80	12.47	14.29	17.60	11.95	12.45	9.60	12.47	8.20
MgO	1.28	1.49	2.67	2.55	3.27	1.49	1.29	2.09	2.45	3.68	1.79	2.20	2.67	3.32
CaO	28.90	10.20	1.50	1.03	2.74	7.02	17.30	5.19	2.20	2.70	1.20	5.95	4.48	8.53
Na_2O	1.65	2.89	2.75	2.49	2.69	3.11	2.47	2.65	1.99	3.16	2.86	3.09	3.03	3.23
K_2O	1.18	2.59	3.14	3.68	2.59	1.66	1.25	2.44	2.18	2.71	4.57	3.16	2.64	1.56
TiO_2	2.11	2.63	1.96	2.61	1.77	4.30	3.55	3.85	4.81	1.78	2.65	2.93	3.10	3.33
P_2O_5	16.70	3.56	0.43	0.37	0.69	2.07	0.44	0.95	0.31	0.61	0.68	1.52	0.73	1.34
MnO	1.09	0.27	3.01	0.66	3.97	0.26	0.09	0.14	0.19	0.28	0.17	0.13	0.21	0.19
LOI	6.84	6.91	15.20	13.50	17.60	6.00	17.80	9.69	13.30	10.10	12.00	7.60	9.51	3.00
Total	94.91	99.63	99.36	99.6	99.22	99.57	99.69	99.82	100.01	99.86	99.63	99.50	99.67	99.88
H_2O+	2.80	3.22	6.66	5.97	6.15	2.87	3.46	4.56	6.39	3.70	6.89	3.87	4.30	1.26
H_2O-	2.22	3.38	7.85	7.35	9.14	2.93	3.66	5.15	7.16	6.30	5.10	3.84	5.33	1.76
CO_2	2.76	0.60	0.19	0.10	1.85	0.30	11.50	0.24	0.05	0.18	0.14	0.21	0.30	0.17
Lithology	Phosphorite cemented breccia	Altered breccia	Mudstone	Mudstone	Phospha-tized mudstone	Vesicular basalt	Calcite cemented breccia	Phosphorite cemented breccia	Vesicular basalt	Breccia with mud matrix	Breccia	Breccia	Breccia	Basalt

	CD13-8F	CD13-13C	CD15-1C	CD15-2D[2]	CD16-6B	CD20-1	CD20-2	CD26-2B	CD26-4C	CD26-5C	CD26-7B	CD28-1F	CD28-2C[2]	CD29-2F
SiO_2	30.70	41.00	42.30	17.3	37.90	41.30	25.80	47.50	12.10	49.20	23.80	11.50	9.3	28.50
Al_2O_3	8.87	12.10	12.40	6.2	10.70	12.80	8.11	16.10	3.41	16.40	7.46	0.69	0.9	8.49
FeO	3.22	0.86	0.42	<0.02	nd	<0.02	<0.02	1.34	<0.02	2.13	nd	nd	<0.02	<0.02
Fe_2O_3	7.62	12.84	11.03	31.0	11.90[1]	11.90	7.27	7.16	2.22	4.77	7.98[1]	19.90[1]	39.3	9.06
MgO	2.37	2.87	3.12	1.6	2.74	2.47	2.14	2.25	0.68	2.08	1.86	1.28	1.1	2.24
CaO	14.80	2.40	0.28	17.8	4.57	0.72	23.90	5.04	39.20	9.34	16.50	29.20	22.3	19.20
Na_2O	1.37	1.67	2.02	1.3	2.12	2.77	1.06	3.70	1.55	4.81	1.81	0.67	0.4	1.41
K_2O	2.38	2.14	1.56	1.1	3.13	2.71	1.19	2.99	0.91	2.77	2.20	1.53	1.0	1.92
TiO_2	2.37	3.29	3.76	1.8	2.64	3.26	1.51	1.66	0.30	1.30	1.88	0.04	0.2	1.73
P_2O_5	9.12	1.64	0.18	8.9	2.76	0.38	0.55	1.63	23.90	3.40	10.10	18.10	13.8	11.60
MnO	0.21	0.68	<0.02	0.7	5.56	0.40	0.09	0.30	0.94	0.26	6.51	4.32	0.4	0.33
LOI	15.40	18.10	22.70	11.5	15.20	20.90	28.50	9.88	8.52	2.19	17.80	9.96	9.8	14.10
Total	98.43	99.59	99.77	99.2	99.22	99.61	100.12	99.55	93.73	98.65	97.90	97.19	98.5	98.58
H_2O+	1.32	2.00	0.40	5.22	4.94	2.70	2.34	4.09	1.94	0.93	<0.01	3.95	6.27	2.92
H_2O-	9.68	12.70	16.00	2.35	8.46	13.60	7.56	5.45	2.73	0.98	11.50	2.42	1.48	7.58
CO_2	1.62	0.14	0.10	3.94	0.48	0.10	17.30	0.33	4.47	0.46	1.79	3.01	2.50	2.30
Lithology	Phosphorite cemented hyalodastite	Phosphorite cemented siltstone	Tuff-aceous siltstone	Altered breccia, phosphorite cemented	Breccia	Breccia	Calcite cemented breccia	Phosphorite cemented breccia	Phosphorite cemented breccia	Vesicular basalt	Phosphorite cemented breccia	Ferruginous phosphorite	Phosphatic ironstone	Phosphorite cemented hyalodastite

Major oxides by X-ray fluorescence; LOI = Loss On Ignition at 900°C; Analysts: J. Taggart, E. Bell, D. Siems, and L. Espos.
nd = not determined
[1] = Total Fe as Fe_2O_3
[2] = Semiquantitative, because Fe contents outside the range of the standards.
[3] = Semiquantitative, because of insufficient sample.

Table 5. Chemical composition of selected, relatively fresh volcanic rocks from Karin Ridge and Johnston Island.

	Karin Ridge			Johnston Island		
Rock Type:	Bm	Haw	AB	AB	Ne	Mu
Sample:	CD1-22	CD12-4	CD29-12	BMDS3-2	CD19-5	CD24-3
SiO_2	55.8	48.0	39.2	40.6	34.4	53.8
Al_2O_3	20.2	15.2	14.2	16.1	12.6	17.3
FeO	0.57	4.62	1.55	5.10	6.18	2.30
Fe_2O_3	2.77	5.82	7.90	7.23	7.95	4.49
MgO	0.42	3.68	3.65	4.33	5.63	2.16
CaO	5.44	9.72	14.0	9.67	13.5	6.28
Na_2O	4.86	3.14	1.65	2.50	1.59	5.09
K_2O	4.44	1.77	1.35	1.51	1.34	3.22
TiO_2	2.36	4.37	2.91	3.36	4.57	1.41
P_2O_5	1.25	1.07	1.83	2.23	3.12	1.26
MnO	0.02	0.12	0.13	0.24	0.26	0.25
H_2O^+	0.58	0.81	2.74	2.84	4.13	1.08
H_2O^-	0.42	1.13	4.18	3.32	4.29	0.45
CO_2	0.08	<0.01	3.40	0.11	0.24	0.05
Total	99.2	99.5	98.7	99.1	99.8	99.1

Major elements by XRF, analysts: J. Taggart, A. Bartel, and D. Siems.
FeO, H_20 and CO_2 by wet chemical techniques, analyst: S. Pribble.
AB = alkalic basalt, Haw = hawaiite, Bm = benmoreite, Ne = nephelinite, and Mu = mugearite; rock classification after MacKenzie et al., (1982).

Table 6. X-Ray diffraction mineralogy of ferromanganese crusts from Cruise F7-86-HW.

Sample Number	Type of Mn Oxide	δMnO_2 (%)	Others (%)
CD1-2A	Bulk Crust (0-15mm)	97	2 - Plagioclase, 1 - Quartz
CD1-3A	Bulk Crust (0-5mm)	97	1 - Plagioclase, 1 - Calcite, 1 - Quartz
CD1-4A	Bulk Crust (0-7mm)	100	Trace - Quartz
CD1-6A	Bulk Crust (0-7mm)	99	<1 - Quartz
CD1-7A-I	Nodule Layer (0-10mm)	99	<1 - Quartz
CD1-7A-II	Nodule Layer (10-20mm)	64	36 - Apatite
CD1-10-A1	Bulk Crust (0-36mm)	99	<1 - Quartz
CD1-10-A2	Layer (0-31mm)	97	1 - Calcite, 1 - Plagioclase, <1 - Quartz
CD1-10-A3	Layer (31-36mm)	90	10 - Apatite
CD1-11A	Bulk Crust (0-4mm)	97	2 - Apatite, 1 - Plagioclase
CD1-14A	Bulk Crust (0-5mm)	98	1 - Quartz, 1 - Plagioclase
CD1-15A	Bulk Crust (0-30mm)	98	2 - Plagioclase, Trace - Quartz
CD1-16A	Bulk Crust (0-5mm)	100	Trace - Plagioclase, Quartz
CD1-17A	Layer (0-10mm)	100	Trace - Quartz
CD1-17B	Layer (10-30mm)	99	1 - Plagioclase, Quartz
CD1-17C	Layer (30-40mm)	46	30 - Todorokite, 24 - Apatite
CD1-17D	Bulk Underside Crust (0-10mm)	100	-
CD1-17E	Bulk Crust (0-45mm)	92	5 - Apatite, 3 - Illite
CD1-19A	Bulk Crust (0-8mm)	100	Trace - Quartz
CD1-20	Bulk Crust (0-25mm)	99	1 - Quartz
CD1-21	Bulk Nodule (0-6mm)	99	1 - Quartz
CD2-3A	Layer (0-10mm)	100	Trace - Quartz
CD2-3B	Layer (10-25mm)	100	Trace - Quartz
CD2-3C	Bulk Crust (0-25mm)	100	Trace - Plagioclase, Quartz
CD2-8A	Layer (0-12.5mm)	100	Trace - Plagioclase, Quartz
CD2-8B	Layer (12.5-32.5mm)	98	1 - Quartz, 1 - Plagioclase
CD2-8C	Layer (32.5-52.5mm)	98	1 - Quartz, 1 - Plagioclase
CD2-8D	Layer (52.5-72.5mm)	97	3 - Apatite
CD2-8E	Layer (72.5-92.5mm)	100	-
CD2-8F	Bulk Crust (0-90mm)	100	-
CD2-10-IVA	Layer (0-35mm)	99	<1 - Plagioclase, Quartz
CD2-10-IVB	Layer (35-54mm)	92	8 - Apatite
CD2-10-IVC	Layer (54-87mm)	93	7 - Apatite
CD2-12	Bulk Crust (0-20mm)	93	4 - Apatite, 2 - Plagioclase, 1 - Quartz
CD2-15A	Layer (0-13mm)	99	<1 - Quartz
CD2-15B	Layer (13-27mm)	100	-
CD2-15C	Layer (27-40mm)	99	<1 - Quartz
CD2-15D	Layer (40-65mm)	88	12 - Apatite
CD2-15E	Bulk Crust (0-68mm)	89	7 - Kutnahorite, 3 - Apatite, 1 - Plagioclase, Trace - Quartz
CD2-19A	Bulk Crust (0-30mm)	99	1 - Quartz
CD2-21	Bulk Nodule (0-8mm)	100	Trace - Plagioclase, Quartz
CD2-23A	Bulk Crust (0-48mm)	100	Trace - Quartz
CD2-23B	Layer (0-16mm)	100	-
CD2-23C	Layer (16-48mm)	100	Trace - Quartz
CD2-28A	Layer (0-35mm)	100	Trace - Calcite
CD2-28B	Layer(35-50mm)	97	2 - Todorokite, 1 - Apatite
CD2-28C	Bulk Crust (0-45mm)	100	-
CD2-37A	Bulk Top Crust (0-35mm)	96	4 - Apatite, Trace - Quartz
CD2-37B	Bulk Underside Crust (0-10mm)	96	2 - Todorokite, 1 - Apatite, 1 - Plagioclase, Trace - Quartz
CD2-38A	Layer (0-10mm)	100	Trace - Quartz
CD2-38B	Layer (10-35mm)	99	1 - Quartz, Trace - Calcite?
CD2-38C	Layer (35-50mm)	99	1 - Quartz
CD2-38D	Layer (50-65mm)	91	8 - Apatite, 1 - Goethite

Table 6. continued

CD2-38E	Layer (65-90mm)	89	10 - Apatite, 1 - Goethite
CD2-38F	Layer (85-90mm)	69	13 - Apatite, 13 - Birnessite, 5 - Todorokite
BMDS3-A	Bulk Crust (0-11mm)	98	1 - Plagioclase, 1 - Quartz
JOD4-1A	Bulk Top Crust (0-20mm)	97	2 - Plagioclase, 1 - Quartz
JOD4-1B	Bulk Underside Crust (0-7mm)	98	1 - Calcite, 1 - Plagioclase
JOD4-2-IIA	Nodule Layer (0-20mm)	99	1 - Plagioclase, Quartz, Goethite
JOD4-2-IIB	Nodule Nucleus (0-27mm)	95	5 - Apatite
JOD4-3-IIA	Bulk Crust (0-13mm)	99	<1 - Plagioclase, Quartz
CD5-1-IIA	Layer (0-18mm)	99	<1 - Quartz
CD5-1-IIB	Layer (18-45mm)	99	1 - Apatite
CD5-2-IIA	Layer (0-7mm)	100	-
CD5-2-IIB	Layer (7-28mm)	97	3 - Apatite, <1 - Quartz
CD5-2-IIC	Layer (28-45mm)	85	15 - Apatite
CD5-3A	Layer (0-11mm)	98	1 - Plagioclase, 1 - Quartz
CD5-3B	Layer (11-21mm)	93	7 - Apatite
CD5-6A	Bulk Crust (0-15mm)	98	1 - Plagioclase, 1 - Quartz
CD5-11A	Layer (0-30mm)	100	Trace - Quartz
CD5-11B	Layer (30-48mm)	100	-
CD6-2B	Bulk Crust (0-35mm)	99	1 - Quartz
CD6-3A	Bulk Crust (0-40mm)	99	1 - Plagioclase, Quartz
CD6-3C	Layer (35-40mm)	81	6 - Todorokite, 5- Phillipsite, 3 - Kutnahorite, 3 - Quartz, 2 - Plagioclase
CD6-4A	Layer (0-5mm)	98	1 - Plagioclase, 1 - Quartz
CD6-4B	Layer (5-35mm)	97	2 - Plagioclase, 1 - Quartz
CD6-7A	Bulk Crust (0-30mm)	97	2 - Plagioclase, 1 - Quartz
CD6-8A	Bulk Top Crust (0-26mm)	99	1 - Quartz
CD6-8B	Bulk Underside Crust (0-4mm)	100	-
CD6-8D	Layer (21-26mm)	96	2 - Plagioclase, 1 - Apatite, 1 - Quartz
CD6-10A	Layer (0-3mm)	98	1 - Plagioclase, 1 - Quartz
CD6-10C	Layer (3-11mm)	98	1 - Plagioclase, 1 - Quartz
CD6-12A	Bulk Crust (0-10mm)	96	1 - Plagioclase, 2 - Quartz
CD6-12C	Layer (6-11mm)	98	1 - Plagioclase, 1 - Quartz
CD6-14A	Bulk Crust (0-30mm)	98	1 - Plagioclase, 1 - Quartz
CD6-15A	Bulk Crust (0-20mm)	100	Trace - Quartz
CD6-21-AI	Bulk Crust (0-20mm)	96	2 - Plagioclase, 2 - Quartz
CD6-22A	Bulk Top Crust (0-25mm)	99	1 - Plagioclase, Quartz
CD6-22B	Bulk Underside Crust (0-5mm)	99	1 - Todorokite?
CD6-22D	Layer (17-22mm)	99	1 - Plagioclase, Quartz
CD6-23A	Bulk Crust (0-15mm)	99	1 - Plagioclase, Quartz
CD6-24A	Bulk Crust (0-55mm)	98	1 - Plagioclase, 1 - Quartz
CD6-24D	Layer (50-55mm)	97	2 - Apatite, 1 - Plagioclase
CD6-25A	Bulk Crust (0-28mm)	99	1 - Plagioclase, Quartz
CD6-25C	Layer (23-28mm)	99	1 - Plagioclase, Quartz
CD7-3A	Bulk Crust (0-25mm)	100	-
CD7-3C	Layer (20-25mm)	97	2 - Plagioclase, 1- Quartz
CD7-9A	Bulk Crust (0-11mm)	96	2 - Plagioclase, 2 - Quartz
CD7-11A	Bulk Top Crust (0-7mm)	99	1 - Plagioclase, Quartz
CD7-11B	Bulk Underside Crust (0-7mm)	98	1 - Plagioclase, 1 - Quartz
CD7-13A	Bulk Crust (0-15mm)	98	1 - Plagioclase, 1 - Quartz
CD7-13C	Layer (10-15mm)	98	1 - Plagioclase, 1 - Quartz
CD7-14A	Bulk Crust (0-14mm)	99	1 - Quartz
CD7-14D	Layer (9-14mm)	99	1 - Quartz
CD7-15A	Bulk Crust (0-1mm)	99	1 - Apatite
CD8-B	Bulk Crust (0-32mm)	100	-
JTD9-1A	Bulk Crust (0-21mm)	100	-

Table 6. continued

JTD9-2A	Layer (0-7mm)	99	1 - Plagioclase, Quartz
JTD9-2B	Layer (7-35mm)	99	1 - Quartz
JTD9-3A	Bulk Crust (0-35mm)	99	1 - Plagioclase, Quartz
CD11-2A	Layer (0-5mm)	99	<1 - Quartz
CD11-2B	Layer (5-15mm)	93	6 - Plagioclase, 1 - Quartz
CD11-11A	Bulk Crust (0-3.5mm)	100	-
CD11-11B	Bulk Underside Crust (0-11mm)	99	<1 - Quartz
CD11-12A	Bulk Crust (0-10mm)	100	-
CD12-1A	Bulk Crust (0-14mm)	97	2 - Plagioclase, 1 - Quartz
CD12-1D	Layer (9-14mm)	94	3 - K-feldspar, 2 - Plagioclase, 1 - Quartz
CD12-2A	Bulk Crust (0-20mm)	100	-
CD13-3A	Bulk Crust (0-30mm)	100	-
CD13-6A	Bulk Crust (0-7mm)	99	1 - Quartz
CD13-8A	Layer (0-10mm)	100	-
CD13-8B	Layer (10-33mm)	100	-
CD13-8C	Layer (33-50mm)	93	7 - Apatite
CD13-9A	Bulk Nodule (0-26mm)	100	-
CD13-9B	Nodule Nucleus (26-51mm)	100	-
CD13-13A	Bulk Crust (0-12mm)	100	-
CD13-27-1	Bulk Nodule (0-13mm)	100	-
CD13-27-3	Bulk Nodule (0-25mm)	100	-
CD13-27-8A	Bulk Nodule (0-6mm)	99	1 - Quartz
CD14-1	Bulk Crust (0-35mm)	98	2 - Quartz
CD14-2A	Bulk Crust (0-15mm)	99	1 - Plagioclase, Quartz
CD14-3	Bulk Crust (0-25mm)	100	-
CD14-5A	Layer (0-8mm)	100	-
CD14-5B	Layer (8-23mm)	99	1 - Quartz
CD14-11A	Bulk Crust (0-6mm)	99	1 - Quartz
CD15-1A	Bulk Crust (0-19mm)	99	1 - Plagioclase, Quartz
CD15-1B	Layer (14-19mm)	96	4 - Apatite, Trace - Quartz?, Goethite?
CD15-2A	Layer (0-20mm)	100	-
CD15-2B	Layer (20-42mm)	92	8 - Apatite
CD16-1A	Bulk Crust (0-105mm)	97	3 - Apatite
CD16-1B	Layer (0-30mm)	100	-
CD16-1C	Layer (30-40mm)	99	<1 - Plagioclase, Quartz
CD16-1D	Layer (40-56mm)	99	<1 - Quartz
CD16-1E	Layer (56-69mm)	98	2 - Goethite, Trace - Plagioclase, Quartz
CD16-1F	Layer (69-102mm)	92	8 - Apatite
CD16-5A	Bulk Top Crust (0-39mm)	95	4 - Phillipsite, 1 - Quartz
CD16-5B	Bulk Underside Crust (0-71mm)	96	2 - Apatite, 1 - Goethite, 1 - Quartz
CD16-6A	Fe-Mn Vein Fill (0-4mm)	60	27 - Apatite, 13 - Todorokite
CD17-4A	Layer (0-12mm)	100	-
CD17-4B	Layer (12-45mm)	100	-
CD17-7A	Nodule Nucleus (30-60mm)	97	3 - Apatite
CD17-7B	Bulk Nodule (0-30mm)	99	<1 - Quartz
CD17-9	Bulk Crust (0-22mm)	100	-
CD18-3	Bulk Crust (0-42mm)	99	<1 - Quartz
CD19-1	Bulk Crust (0-14mm)	99	<1 - Quartz
CD19-4	Bulk Nodule (0-5mm)	99	1 - Quartz
CD21-6A	Bulk Crust (0-6mm)	99	1 - Plagioclase, Quartz
CD21-7B	Layer (0-28mm)	99	<1 - Quartz
CD21-7C	Layer (28-65mm)	100	-
CD21-7D	Layer (65-80mm)	91	9 - Apatite, Trace - Quartz
CD23-1A	Bulk Crust (0-50mm)	100	-
CD23-2	Bulk Crust (0-27mm)	94	3 - Plagioclase, 3 - Quartz
CD24-1A	Layer (0-22mm)	99	1 - Plagioclase, Quartz
CD24-1B	Layer (22-50mm)	89	11 - Apatite, Trace - Quartz
CD25-A1-A	Bulk Crust (0-8mm)	99	1 - Quartz

Table 6. continued

CD26-2A	Bulk Crust (0-4mm)	97	2 - Phillipsite, 1 - Plagioclase, Trace - Quartz
CD26-4A	Bulk Crust (0-27mm)	100	Trace - Quartz
CD26-4B	Crust Clast in Substrate (0-23mm)	90	8 - Apatite, 1 - Quartz, 1 - Plagioclase
CD26-4D	Layer (22-27mm)	99	1 - Plagioclase, Quartz
CD26-5A	Bulk Crust (0-37mm)	100	-
CD26-5B	Layer (32-37mm)	99	1 - Plagioclase, Quartz
CD26-7A	Bulk Crust (0-32mm)	100	-
CD26-7C	Stratabound Layer (0-5mm)	73	11 - Todorokite, 7 - Birnessite, 9 - Apatite, Trace - Quartz?
CD26-9-2A	Bulk Nodule (0-10mm)	99	1 - Quartz
CD26-9-2B	Nodule Layer (5-10mm)	98	2 - Plagioclase, Trace - Quartz
CD26-9-2C	Nodule Nucleus (10-30mm)	93	7 - Apatite
CD28-1B	Layer (0-20mm)	99	1 - Quartz
CD28-1C	Layer (20-34mm)	99	1 - Apatite
CD28-1D	Layer (34-65mm)	93	7 - Apatite
CD28-1E	Layer (60-65mm)	91	9 - Apatite
CD28-2A	Bulk Crust (0-50mm)	97	2 - Apatite, 1 - Plagioclase
CD28-2B	Layer (45-50mm)	94	6 - Apatite
CD29-2A	Bulk Crust (0-110mm)	93	6 - Apatite, 1 - Plagioclase, Quartz
CD29-2B	Layer (0-9mm)	96	2 - Quartz, 2 - Plagioclase
CD29-2C	Layer (9-49mm)	99	1 - Plagioclase, Quartz
CD29-2D	Layer (49-76mm)	89	10 - Apatite, 1 - Plagioclase, Quartz
CD29-2E	Layer (76-105mm)	93	7 - Apatite
CD29-7A	Layers (0-80mm)	94	5 - Apatite, 1 - Plagioclase, Quartz
CD29-7B	Layer (80-138mm)	85	15 - Apatite
CD29-11	Bulk Crust (0-35mm)	100	-
CD30-1	Bulk Crust (0-12mm)	98	1 - Plagioclase, 1 - Quartz
CD30-2	Bulk Crust (0-12mm)	97	2 - Plagioclase, 1 - Quartz
CD30-10A	Bulk Crust (0-75mm)	94	6 - Apatite, Trace - Quartz
CD30-10B	Layer (0-25mm)	100	Trace - Quartz
CD30-10C	Layer (25-39mm)	98	1 - Apatite, 1 - Plagioclase, Trace - Quartz
CD30-10D	Layer (39-70mm)	93	7 - Apatite

Percentages were determined by using the following weighting factors relative to quartz set at 1: δ-MnO_2 75; Todorokite 10; Birnessite 12 (Hein et al., 1988); Carbonate fluorapatite 3.1; Plagioclase 2.8; Calcite 1.65; Smectite 3.0; Goethite 7.0; Phillipsite 17.0; Illite 6.0 (From Cook et al., 1975). The limit of detection for each mineral falls between 0.2 and 1.0%, except the manganese minerals which are greater, perhaps as much as 10% for δ-MnO_2. Intervals measured from the outer surface of crusts and nodules.

Table 7. Chemical composition of ferromanganese crusts in weight percent for major elements and ppm for minor elements.*

	CD1-2A†	CD1-3A	CD1-4A	CD1-6A	CD1-7A-I	CD1-7A-II	CD1-10A1	CD1-10A2	CD1-10A3	CD1-11A	CD1-14A	CD1-15A	CD1-16A	CD1-17A	CD1-17B
Fe %	14.7	14.4	13.7	13.9	15.6	5	12.2	12.1	10.6	14.4	14.1	14.1	16.6	13.1	12.2
Mn	19.4	18.3	22.1	20.8	18.1	11.3	18.5	19.1	12.4	18.5	19.5	18.5	19.5	20.2	21.5
Mn/Fe	1.32	1.27	1.61	1.50	1.16	2.26	1.52	1.58	1.17	1.28	1.38	1.31	1.17	1.54	1.76
Si	3.74	4.25	2.85	2.95	3.83	1.63	2.99	3.22	2.76	4.30	3.32	3.97	3.69	2.24	2.52
Na	1.45	1.32	1.39	1.39	1.19	0.72	1.35	1.33	1.14	1.33	1.33	1.22	1.19	1.21	1.31
Mg	0.87	0.9	0.92	0.9	0.84	0.75	0.82	0.8	0.68	0.94	0.9	0.9	0.92	0.84	0.86
K	0.48	0.54	0.43	0.43	0.42	0.41	0.49	0.56	0.45	0.46	0.44	0.47	0.39	0.38	0.47
Ca	2.01	2.15	2.16	2.09	2.35	20.8	4.9	2.26	14.7	2.02	2.03	2.34	2.12	2.01	2.07
Ti	0.94	0.96	0.84	0.87	0.88	0.31	0.98	1.04	0.7	1	0.88	0.98	0.96	0.78	1.01
Al	0.71	0.94	0.45	0.52	0.63	0.61	0.70	0.75	0.76	0.87	0.64	0.89	0.59	0.28	0.44
P	0.36	0.38	0.37	0.38	0.56	8.2	1.43	0.37	5.4	0.37	0.38	0.4	0.44	0.36	0.3
H2O+	3.00	3.50	4.60	2.90	5.00	2.50	6.90	4.00	3.70	5.10	5.30	4.00	5.20	4.20	5.00
H2O-	21.3	19.3	18.9	21.6	18.8	3.5	20.2	23.4	8.7	19.2	19.7	20.3	16.8	24.6	21.4
CO2	0.49	0.64	0.47	0.44	0.54	3.3	0.77	0.58	1.4	0.47	0.48	0.67	0.51	0.46	0.43
LOI	-	-	-	-	-	-	-	-	-	-	-	-	-	-	-
Ba ppm	1200	1500	1200	1100	1600	28800	1500	1600	1600	1100	1100	1100	1300	990	1400
Co	7700	7500	8400	7700	5200	1800	5400	6000	1800	7300	7600	7500	5800	7800	7500
Cu	640	470	480	650	410	790	870	920	950	500	520	540	470	290	680
Mo	380	340	520	440	370	160	330	380	210	330	410	340	380	460	450
Ni	3600	3400	4600	4000	3100	3600	3600	4100	2500	3200	3600	3300	3300	4000	4700
Sr	1300	1300	1400	1300	1400	2700	1300	1300	1500	1200	1300	1200	1400	1300	1300
V	530	520	600	560	610	470	460	490	380	530	550	500	640	530	510
Y	180	160	170	175	200	460	230	145	520	150	160	150	200	170	130
Ce	840	880	740	740	910	660	1000	1000	1000	900	810	810	910	720	860
As	240	230	250	240	270	60	170	190	110	240	250	230	280	240	210
Cd	2.7	2.6	3.4	3.1	2.5	1.1	2.2	2.5	1.1	2.8	2.9	2.9	2.8	3.0	3.2
Cr	12	14	2.5	13	6	14	6.5	19	5.3	6.3	7	9.8	6.8	1.25	5.5
Pb	1400	1400	1500	1500	1600	970	1200	1200	790	1500	1500	1500	1800	1500	1400
Zn	490	480	520	500	550	720	550	560	460	500	490	500	560	470	560
Pd	-	-	-	-	-	-	0.0005	-	-	-	-	-	-	-	-
Pt	-	-	-	-	-	-	0.30	-	-	-	-	-	-	-	-
Rh	-	-	-	-	-	-	0.021	-	-	-	-	-	-	-	-
Interval	B 0-15	B 0-5	B 0-7	B 0-7	NL 0-10	NL 10-20	B 0-36	L 0-31	L 31-36	B 0-4	B 0-5	B 0-4	B 0-5	L 0-10	L 10-30
Type	Crust	Crust	Crust	Crust	Nodule	Nodule	Crust	Crust	Crust	Crust	Crust	Crust	Crust	Crust	Crust
Comments					Outer layer	Inner			Inner						
						layer			5 mm						

Table 7. continued

	CD1-17C	CD1-17D	CD1-17E	CD1-19A	CD1-20	CD1-21	CD2-3A	CD2-3B	CD2-3C	CD2-8A	CD2-8B	CD2-8C	CD2-8D	CD2-8E	CD2-8F
Fe %	2.85	11.6	11.8	14.4	13.5	13.7	14.5	13.4	14.3	14.7	13.3	12.4	15.2	12.7	13.4
Mn	10.8	22.8	20.7	20	18.4	18.4	19.6	19.6	20.1	20.1	20.7	22.4	19.1	21.3	19.6
Mn/Fe	3.79	1.97	1.75	1.39	1.36	1.34	1.35	1.46	1.41	1.37	1.56	1.81	1.26	1.68	1.46
Si	2.85	1.45	2.85	2.96	3.27	3.65	2.95	3.65	2.85	2.20	2.62	2.76	2.90	1.50	2.62
Na	1.10	1.08	1.32	1.22	1.07	1.32	1.37	1.40	1.36	1.28	1.42	1.42	1.29	1.20	1.27
Mg	1.03	0.90	0.92	0.84	0.78	0.85	0.83	0.9	0.87	0.82	0.85	0.92	0.80	0.75	0.82
K	0.81	0.35	0.46	0.41	0.39	0.44	0.42	0.54	0.41	0.33	0.44	0.53	0.44	0.35	0.41
Ca	20	2.24	3.5	2.02	1.98	2.28	2	2.04	2.01	2.01	2.08	2.21	2.10	2.29	2.54
Ti	0.25	1.01	0.97	0.87	0.83	0.88	0.93	1.11	0.96	0.82	1.05	0.94	0.95	1.08	0.85
Al	1.21	0.22	0.59	0.46	0.53	0.82	0.44	0.72	0.47	0.23	0.48	0.65	0.72	0.33	0.51
P	7.7	0.33	0.85	0.37	0.38	0.45	0.35	0.31	0.32	0.35	0.30	0.25	0.29	0.29	0.49
H2O+	4.20	8.80	7.60	5.00	3.50	7.90	3.90	6.20	8.40	8.50	8.20	8.20	8.60	8.20	7.40
H2O-	5.2	23.1	20.2	21.4	25.1	22.3	20.9	20	21.0	22.9	21.7	21.7	20.8	23.6	22.6
CO2	2.5	0.50	0.59	0.43	0.52	0.43	0.5	0.54	0.43	0.42	0.40	0.36	0.34	0.36	0.47
LOI	-	-	-	-	-	-	-	-	-	-	-	-	-	-	-
Ba ppm	28500	1300	3100	1200	1200	1100	1200	1500	1200	1100	1400	1800	2400	2700	2200
Co	1300	10800	6400	7100	6300	6200	7200	5900	6800	6100	5800	4700	2900	4200	4300
Cu	2600	340	850	350	380	380	540	990	610	410	870	1500	1500	1300	1200
Mo	140	430	410	470	400	340	400	340	380	490	380	490	400	570	450
Ni	7500	4600	4900	3500	3200	3400	3500	4300	3600	3200	3900	4900	3100	3500	3700
Sr	2200	1300	1300	1300	1200	1200	1300	1300	1300	1300	1300	1400	1500	1600	1400
V	160	490	470	610	520	520	540	470	520	600	480	520	600	620	560
Y	490	155	160	180	170	150	170	140	160	195	160	130	140	170	210
Ce	150	900	800	760	710	730	850	880	840	750	880	1000	1500	1700	1200
As	39	230	190	260	240	230	240	190	230	260	200	190	210	200	210
Cd	2.6	3.7	2.9	2.4	2.3	2.4	2.6	2.9	2.4	2.2	2.5	2.7	1.6	2.0	2.0
Cr	4	1.0	5.0	5	8.5	11	5.5	5.5	5.0	1.0	3.5	1.0	1.5	1.5	2.0
Pb	270	1600	1300	1500	1400	1500	1400	1100	1400	1500	1200	840	1000	1700	1200
Zn	730	550	620	490	450	510	490	560	530	500	560	680	690	630	600
Pd	-	0.0007	0.0012	-	-	< 0.0005	-	-	0.0007	0.0008	0.0018	0.0060	0.0007	< 0.0005	0.0015
Pt	-	0.17	0.25	-	-	0.081	-	-	0.015	0.086	0.15	0.29	0.46	0.35	0.27
Rh	-	0.016	0.017	-	-	0.0065	-	-	0.012	0.0090	0.014	0.019	0.022	0.017	0.012
Interval	L 30-40	B 0-10	B 0-45	B 0-8	B 0-25	N ~0-4	L 0-10	L 10-25	B 0-25	L 0-12.5	L 12.5-32.	L 32.5-52.	L 52.5-72.	L 72.5-92.	B 0-90
Type	Crust	Crust	Crust	Crust	Crust	Nodules	Crust	Crust	Crust	Crust	Crust	Crust	Crust	Crust	Crust
Comments		Underside				Bulk									

Table 7. continued

	CD2-10-A	CD2-10-B	CD2-10-C	CD2-10-D	CD2-12	CD2-15A	CD2-15B	CD2-15C	CD2-15D	CD2-15E	CD2-19A	CD2-21-I	CD2-23A	CD2-23B	CD2-23C
Fe %	11.2	10.2	9.8	10.8	12.3	12.9	11.6	11.8	10.5	12.2	13.8	13.9	11.7	12.4	11.2
Mn	20.2	12.6	16	17.8	19.1	19	21.5	22	17.8	20.2	19.1	21.1	20.4	20.8	22.2
Mn/Fe	1.80	1.24	1.63	1.65	1.55	1.47	1.85	1.86	1.70	1.66	1.38	1.52	1.74	1.68	1.98
Si	2.01	2.06	1.54	1.87	3.32	2.34	2.43	2.24	1.35	2.43	2.76	2.90	2.15	2.15	1.87
Na	1.28	1.04	1.09	1.18	1.41	1.27	1.45	1.45	1.14	1.36	1.30	1.39	1.35	1.38	1.39
Mg	0.82	0.59	0.61	0.73	0.88	0.78	0.92	0.88	0.65	0.85	0.83	0.91	0.84	0.87	0.85
K	0.43	0.34	0.36	0.39	0.53	0.38	0.49	0.51	0.35	0.46	0.42	0.46	0.42	0.41	0.44
Ca	2.1	12.5	10	5.4	2.55	1.93	2.26	2.37	8.9	2.76	1.94	2.11	2.02	2.00	2.21
Ti	0.86	0.58	0.77	0.74	0.97	0.79	1	0.85	0.86	0.92	0.84	0.96	0.90	0.91	0.80
Al	0.38	0.48	0.33	0.38	0.76	0.32	0.46	0.5	0.28	0.47	0.43	0.57	0.41	0.36	0.37
P	0.32	4.5	3.5	1.64	0.49	0.32	0.31	0.33	2.97	0.53	0.33	0.34	0.28	0.30	0.26
H2O+	4.20	4.40	5.10	5.10	6.80	5.70	7.00	7.20	6.50	7.20	7.10	7.10	8.10	8.40	8.40
H2O-	26.8	17.7	19.7	25.1	22.2	26.8	21.6	20.6	18	22.6	23.9	20.2	25.4	23.8	23.6
CO2	0.41	1.9	1.6	0.9	0.57	0.49	0.78	0.54	1.4	0.66	0.5	0.43	0.40	0.39	0.39
LOI	-	-	-	-	-	-	-	-	-	-	-	-	-	-	-
Ba ppm	1400	1600	2200	1600	1400	1100	1500	1800	2200	1400	1100	1200	1400	1200	1700
Co	5900	2000	3100	4200	6100	6400	6300	5000	3700	5900	6600	7100	6100	6900	5100
Cu	1100	1200	1200	1100	1100	460	1300	1800	1400	1000	490	770	1000	780	1500
Mo	440	260	430	400	340	440	440	500	470	430	390	400	420	430	530
Ni	4700	2200	2600	3800	4300	3500	5000	5000	2900	4200	3500	4200	4300	4300	4900
Sr	1300	1400	1500	1300	1200	1200	1300	1400	1500	1300	1200	1300	1200	1200	1300
V	480	410	520	470	450	520	470	500	500	490	520	520	470	490	510
Y	140	260	180	200	170	160	145	110	200	160	170	155	140	160	100
Ce	810	1000	1400	1000	810	700	830	990	1300	870	760	810	830	790	990
As	190	110	130	140	180	190	190	190	150	200	240	230	200	210	190
Cd	3.0	1.1	1.8	2.0	2.8	4.6	3.2	2.9	1.9	2.8	2.7	3.2	2.5	2.7	2.8
Cr	1.5	2.25	2.75	2.5	3	2.83	4	4	<1.0	3	4.5	4	2.5	3.5	1.0
Pb	1000	650	1400	1000	1200	1300	1100	800	1300	1200	1400	1400	1100	1300	770
Zn	570	460	560	570	550	470	580	640	550	560	490	560	550	550	620
Pd	-	-	-	-	-	-	-	-	-	-	-	-	0.0007	0.0017	0.0007
Pt	-	-	-	-	-	-	-	-	-	-	-	-	0.20	0.20	0.29
Rh	-	-	-	-	-	-	-	-	-	-	-	-	0.016	0.0075	0.018
Interval	L 0-35	L 35-54	L 54-87	B 0-83	B 0-20	L 0-13	L 13-27	L 27-40	L 40-65	B 0-68	B 0-30	N 0-8	B 0-48	L 0-16	L 16-48
Type	Crust	Crust	Crust	Crust	Crust	Crust	Crust	Crust	Crust	Crust	Crust	Nodule	Crust	Crust	Crust
Comments															

Table 7. continued

	CD2-28A	CD2-28B	CD2-28C	CD2-37A	CD2-37B	CD2-38A	CD2-38B	CD2-38C	CD2-38D	CD2-38E	CD2-38F	CD2-38H	BMDS3-A	JOD4-1A
Fe %	10.5	10.2	10.4	11.8	12	14.1	10.7	11.3	10.6	10.4	6.3	11.7	15.4	15.3
Mn	20.7	21.8	22.5	19.3	20.5	19.9	20.7	21.4	13.2	18.1	18	19	16.4	15.7
Mn/Fe	1.97	2.14	2.16	1.64	1.71	1.41	1.93	1.89	1.25	1.74	2.86	1.62	1.06	1.03
Si	1.59	1.14	1.22	2.66	3.13	2.24	2.71	2.06	2.43	1.15	1.64	2.06	3.97	5.14
Na	1.28	1.36	1.34	1.35	1.24	1.25	1.40	1.33	1.11	1.12	0.93	1.24	1.38	1.34
Mg	0.84	0.81	0.89	0.84	0.94	0.83	0.91	0.83	0.68	0.65	1.17	0.79	0.78	0.81
K	0.4	0.41	0.42	0.49	0.52	0.33	0.46	0.43	0.36	0.28	0.72	0.38	0.38	0.47
Ca	2.08	4.6	2.92	3.3	2.28	2.03	2.10	2.15	12.1	8.8	16	5.8	1.86	2.01
Ti	0.95	1	0.97	0.87	1.08	0.80	0.96	0.86	0.66	0.95	0.22	0.92	0.86	0.96
Al	0.23	0.22	0.22	0.64	0.7	0.27	0.53	0.44	0.67	0.21	0.53	0.46	0.58	0.93
P	0.24	1.16	0.51	0.71	0.33	0.36	0.28	0.26	4.3	2.91	5.8	1.73	0.33	0.38
H2O+	3.30	6.50	7.40	10.40	6.70	8.40	7.70	7.50	6.10	6.80	6.50	7.20	6.20	6.70
H2O-	28	22	23.9	21.9	21	23.8	24.8	25.5	15.9	18.9	5.1	20.3	23.9	21.1
CO2	0.73	0.71	0.5	0.7	0.14	0.41	0.49	0.37	1.8	1.3	0.15	0.93	0.43	0.55
LOI	-	-	-	-	-	-	-	-	-	-	-	-	-	-
Ba ppm	1400	2400	1900	1700	1700	1100	1300	1700	1700	2200	3600	1800	1200	1300
Co	8500	5400	7600	4700	6200	6500	6300	5200	2000	4000	1100	4900	4100	4300
Cu	650	1500	1200	1600	1700	390	1100	1500	1400	1300	1200	1200	460	610
Mo	370	550	460	370	360	450	400	470	230	440	270	400	320	260
Ni	4900	4900	5300	4200	5100	3400	5000	4600	2600	2800	6500	3600	2300	2400
Sr	1200	1500	1300	1300	1200	1300	1200	1300	1400	1600	1400	1400	1200	1200
V	400	490	430	460	460	550	420	480	390	540	370	500	510	480
Y	140	350	230	150	58	180	140	94	330	93	350	160	185	170
Ce	1100	1500	1200	910	970	750	760	920	980	1400	920	1100	830	870
As	180	160	170	170	170	240	170	180	115	140	68	150	230	220
Cd	3.3	3.5	3.5	3.3	2.8	2.4	3.0	2.7	1.4	1.8	4.1	2.3	1.8	1.8
Cr	1.75	<1.0	<1.0	5.5	4	2.0	4.0	1.5	4.0	1.5	17	3.5	3	5.5
Pb	1200	1500	1300	930	1100	1400	1000	820	680	1400	1000	1100	1200	1200
Zn	550	630	630	590	680	490	570	630	510	620	1000	610	480	510
Pd	-	-	-	-	-	0.0018	0.0043	0.0030	0.0017	0.0017	-	0.0017	-	-
Pt	-	-	-	-	-	0.077	0.19	0.36	0.30	0.19	-	0.21	-	-
Rh	-	-	-	-	-	0.0077	0.013	0.020	0.024	0.015	-	0.014	-	-
Interval	L 0-35	L 35-50	B 0-45	B 0-35	B 0-10	L 0-10	L 10-35	L 35-50	L 50-65	L 65-90	L 85-90	B 0-90	B 0-11	B 0-20
Type	Crust	Crust	Crust	Crust	Crust	Crust	Crust	Crust	Crust	Crust	Crust	Crust	Crust	Crust
Comments				Top	Underside						Inner			Top
											5 mm			

Table 7. continued

	JOD4-1B	JOD4-2-IIA	JOD4-2-IIB	JOD4-2-III	JOD4-3-IIA	CD5-I-IIA	CD5-I-IIB	CD5-I-IIC	CD5-2-IIA	CD5-2-IIB	CD5-2-IIC	CD5-2-IID	CD5-3A	CD5-3B
Fe %	13.8	14.3	13.5	12.4	13.5	11.9	10.6	11.3	12.7	15.4	8.8	12.0	14.1	11.6
Mn	19.2	17.5	18.2	15.7	18.3	20.9	19.3	20.4	20.4	20.7	20.4	20.4	19.9	20.7
Mn/Fe	1.39	1.22	1.35	1.27	1.36	1.76	1.82	1.81	1.61	1.34	2.32	1.70	1.41	1.78
Si	3.09	4.77	2.01	4.25	3.74	1.73	1.08	1.54	1.82	2.06	1.03	1.40	2.90	1.32
Na	1.29	1.46	1.16	1.31	1.31	1.28	1.15	1.28	1.13	1.24	1.18	1.17	1.28	1.22
Mg	0.89	0.78	0.68	0.72	0.83	0.80	0.69	0.77	0.73	0.74	0.74	0.72	0.84	0.72
K	0.41	0.77	0.37	0.67	0.47	0.36	0.31	0.36	0.34	0.42	0.39	0.35	0.37	0.33
Ca	2.26	2.22	7.0	3.5	1.93	2.06	6.5	4.1	2.43	2.99	7.1	3.8	2.01	5.2
Ti	0.93	0.85	1.01	0.87	1.06	0.84	0.67	0.77	1.16	1.07	0.40	0.81	0.83	0.91
Al	0.61	1.31	0.47	1.16	0.88	0.29	0.23	0.28	0.40	0.51	0.28	0.30	0.48	0.27
P	0.32	0.30	2.17	0.87	0.27	0.27	1.95	1.04	0.37	0.59	2.13	0.89	0.34	1.33
H2O+	7.20	8.40	8.60	9.80	5.40	7.30	5.90	7.50	8.70	9.80	6.50	8.50	5.50	9.00
H2O-	21.5	18.6	16.1	24.1	23.1	26.5	22.3	22.6	25.3	16.5	23.5	24.2	21.2	20.7
CO2	0.82	0.68	1.1	0.61	0.39	0.37	1.0	0.66	0.43	0.56	1.1	0.62	0.45	0.83
LOI	-	-	-	-	-	-	-	-	-	-	-	-	-	-
Ba ppm	1300	2000	2500	2000	1500	1700	2300	1800	2700	3200	2500	2700	1200	2300
Co	6300	3300	3100	3200	4900	5600	3600	5200	4000	3200	3100	3500	6500	4600
Cu	920	2800	1900	1800	1500	670	550	650	1100	1100	920	890	430	730
Mo	340	270	470	270	280	490	620	530	480	720	730	660	420	560
Ni	3500	3200	2600	2900	3500	3800	3100	3700	3100	2600	4200	3400	3400	3300
Sr	1200	1300	1700	1200	1200	1300	1500	1400	1500	1700	1400	1500	1300	1500
V	490	510	630	450	460	550	650	570	610	850	620	700	570	610
Y	160	87	140	130	110	120	170	150	80	100	270	140	150	130
Ce	780	1100	1600	1100	910	1100	1700	1300	1800	2200	2000	1900	820	1600
As	220	170	160	150	160	200	180	200	180	250	150	190	250	170
Cd	2.5	1.9	1.6	1.9	2.3	2.7	2.5	2.7	2.2	2.0	3.3	2.7	2.8	2.5
Cr	1.75	5.5	< 1.0	1.5	6.3	2.0	3.5	1.5	< 1.0	2.0	3.3	< 1.0	3.0	< 1.0
Pb	1300	890	1500	990	1100	1400	2000	1600	1500	2300	2300	2100	1500	1600
Zn	530	590	600	530	570	570	630	590	630	700	750	690	520	590
Pd	-	-	-	-	0.0017	0.0008	0.0013	0.0005	-	-	-	-	-	-
Pt	-	-	-	-	0.10	0.47	0.13	0.10	-	-	-	-	-	-
Rh	-	-	-	-	0.011	0.015	0.010	0.0084	-	-	-	-	-	-
Interval	B 0-7	LN 0-20	LN 0-27	BN 0-78	B 0-13	L 0-18	L18-45	B 0-50	L 0-7	L 7-28	L 28-45	B 0-45	L 0-11	L 11-21
Type	Crust	Nodule	Nodule	Nodule	Crust	Crust	Crust	Crust	Crust	Crust	Crust	Crust	Crust	Crust
Comments	Underside	Outer layer	Nucleus	Bulk										

Table 7. continued

	CD5-3C	CD5-6A	CD5-11A	CD5-11B	CD5-11C	CD6-3A	CD6-3C	CD6-4A	CD6-4B	CD6-4D	CD6-7A	CD6-7D	CD6-8A	CD6-8B	CD6-8D
Fe %	13.5	13.4	12.3	11.9	12.1	12.6	13.5	16.8	13.6	13.3	14.5	14.0	15.1	11.9	13.8
Mn	20.6	20.3	18.3	20.4	19.2	17.3	20.9	16.3	18.1	19.4	16.6	18.2	17.2	22.3	18.7
Mn/Fe	1.53	1.51	1.49	1.71	1.59	1.37	1.55	0.97	1.33	1.46	1.14	1.30	1.14	1.87	1.36
Si	2.15	2.52	2.20	1.31	1.78	3.60	3.74	4.44	4.68	4.25	4.53	5.47	5.84	2.52	4.77
Na	1.28	1.34	1.20	1.15	1.25	1.31	1.40	1.22	1.42	1.36	1.30	1.41	1.46	1.38	1.48
Mg	0.80	0.89	0.75	0.72	0.74	0.78	0.94	0.81	0.90	0.96	0.77	0.91	0.80	0.98	0.87
K	0.36	0.36	0.34	0.31	0.33	0.45	0.59	0.38	0.58	0.58	0.42	0.61	0.50	0.46	0.60
Ca	3.4	2.16	1.92	2.54	3.2	1.81	2.18	1.87	1.99	2.22	1.93	2.14	2.44	2.16	2.42
Ti	0.92	0.85	0.76	1.02	0.85	0.95	1.17	0.98	1.05	1.25	0.95	1.16	1.07	1.27	1.18
Al	0.42	0.48	0.36	0.28	0.34	0.72	0.88	0.73	1.15	1.11	0.89	1.27	1.21	0.58	1.08
P	0.79	0.35	0.33	0.41	0.73	0.29	0.30	0.35	0.31	0.32	0.33	0.33	0.45	0.26	0.44
H2O+	9.70	10.00	8.10	8.50	2.40	6.10	6.80	8.40	8.20	6.90	9.00	7.00	7.20	8.30	7.40
H2O-	18.0	20.4	28.4	26.7	25.1	26.8	18.0	20.5	19.7	18.4	22.5	18.0	15.9	20.7	18.7
CO2	0.66	0.44	0.42	0.36	0.56	0.34	0.33	0.37	0.41	0.37	0.38	0.32	0.51	0.43	0.43
LOI	-	-	-	-	-	-	31.6	-	-	32.3		31.0	-	-	31.6
Ba ppm	1900	1700	1300	2500	1800	1200	1800	1100	1400	1600	1300	1700	1300	1300	1700
Co	5500	6400	5800	5300	5000	5600	6200	5000	5800	6100	4400	4800	4800	10400	5000
Cu	650	820	550	1100	820	850	1500	390	860	1100	640	1300	620	400	800
Mo	490	450	410	560	490	300	340	280	310	290	310	270	300	320	320
Ni	3400	3800	3400	3400	3300	3300	4200	2300	3800	4200	2600	3600	2700	5200	3500
Sr	1500	1400	1200	1500	1400	1100	1300	1200	1100	1200	1200	1200	1200	1100	1300
V	620	590	510	620	570	430	460	520	440	390	490	410	510	400	460
Y	140	150	150	110	170	170	170	180	190	170	170	160	170	150	200
Ce	1300	1000	830	1800	1300	810	1100	960	840	1000	790	980	810	1200	870
As	220	220	200	200	200	180	200	240	170	170	200	170	200	170	190
Cd	2.5	2.8	2.5	2.2	2.3	2.2	2.9	1.9	2.4	3.0	1.6	2.1	2.0	3.8	2.4
Cr	2.0	3.0	2.5	1.0	4.8	7.5	7.0	9.0	12	10	6.0	14	10	5.5	16
Pb	1600	1700	1300	1600	1500	1200	1100	1500	1100	1200	1200	970	1300	1500	1200
Zn	590	570	500	610	530	470	640	500	510	640	490	580	500	650	570
Pd	-	-	-	-	-	0.0005	-	-	-	-	< 0.0005	-	-	-	-
Pt	-	-	-	-	-	0.12	-	-	-	-	0.10	-	-	-	-
Rh	-	-	-	-	-	0.091	-	-	-	-	0.0060	-	-	-	-
Interval	B 0-21	B 0-15	L 0-30	L 30-48	B 0-48	B 0-40	L 35-40	L 0-5	L 5-35	L 30-35	B 0-30	L 25-30	B 0-26	B 0-4	L 21-26
Type	Crust	Crust	Crust	Crust	Crust	Crust	Crust	Crust	Crust	Crust	Crust	Crust	Crust	Crust	Crust
Comments							Inner			Inner		Inner 5 mm	Top	Underside	Inner
							5 mm			5 mm					5 mm

Table 7. continued

	CD6-10A	CD6-10C	CD6-12A	CD6-12C	CD6-15A	CD6-21A	CD6-21B	CD6-22A	CD6-22B	CD6-22D	CD6-23A	CD6-23B	CD6-24A	CD6-24D	CD6-25A
Fe %	17.2	14.6	15.2	15.7	14.7	14.4	14.1	15.6	10.6	13.5	14.6	14.2	14.0	11.9	14.8
Mn	15.9	16.7	16.2	16.7	17	17.3	17.6	18.5	23.2	21.0	16.5	18.4	17.2	20.9	19.7
Mn/Fe	0.92	1.14	1.07	1.06	1.16	1.20	1.25	1.19	2.19	1.56	1.13	1.30	1.23	1.76	1.33
Si	4.25	5.10	4.86	5.98	5.14	4.44	4.02	4.25	1.92	3.18	4.16	4.86	4.91	2.95	2.95
Na	1.25	1.33	1.25	1.38	1.33	1.29	1.29	1.35	1.39	1.32	1.23	1.41	1.39	1.34	1.36
Mg	0.81	0.81	0.75	0.85	0.84	0.77	0.77	0.81	1.07	0.85	0.76	0.87	0.82	0.97	0.83
K	0.39	0.49	0.45	0.60	0.48	0.43	0.45	0.42	0.46	0.47	0.38	0.57	0.54	0.57	0.37
Ca	1.80	1.97	1.93	2.04	2.05	1.87	1.92	2.01	2.17	2.09	1.79	1.95	1.91	3.9	1.98
Ti	0.91	1.02	1.04	1.21	1.04	0.96	1.01	1.12	1.21	1.16	0.93	1.08	1.04	0.90	0.92
Al	0.69	1.16	1.00	1.43	1.20	0.81	0.82	0.81	0.58	0.59	0.69	0.98	1.06	0.76	0.43
P	0.37	0.31	0.31	0.30	0.32	0.30	0.29	0.32	0.25	0.28	0.32	0.30	0.31	0.98	0.32
H2O+	8.00	6.90	6.70	6.60	8.40	7.60	7.50	8.00	8.20	7.20	6.40	5.50	7.30	6.80	8.20
H2O-	20.4	19.8	20.5	18.3	19.6	22.1	23.0	18.4	21.1	21.0	24.9	20.6	20.8	18.0	20.7
CO2	0.40	0.42	0.43	0.35	0.48	0.39	0.40	0.43	0.53	0.37	0.37	0.33	0.36	0.61	0.44
LOI	-	-	-	30.4	-	-	-	-	-	34.8	-	32.8	-	31.4	-
Ba ppm	1200	1500	1500	1700	1500	1300	1300	1400	1300	1600	1200	1400	1300	2000	1200
Co	3900	4000	3600	3700	4000	5300	5700	4900	10200	5200	5500	5900	5900	4700	6100
Cu	560	1300	900	1200	1200	680	610	790	770	1100	480	730	1100	1700	540
Mo	260	270	260	240	270	310	290	320	350	370	300	310	290	430	390
Ni	2000	2900	2300	2500	2900	3000	3000	3000	6100	3800	2700	3600	3200	4800	3300
Sr	1200	1200	1200	1300	1200	1200	1100	1300	1100	1400	1200	1200	1200	1400	1300
V	550	470	480	410	470	490	450	570	380	510	490	440	450	470	560
Y	180	170	180	180	180	170	170	160	130	150	170	170	170	260	180
Ce	1000	820	900	960	800	820	860	830	1000	1000	800	790	910	1000	790
As	250	180	200	180	190	200	200	230	170	200	220	190	200	170	240
Cd	1.7	2.1	2.0	2.5	2.2	2.0	2.3	2.1	3.8	2.5	1.9	2.7	2.0	2.8	2.1
Cr	5.5	11	8.0	13	6.5	7.0	7.0	10	5.0	3.5	6.5	10	18	13	4.5
Pb	1400	1100	1100	1100	1100	1200	1200	1300	1300	1200	1400	1200	1200	1000	1400
Zn	500	520	540	580	540	490	480	550	670	610	480	560	490	690	500
Pd	0.0007	-	-	-	-	-	-	-	-	-	0.0005	-	-	-	-
Pt	0.053	-	-	-	-	-	-	-	-	-	0.081	-	-	-	-
Rh	0.0054	-	-	-	-	-	-	-	-	-	0.0063	-	-	-	-
Interval	L 0-3	L 3-11	B 0-10	L 6-11	B 0-20	B 0-20	B 0-20	B 0-25	B 0-5	L 17-22	B 0-15	L 10-15	B 0-55	L 50-55	B 0-28
Type	Crust	Crust	Crust	Crust	Crust	Crust	Crust	Crust	Crust	Crust	Crust	Crust	Crust	Crust	Crust
Comments				Inner		Breccia	Basalt	Top	Underside	Inner		Inner		Inner	
				5 mm		substrate	substrate			5 mm		5 mm		5 mm	

Table 7. continued

	CD6-25C	CD7-3A	CD7-3C	CD7-9A	CD7-11A	CD7-11B	CD7-13A	CD7-13C	CD7-14A	CD7-14D	CD8-B	JTD9-1A	JTD9-2A	JTD9-2B	JTD9-2C
Fe %	13.1	14.5	14.0	15.3	15.5	16.3	13.8	14.0	14.7	13.3	13.5	12.8	18.1	15.2	16.1
Mn	20.9	18.2	18.7	15.7	17.8	16.1	17.3	20.0	18.4	21.0	20.6	20.3	15.1	17.8	17.3
Mn/Fe	1.60	1.26	1.34	1.03	1.15	0.99	1.25	1.43	1.25	1.58	1.53	1.59	0.8	1.2	1.1
Si	3.46	4.02	4.96	6.45	3.79	5.19	3.65	3.60	3.97	3.41	2.38	2.57	4.91	4.07	4.49
Na	1.54	1.33	1.35	1.38	1.34	1.24	1.38	1.50	1.35	1.37	1.42	1.23	1.19	1.27	1.28
Mg	0.92	0.82	0.89	0.91	0.83	0.98	0.78	0.90	0.82	0.93	0.85	0.85	0.80	0.82	0.83
K	0.53	0.45	0.59	0.79	0.40	0.49	0.41	0.50	0.40	0.50	0.37	0.37	0.38	0.46	0.45
Ca	2.07	2.02	2.10	1.89	1.90	1.99	1.89	1.97	1.93	2.02	2.03	2.01	1.93	2.08	2.05
Ti	1.06	1.04	1.16	0.98	1.02	1.23	0.91	0.97	0.93	0.99	0.86	0.98	1.00	1.08	1.07
Al	0.71	0.77	1.14	1.53	0.71	1.29	0.65	0.62	0.63	0.60	0.35	0.43	0.88	0.88	0.91
P	0.28	0.32	0.28	0.34	0.31	0.33	0.34	0.30	0.33	0.30	0.36	0.29	0.33	0.32	0.32
H2O+	7.00	8.20	7.20	6.20	10.40	8.90	8.50	7.20	7.10	6.60	8.00	6.90	6.70	6.30	6.90
H2O-	20.4	20.5	19.4	16.7	18.4	15.0	22.7	20.8	19.6	20.9	22.3	23.6	15.4	17.5	17.4
CO2	0.33	0.40	0.32	0.40	0.44	0.55	0.39	0.36	0.42	0.37	0.42	0.44	0.55	0.43	0.41
LOI	34.2	-	32.7	-	-	-	-	34.3	-	34.4	-	-	28.4	31	30.5
Ba ppm	1400	1400	1600	1600	1400	1600	1100	1300	1100	1300	1200	1200	1200	1500	1500
Co	6500	4600	4800	4100	5100	5600	6300	6800	6700	7700	7000	7400	3200	4100	3800
Cu	910	1100	1600	1200	1200	1300	460	640	500	880	340	900	570	1200	1000
Mo	400	340	300	220	310	200	320	400	350	430	470	390	250	320	300
Ni	4500	2900	3600	2500	2800	3100	3100	3800	3200	4500	3700	4000	1500	2600	2300
Sr	1300	1200	1200	1100	1300	1200	1200	1300	1300	1300	1300	1200	1100	1200	1200
V	480	490	410	460	540	470	480	490	510	500	560	470	490	470	480
Y	160	190	170	150	180	160	160	160	170	150	170	180	170	190	190
Ce	800	870	980	880	880	1100	800	760	860	780	830	860	930	900	900
As	180	200	180	200	210	190	210	220	230	210	250	190	220	190	200
Cd	3.4	2.0	2.6	1.9	1.9	2.3	2.1	2.6	2.3	3.0	2.4	2.7	1.8	2.0	1.8
Cr	6.0	6.8	13	12	7.0	12	8.0	8.0	6.5	8.0	2.5	2.8	8.5	9.5	7.5
Pb	1300	1100	970	1200	1300	1400	1300	1400	1400	1400	1600	1300	1300	1000	1100
Zn	590	510	570	530	530	600	450	560	480	580	500	490	520	540	530
Pd	-	0.0018	-	0.0027	-	-	-	-	-	-	0.0005	-	0.0027	0.0047	0.0050
Pt	-	0.18	-	0.14	-	-	-	-	-	-	0.13	-	0.077	0.18	0.11
Rh	-	0.0099	-	0.011	-	-	-	-	-	-	0.013	-	0.0081	0.011	0.0089
Interval	L 23-28	B 0-25	L 20-25	B 0-11	B 0-7	B 0-7	B 0-15	L 10-15	B 0-14	L 9-14	B 0-32	B 0-21	L 0-7	L 7-35	B 0-35
Type	Crust	Crust	Crust	Crust	Crust	Crust	Crust	Crust	Crust	Crust	Crust	Crust	Crust	Crust	Crust
Comments	Inner		Inner		Top	Underside		Inner		Inner					
	5 mm		5 mm					5 mm		5 mm					

Table 7. continued

	JTD9-3A	CD11-2A	CD11-2B	CD11-2C	CD11-11A	CD11-11B	CD11-12A	CD12-1A	CD12-1D	CD12-2A	CD13-3A	CD13-6A	CD13-8A	CD13-8B	CD13-8C
Fe %	14.6	17.5	15.5	17.6	14.5	16.2	16.5	15.8	15.6	14.2	11.9	14.3	14.4	14.4	11.3
Mn	16.6	17	17.9	17.5	20.1	18.5	17.1	15.2	15.9	20.6	22.4	19.6	20.2	19.3	20.0
Mn/Fe	1.14	0.97	1.15	0.99	1.39	1.14	1.04	0.96	1.02	1.45	1.88	1.37	1.4	1.3	1.8
Si	4.53	3.74	4.11	4.11	2.48	3.04	3.83	6.26	6.36	2.66	2.15	3.83	2.43	2.85	1.22
Na	1.25	1.25	1.34	1.29	1.26	1.25	1.26	1.48	1.46	1.39	1.38	1.37	1.26	1.25	1.19
Mg	0.77	0.81	0.81	0.83	0.86	0.81	0.80	0.87	0.83	0.90	0.96	0.93	0.87	0.89	0.73
K	0.47	0.33	0.41	0.37	0.36	0.32	0.37	0.66	0.69	0.42	0.47	0.48	0.35	0.44	0.31
Ca	1.86	1.81	1.89	1.96	2.10	1.94	1.88	2.06	1.79	2.06	2.18	2.02	2.00	2.16	6.5
Ti	1.02	0.95	1.04	0.99	1.00	0.94	1.00	1.11	1.03	0.98	0.98	0.97	0.89	0.83	0.91
Al	0.94	0.51	0.69	0.64	0.38	0.39	0.61	1.43	1.34	0.42	0.39	0.72	0.33	0.71	0.25
P	0.30	0.37	0.31	0.36	0.35	0.34	0.34	0.32	0.31	0.31	0.25	0.33	0.31	0.30	1.82
H2O+	9.00	8.40	8.60	8.00	8.00	8.70	8.80	6.50	6.90	6.70	6.20	7.00	6.40	6.60	5.00
H2O-	21.5	20.0	19.5	16.6	20.6	21.1	20.0	18.7	18.4	21.6	21.3	20.4	16.6	20.1	12.6
CO2	0.38	0.44	0.40	0.42	0.51	0.44	0.39	0.55	0.33	0.38	0.49	0.36	0.47	0.44	1.1
LOI	-	-	-	-	-	-	-	30.8	31.2	34.7	35.0	33.4	31.4	33.6	24.8
Ba ppm	1300	1100	1300	1300	1000	1100	1200	1300	1300	1100	1700	1300	1100	1800	2300
Co	4600	4300	5400	4200	6900	5200	5100	5600	5400	7300	7100	5200	7000	4200	4000
Cu	850	480	830	660	480	440	540	670	860	540	1100	920	560	1100	1000
Mo	270	290	350	330	350	360	300	230	260	410	500	360	410	370	550
Ni	2800	2100	2700	2200	3100	2600	2400	2400	2700	3600	4800	3900	3500	3700	3200
Sr	1200	1300	1300	1300	1300	1300	1300	1100	1100	1300	1300	1300	1300	1300	1600
V	450	530	500	560	520	540	510	420	420	470	500	500	510	510	580
Y	180	190	190	200	190	200	200	160	170	180	140	150	170	150	190
Ce	950	1100	940	1000	1000	940	1000	870	780	820	1100	780	770	1200	1600
As	190	240	210	240	240	240	240	200	190	230	200	230	220	180	150
Cd	1.9	2.0	1.9	1.8	2.5	2.1	2.1	2.1	2.1	2.5	3.3	2.8	2.5	2.4	2.3
Cr	9.5	2.8	4.0	3.0	2.5	1.5	4.5	17	20	5.5	6.5	8.0	4.5	6.5	1.3
Pb	1100	1500	1300	1400	1500	1400	1400	1300	1200	1500	1500	1400	1400	1000	1500
Zn	490	480	500	500	490	480	480	490	510	530	630	630	510	600	600
Pd	-	-	-	-	-	-	-	-	-	-	-	-	0.0050	0.062	0.0040
Pt	-	-	-	-	-	-	-	-	-	-	-	-	0.15	0.51	0.33
Rh	-	-	-	-	-	-	-	-	-	-	-	-	0.0084	0.019	0.013
Interval	B 0-40	L 0-5	L 5-15	B 0-15	B 0-3.5	B 0-11	B 0-10	B 0-14	L 9-14	B 0-20	B 0-30	B 0-7	L 0-10	L 10-33	L 33-50
Type	Crust	Crust	Crust	Crust	Crust	Crust	Crust	Crust	Crust	Crust	Crust	Crust	Crust	Crust	Crust
Comments					side	top			Inner						
									5 mm						

Table 7. continued

	CD13-8D	CD13-8E	CD13-9A	CD13-9B	CD13-13A	CD13-13B	CD13-27-1	CD13-27-3	CD13-27-8A	CD14-1	CD14-3	CD14-5A	CD14-5B	CD14-5C
Fe %	13.8	11.7	12.9	14.8	13.7	13.7	14.3	13.4	12.9	11.9	11.4	14.4	12.3	13.6
Mn	20.1	18.1	18.6	18.3	20.3	21.9	20.3	21.5	21.9	20.1	23.2	19.5	18.8	19.2
Mn/Fe	1.5	1.5	1.44	1.24	1.5	1.60	1.42	1.60	1.70	1.7	2.04	1.4	1.5	1.4
Si	2.20	1.31	2.76	2.52	2.62	2.38	3.18	3.18	2.52	2.20	1.73	3.18	4.53	3.74
Na	1.28	1.08	1.28	1.17	1.29	1.34	1.35	1.42	1.41	1.37	1.60	1.45	1.53	1.49
Mg	0.85	0.66	0.88	0.76	0.87	0.94	0.97	0.98	0.97	0.85	1.01	0.92	1.10	0.98
K	0.38	0.27	0.44	0.46	0.38	0.43	0.47	0.46	0.43	0.40	0.46	0.42	0.74	0.54
Ca	3.3	7.9	2.01	2.05	2.03	2.10	2.56	2.27	2.06	1.97	2.17	1.95	2.24	2.10
Ti	0.91	0.77	0.88	1.13	0.91	1.08	1.03	0.99	0.87	0.95	1.12	0.94	1.17	1.06
Al	0.49	0.28	0.69	0.62	0.41	0.36	0.69	0.69	0.47	0.40	0.25	0.55	1.29	0.86
P	0.70	2.38	0.31	0.31	0.31	0.30	0.52	0.37	0.31	0.26	0.27	0.31	0.30	0.30
H2O+	7.90	3.90	6.80	7.90	6.90	7.90	7.50	8.20	7.40	5.20	7.40	6.50	6.90	7.40
H2O-	15.6	11.8	24.4	22.2	18.3	21.4	19.6	19.4	22.0	26.3	20.8	18.2	13.9	15.5
CO2	0.63	1.4	0.36	0.32	0.5	0.37	0.42	0.34	0.33	0.4	0.40	0.5	0.76	0.59
LOI	30.4	22.4	37.5	35.2	32.4	35.5	33.4	33.8	35.9	38.5	35.6	32.4	27.5	29.6
Ba ppm	2000	2000	1700	2700	1300	1400	1800	1400	1200	1300	1300	1200	1500	1300
Co	4500	3200	4100	3200	5800	5700	5600	6300	6800	6400	10300	3600	6600	6800
Cu	990	780	1400	1200	650	840	1100	950	760	940	630	690	950	830
Mo	460	520	340	510	440	450	450	420	450	390	400	360	280	330
Ni	3300	2400	4100	2800	3800	4100	4300	4500	4600	4100	5000	3600	4300	3900
Sr	1400	1600	1300	1600	1300	1400	1400	1300	1300	1200	1300	1200	1100	1200
V	560	570	450	650	560	530	600	510	530	440	450	500	400	450
Y	170	150	150	140	170	160	160	170	150	140	150	160	170	170
Ce	1300	1500	960	1800	750	810	1000	820	670	900	1100	790	940	890
As	190	150	180	210	220	240	220	220	230	180	200	220	150	180
Cd	2.4	1.9	2.5	2.1	2.7	2.6	2.6	3.1	3.3	3.0	3.8	2.2	2.8	2.6
Cr	4.0	3.5	3.5	4.0	5.5	4.5	11	7.0	6.0	2.5	6.5	7.5	17	12
Pb	1300	1700	1000	1900	1400	1300	1600	1500	1500	1100	1500	1400	1100	1200
Zn	600	530	660	750	550	590	700	660	620	540	640	530	560	550
Pd	0.0028	0.0043	-	-	0.0038	-	-	-	-	0.0025	-	0.0090	0.0025	0.0082
Pt	0.35	0.31	-	-	0.12	-	-	-	-	0.23	-	0.22	0.28	0.27
Rh	0.012	0.014	-	-	0.012	-	-	-	-	0.016	-	0.010	0.011	0.013
Interval	B 0-50	L 45-50	N 0-26	N 26-51	B 0-12	L 9-13	N 0-13	N 0-25	N 0-6	B 0-35	B 0-25	L 0-8	L 8-23	B 0-22
Type	Crust	Crust	Nodule	Nodule	Crust	Crust	Nodule	Nodule	Nodule	Crust	Crust	Crust	Crust	Crust
Comments		Inner 5 mm	Outer	nucleus		Inner	Bulk	Bulk	Bulk					
			layer			5 mm								

Table 7. continued

	CD15-1A	CD15-1B	CD15-2A	CD15-2B	CD15-2C	CD16-1A	CD16-1B	CD16-1C	CD16-1D	CD16-1E	CD16-1F	CD16-5A	CD16-5B	CD16-6A
Fe %	12.9	14.2	12.4	6.2	8.0	11.6	12.3	11.1	11.9	15.2	10.8	12.4	13.8	6.6
Mn	22.3	23.1	22.6	23.8	23.0	19.0	20.2	21.3	21.2	16.8	17.0	18.1	17.6	14.7
Mn/Fe	1.73	1.63	1.82	3.84	2.88	1.64	1.64	1.92	1.78	1.11	1.57	1.46	1.28	2.23
Si	2.06	1.64	1.64	0.52	0.76	2.06	2.10	3.04	2.01	2.81	1.35	3.74	2.52	2.52
Na	1.33	1.28	1.37	1.35	1.39	1.30	1.40	1.45	1.38	1.22	1.15	1.39	1.18	1.10
Mg	0.87	0.83	0.85	0.97	0.93	0.79	0.86	0.95	0.84	0.80	0.65	0.87	0.76	1.30
K	0.43	0.41	0.44	0.55	0.52	0.40	0.41	0.56	0.49	0.46	0.33	0.62	0.42	0.59
Ca	2.23	2.37	2.77	10.3	8.8	4.4	1.90	2.03	2.08	2.46	9.5	2.04	2.58	15.0
Ti	0.87	0.90	0.89	0.29	0.38	0.89	0.92	1.09	0.83	0.91	0.88	0.93	0.97	0.54
Al	0.36	0.30	0.29	0.13	0.16	0.36	0.29	0.62	0.41	0.73	0.25	0.86	0.56	1.25
P	0.27	0.25	0.44	3.3	2.80	1.17	0.28	0.24	0.24	0.52	3.1	0.34	0.52	5.6
H2O+	8.20	8.20	7.30	6.30	6.90	7.10	6.60	7.10	7.50	6.80	6.20	6.10	6.20	5.00
H2O-	21.4	20.2	20.4	13.8	13.9	23.4	24.4	22.6	24.0	23.4	17.1	23.3	24.4	6.8
CO2	0.36	0.34	0.40	1.5	1.2	0.64	0.39	0.31	0.35	0.42	1.5	0.47	0.41	2.3
LOI	35.3	35.0	34.4	27.3	28.8	36.5	37.7	36.0	37.1	36.3	29.5	36.2	37.1	18.0
Ba ppm	1900	2600	2200	2700	2800	1700	1200	1500	1700	2400	2200	1400	2800	3100
Co	5600	3900	5500	4000	3600	5000	6900	6500	4400	2600	3400	5100	3100	1400
Cu	960	1100	990	500	400	1100	600	1200	1500	1700	1100	1100	1400	880
Mo	610	790	690	780	730	420	420	370	500	360	460	340	460	220
Ni	3800	3200	3700	6000	5000	3500	3900	4600	4100	2600	2500	3600	2600	7700
Sr	1500	1800	1600	1500	1600	1400	1200	1200	1400	1400	1600	1200	1500	1400
V	630	760	700	610	660	480	470	430	520	560	500	440	600	410
Y	110	94	88	240	210	180	150	130	110	230	220	160	140	520
Ce	1400	2000	1500	1700	2100	1100	750	960	1000	1500	1400	770	1500	960
As	230	240	200	110	130	180	220	180	210	190	140	190	200	56
Cd	2.8	2.4	2.8	5.2	3.6	2.2	2.5	3.1	2.4	1.4	2.0	2.4	1.6	3.2
Cr	5.0	2.0	4.0	2.5	4.5	3.5	6.0	5.0	1.0	3.5	2.0	11	3.0	37
Pb	1900	2400	2000	2500	2500	1100	1300	960	740	970	1400	1100	1500	1300
Zn	620	660	700	1200	1000	570	530	600	610	650	550	560	660	1200
Pd	-	-	-	-	-	-	-	-	-	-	-	-	-	-
Pt	-	-	-	-	-	-	-	-	-	-	-	-	-	-
Rh	-	-	-	-	-	-	-	-	-	-	-	-	-	-
Interval	B 0-19	L 15-20	L 0-20	L 20-42	L 38-43	B 0-105	L 0-30	L 30-40	L 40-56	L 56-69	L 69-102	B 0-39	B 0-71	B 0-4
Type	Crust	Crust	Crust	Crust	Crust	Crust	Crust	Crust	Crust	Crust	Crust	Crust	Crust	Vein
Comments		Inner			Inner							Top	Underside	fracture
		5 mm			5 mm									fill

Table 7. continued

	CD17-4A	CD17-4B	CD17-4C	CD17-7A	CD17-7B	CD17-9	CD18-3	CD19-1	CD19-4	CD21-6A	CD21-7A	CD21-7B	CD21-7C	CD21-7D	CD23-1A
Fe %	15.8	12.5	12.8	10.3	12.4	12.6	14.3	11.8	13.9	16.8	13.7	13.2	14.5	12.6	16.2
Mn	19.3	21.3	21.9	16.8	19.6	20.2	19.2	24.3	20.8	17.6	20.7	19.9	19.9	16.9	19.9
Mn/Fe	1.2	1.7	1.7	1.63	1.58	1.60	1.34	2.06	1.50	1.0	1.5	1.5	1.4	1.3	1.23
Si	2.48	2.29	1.73	1.37	2.95	2.06	3.27	2.24	2.66	3.83	2.43	2.66	2.57	1.78	2.62
Na	1.22	1.38	1.34	1.16	1.39	1.28	1.32	1.38	1.44	1.31	1.34	1.32	1.28	1.11	1.23
Mg	0.83	0.87	0.86	0.67	0.89	0.86	0.84	1.10	0.94	0.88	0.85	0.87	0.84	0.64	0.82
K	0.32	0.43	0.38	0.36	0.49	0.40	0.44	0.44	0.41	0.37	0.40	0.40	0.42	0.30	0.41
Ca	2.00	2.22	2.14	8.0	1.99	1.90	2.01	2.43	2.07	1.93	2.82	1.94	2.49	8.4	2.07
Ti	0.82	0.97	0.87	0.80	0.95	0.91	0.99	0.94	0.86	0.89	0.91	1.00	0.87	0.97	1.13
Al	0.24	0.42	0.24	0.35	0.62	0.33	0.59	0.45	0.46	0.58	0.50	0.46	0.64	0.38	0.51
P	0.35	0.29	0.27	2.60	0.29	0.27	0.31	0.31	0.35	0.35	0.52	0.27	0.40	2.65	0.29
H2O+	5.00	5.50	6.20	6.20	6.80	5.00	5.50	6.00	5.70	7.00	6.00	5.90	5.90	5.90	6.00
H2O-	20.1	22.5	21.3	20.4	24.0	27.0	22.3	18.4	21.0	16.8	19.8	24.3	21.6	16.1	18.6
CO2	0.48	0.43	0.43	1.2	0.33	0.37	0.42	0.50	0.38	0.45	0.51	0.39	0.41	1.3	0.35
LOI	33.9	33.5	35	32.7	37.6	39.9	35.1	32.1	34.2	30.4	33.1	36.5	33.9	28.3	32.1
Ba ppm	1200	1600	1400	2000	1500	1100	1400	1400	1100	1100	1800	1200	2000	2300	2500
Co	5300	5000	5500	3300	5500	7000	5200	8200	6200	4800	4700	6400	3700	3000	4000
Cu	370	1300	1000	1200	1000	630	930	1300	550	420	1300	870	1500	1200	1300
Mo	450	430	500	390	350	390	370	480	410	340	430	350	380	450	550
Ni	2700	4100	4100	2700	4000	3900	3200	5900	3800	2400	3800	3800	3600	2300	2800
Sr	1400	1300	1400	1500	1200	1200	1300	1300	1300	1300	1400	1200	1400	1600	1600
V	580	490	530	480	450	450	490	480	560	520	520	440	510	590	710
Y	200	160	160	320	150	130	170	130	160	180	150	170	160	210	130
Ce	790	900	850	1300	940	760	860	680	730	980	1100	820	1200	1500	1600
As	250	190	210	130	190	170	210	200	230	240	190	190	180	150	230
Cd	2.0	2.3	2.5	1.9	3.2	2.8	2.3	4.2	3.1	1.6	2.3	2.5	2.2	1.5	2.0
Cr	5.5	3.0	3.0	3.0	4.5	7.0	7.5	6.5	4.0	7.5	3.0	7.0	4.0	3.0	5.0
Pb	1600	890	1200	1200	1100	1300	1100	1300	1600	1400	1100	1200	890	1400	1700
Zn	510	580	580	580	600	520	540	680	570	510	610	510	630	610	680
Pd	0.0042	0.015	0.0045	-	-	-	-	-	-	0.0027	0.0057	0.0048	0.0050	0.0042	-
Pt	0.075	0.20	0.17	-	-	-	-	-	-	0.063	0.29	0.14	0.94	0.26	-
Rh	0.0077	0.015	0.012	-	-	-	-	-	-	0.0027	0.013	0.0066	0.014	0.011	-
Interval	L 0-12	L 12-45	B 0-45	N 30-60	N 0-30	B 0-22	B 0-42	B 0-14	N 0-5	B 0-6	B 0-79	L 0-28	L 28-65	L 65-80	B 0-50
Type	Crust	Crust	Crust	Nodule	Nodule	Crust	Crust	Crust	Nodule	Crust	Crust	Crust	Crust	Crust	Crust
Comments				nucleus	Outer				Bulk						
					layer										

Table 7. continued

	CD23-2	CD24-1A	CD24-1B	CD25-A1A	CD26-2A	CD26-4A	CD26-4B	CD26-4D	CD26-5A	CD26-5B	CD26-7A	CD26-7C	CD26-9-2A	CD26-9-2B
Fe %	15.2	14.4	12.5	14.8	12	15.1	13.2	12.9	13.4	12.2	13.6	1.98	13.6	13.2
Mn	17.5	17.7	16.7	18.3	21	18.3	12	18.5	21.3	21.8	22.2	15.1	19.8	18.3
Mn/Fe	1.15	1.2	1.3	1.24	1.75	1.21	0.91	1.43	1.59	1.79	1.63	7.63	1.46	1.39
Si	5.70	4.07	1.92	4.02	3.09	4.25	5.33	4.11	2.34	2.52	2.76	3.69	3.74	4.35
Na	1.38	1.25	1.04	1.45	1.33	1.31	1.08	1.40	1.35	1.39	1.44	1.09	1.37	1.37
Mg	0.87	0.82	0.60	0.92	0.94	0.89	0.66	0.91	0.89	0.89	0.94	1.00	0.89	0.89
K	0.48	0.45	0.31	0.46	0.56	0.51	0.71	0.55	0.41	0.50	0.46	0.95	0.50	0.56
Ca	2.08	2.15	8.9	2.03	2.20	1.96	9.2	2.04	2.09	2.15	2.15	18.6	2.00	2.02
Ti	1.01	0.99	0.85	1.04	0.96	1.05	1.09	1.09	0.98	0.93	1.04	0.31	1.07	1.08
Al	1.11	0.87	0.38	0.74	0.80	0.84	1.33	0.97	0.35	0.52	0.41	1.52	0.77	0.99
P	0.31	0.35	2.89	0.31	0.27	0.32	3.1	0.29	0.29	0.24	0.29	6.9	0.27	0.28
H2O+	5.70	6.20	5.70	5.50	5.80	5.90	4.30	5.70	5.20	5.30	5.40	4.20	5.50	4.60
H2O-	17.4	21.6	16.5	18.5	18.0	21.5	11.2	16.5	20.9	19.8	18.8	3.0	18.5	17.0
CO2	0.55	0.51	1.4	0.52	0.39	0.42	1.4	0.44	0.36	0.35	0.41	2.6	0.38	0.51
LOI	29.9	33.9	28.7	31.6	31.6	33.9	21.6	29.8	34.4	32.5	31.7	13.0	31.7	29.6
Ba ppm	1300	1600	2900	1200	1600	1400	2600	1600	1300	1700	1400	7400	1300	1400
Co	4400	4100	1900	6600	6400	6100	1800	5200	6200	6100	7000	730	6200	5400
Cu	730	1200	930	600	2300	850	1700	1100	960	1500	900	1800	1700	1600
Mo	310	340	440	310	370	330	290	290	430	450	430	47	310	280
Ni	2800	2900	1900	3100	4400	3400	1900	4000	4000	4500	4500	1800	3800	3700
Sr	1200	1300	1700	1200	1300	1300	1500	1200	1300	1400	1400	1200	1200	1200
V	480	520	670	470	420	490	490	410	500	490	490	750	460	420
Y	160	170	220	170	83	170	140	150	160	130	170	470	110	120
Ce	750	970	2100	840	910	910	1400	930	840	910	850	84	830	890
As	200	170	130	200	170	190	110	160	210	190	200	16	180	160
Cd	2.1	1.9	1.3	2.5	3.3	2.4	1.4	2.6	2.6	2.9	3.1	2.3	2.3	2.4
Cr	6.5	9.0	2.0	9.0	3.0	12	10	7.0	3.5	2.5	7.0	25	5.0	7.0
Pb	1300	1200	2000	1300	1000	1200	1300	1000	1200	870	1300	120	1200	1100
Zn	550	560	630	560	660	560	660	610	570	650	580	460	600	590
Pd	-	0.0052	0.0065	-	-	-	-	-	-	-	-	-	-	-
Pt	-	0.19	0.084	-	-	-	-	-	-	-	-	-	-	-
Rh	-	0.0091	0.0077	-	-	-	-	-	-	-	-	-	-	-
Interval	B 0-27	L 0-22	L 22-50	B 0-8	B 0-4	B 0-27	B 0-23	L 22-27	B 0-37	L 32-37	B 0-32	B 0-4	N 0-10	N 5-10
Type	Crust	Crust	Crust	Crust	Crust	Crust	Crust	Crust	Crust	Crust	Crust	Strat-	Nodule	Nodule
Comments							Clast in	Inner		Inner		bound	Bulk	Inner 5 mm
							breccia	5 mm		5 mm		layer		

Table 7. continued

	CD26-9-2C	CD28-1A	CD28-1B	CD28-1C	CD28-1D	CD28-1E	CD28-2A	CD28-2B	CD29-2A	CD29-2B	CD29-2C	CD29-2D	CD29-2E	CD29-7A	CD29-7B
Fe %	14.2	13.5	15.7	14.7	12.3	10.3	11.6	9.4	11.2	15.4	12.3	10.6	10.1	12.4	9.5
Mn	17.2	19.9	19.2	22	20.3	18.5	18.4	20.8	18.7	18.2	19.9	14.0	20.0	17.4	17.7
Mn/Fe	1.21	1.47	1.22	1.50	1.65	1.80	1.59	2.21	1.7	1.2	1.6	1.3	2.0	1.40	1.86
Si	2.76	2.38	4.07	2.24	1.45	1.26	2.24	1.45	1.96	4.21	3.04	2.38	1.08	3.13	1.08
Na	1.11	1.22	1.32	1.28	1.19	1.14	1.16	1.14	1.26	1.38	1.35	1.19	1.16	1.23	1.12
Mg	0.70	0.80	0.88	0.84	0.73	0.66	0.73	0.80	0.75	0.84	0.85	0.65	0.71	0.79	0.65
K	0.48	0.42	0.47	0.44	0.37	0.34	0.44	0.47	0.36	0.39	0.48	0.34	0.32	0.46	0.31
Ca	5.6	5.3	1.98	2.43	7.8	10.1	4.9	8.0	5.9	1.96	2.05	12.2	6.7	4.0	10.2
Ti	1.11	0.92	1.02	1.22	0.74	0.54	0.75	0.50	0.81	0.96	0.96	0.63	0.79	0.81	0.69
Al	0.62	0.48	0.72	0.45	0.26	0.24	0.45	0.32	0.42	0.70	0.69	0.59	0.21	0.70	0.19
P	1.65	1.40	0.31	0.34	2.26	3.2	1.34	2.39	1.72	0.35	0.28	4.2	1.94	1.04	3.2
H2O+	5.20	5.20	4.90	6.10	4.30	3.50	4.80	5.40	4.40	6.40	5.00	5.10	5.40	4.20	3.90
H2O-	15.4	17.2	18.5	17.7	14.3	13.2	23.6	15.8	22.2	18.4	24.7	13.9	22	24.5	17.6
CO2	0.84	0.86	0.41	0.36	1.2	1.5	0.76	1.2	0.95	0.44	0.38	1.8	0.99	0.65	1.5
LOI	28.1	29.6	30.8	31.2	27.1	24.8	35.2	28.6	34.2	31.4	36.7	25.2	34	35.7	28.8
Ba ppm	2700	2100	1300	2700	2400	2400	2400	3200	1700	1200	1600	1800	2200	1400	2200
Co	2800	4700	6700	4700	3200	2800	3300	2900	4100	6000	5000	2100	4100	4300	3300
Cu	1900	1100	690	1500	1100	680	680	850	940	380	1000	1100	1300	1100	1100
Mo	440	450	330	480	550	460	480	640	410	340	370	250	550	310	480
Ni	2600	3100	3400	3500	2500	2300	2900	3700	3400	2700	4100	2500	3200	3200	2800
Sr	1600	1500	1300	1600	1700	1700	1400	1600	1400	1300	1300	1400	1500	1200	1600
V	660	570	480	610	660	580	580	660	510	520	470	410	630	410	520
Y	180	200	170	160	270	420	140	360	130	170	120	200	100	230	130
Ce	1700	1500	830	1700	1900	1900	1300	1500	1100	860	910	1000	1400	820	1300
As	160	170	210	160	170	140	160	140	150	230	170	110	150	160	130
Cd	1.4	2.3	2.7	2.2	1.9	2.0	2.3	3.3	2.1	2.0	2.3	1.3	2.3	2.2	2.1
Cr	2.5	5.5	9.5	6.5	1.5	2.0	4.0	7.0	2.5	8.0	5.5	2.5	1.5	6.5	1.0
Pb	1500	1800	1400	1600	2200	2200	1600	2000	1100	1500	960	670	1500	930	1500
Zn	720	640	570	710	670	630	640	720	570	500	610	510	620	530	580
Pd	-	-	-	-	-	-	-	-	0.0043	0.0031	0.0048	0.0073	0.0045	-	-
Pt	-	-	-	-	-	-	-	-	0.33	0.30	0.28	0.43	0.22	-	-
Rh	-	-	-	-	-	-	-	-	0.017	0.0091	0.010	0.019	0.011	-	-
Interval	N 10-30	B 0-59	L 0-20	L 20-34	L 34-65	L 60-65	B 0-50	L 45-50	B 0-110	L 0-9	L 9-49	L 49-76	L 76-105	L 0-80	L 80-138
Type	Nodule	Crust	Crust	Crust	Crust	Crust	Crust	Crust	Crust	Crust	Crust	Crust	Crust	Crust	Crust
Comments	nucleus					Inner		Inner						layers 1-4	layer 5
						5 mm		5 mm							

Table 7. continued

	CD29-11	CD30-1	CD30-2	CD30-10A	CD30-10B	CD30-10C	CD30-10D
Fe %	12.6	14.1	15.1	11.4	12.5	10.4	10.6
Mn	19.9	17.4	18.7	18.8	19.5	21.5	18.5
Mn/Fe	1.58	1.2	1.24	1.65	1.6	2.1	1.7
Si	2.90	4.07	4.25	2.24	2.76	2.24	1.54
Na	1.33	1.29	1.37	1.19	1.34	1.34	1.17
Mg	0.88	0.79	0.86	0.80	0.83	0.88	0.71
K	0.48	0.43	0.47	0.43	0.41	0.48	0.36
Ca	2.04	1.92	1.99	5.7	1.92	2.50	7.5
Ti	1.01	0.85	0.90	0.87	0.88	0.95	0.81
Al	0.56	0.72	0.72	0.50	0.48	0.54	0.40
P	0.31	0.36	0.34	1.62	0.30	0.40	2.29
H2O+	4.80	6.40	4.60	4.30	6.10	6.30	5.90
H2O-	24.0	20.2	19.2	20.4	20.9	22.5	17.5
CO2	0.38	0.44	0.36	0.89	0.4	0.44	1.2
LOI	36.0	32.7	31.0	31.9	34.1	35.8	29.3
Ba ppm	1300	1100	1200	2200	1200	1600	3600
Co	6800	5800	6200	4500	6800	5200	3600
Cu	920	560	690	900	480	1100	1200
Mo	350	320	330	400	390	440	450
Ni	4000	2900	3000	3500	3800	5100	2900
Sr	1200	1200	1300	1400	1200	1300	1600
V	410	480	480	500	470	460	580
Y	170	140	140	150	150	130	170
Ce	850	780	860	1300	760	960	1600
As	180	220	220	150	210	160	150
Cd	3.0	2.2	2.7	2.5	2.9	2.9	1.9
Cr	9.5	8.5	12	13	4.0	3.5	< 1.0
Pb	1200	1400	1400	1400	1400	1100	1500
Zn	540	490	520	650	540	680	650
Pd	-	0.0025	-	-	0.0032	0.010	0.0085
Pt	-	0.14	-	-	0.18	0.64	0.39
Rh	-	0.011	-	-	0.0082	0.0082	0.013
Interval	B 0-35	B 0-12	B 0-12	B 0-75	L 0-25	L 25-39	L 39-70
Type	Crust	Crust	Crust	Crust	Crust	Crust	Crust
Comments							

*Major and minor elements determined by Inductively Coupled Plasma-Atomic Emission Spectrometry; except K, Zn, Pb by Flame Atomic-Absorption Spectroscopy, and As, Cr, Cd by Graphite-Furnace Atomic Absorption Spectroscopy on air dried samples. Pt, Pd, and Rh determined by fire assay.

•Analysts: H. Kirschenbaum, C.L. Prosser, Hezekiah Smith, J.W. Marinenko, Norma Rait, M. Kavulak, Roosevelt Moore.

•Au was below the detection limit of 0.04 ppm in 31 samples analyzed. Analysts: P. Aruscavage and R. Moore.

•Hg was below the detection limit of 0.02 ppm in 8 samples analyzed. Analyst: P. Hageman.

•Sample numbers which are identical except for the suffixes -A, -B, -C, and -D represent different sample intervals from the crust.

†Intervals measured from outer surface of crust; B = bulk, which means the entire crust thickness was sampled and analyzed; L = layer; N = nodule. Top crust is on top side of substrate rock, at seawater substrate contact; underside crust is from bottom side of substrate, not in direct (or most recent) contact with seawater.

Table 8. Chemical composition of ferromanganese crusts in weight percent, except Pt in ppm; analyses by the Japanese Geological Survey.

	JOD4-A1	JOD4-A2	CD6-A1	CD6-B2	CD7-A	JTD9-A1	JTD9-A2	JTD9-B1	JTD9-B2	CD11-A	CD13-A	CD13-B	CD15-A	CD15-B1	CD15-B2	CD16-A1	CD16-A2	CD16-A3
Mn	21.08	23.48	18.94	23.17	19.30	24.37	20.27	19.89	20.60	26.15	26.06	27.00	23.66	24.60	24.32	26.03	25.25	25.72
Fe	18.51	15.98	18.85	16.29	18.35	16.93	19.46	20.00	17.86	17.02	15.52	15.28	14.29	13.70	7.67	17.02	14.44	16.11
Mn/Fe	1.14	1.47	1.00	1.42	1.05	1.44	1.04	0.99	1.15	1.54	1.68	1.77	1.66	1.80	3.17	1.53	1.75	1.6
Si	4.49	4.26	6.24	4.41	5.88	2.78	5.43	5.36	5.54	2.21	3.13	2.86	1.77	2.36	0.53	2.29	3.71	3.22
Al	0.82	0.87	1.17	1.01	1.37	0.47	0.99	0.97	1.15	0.35	0.79	0.55	0.53	0.88	0.20	0.31	0.78	0.76
LOI	11.13	10.35	10.45	10.72	10.47	11.41	11.36	11.12	10.99	12.62	10.39	10.83	9.83	9.25	8.47	11.54	10.79	11.64
Co	0.67	0.72	0.57	0.68	0.53	0.77	0.54	0.48	0.52	0.95	0.77	0.88	0.49	0.60	0.32	0.89	0.76	0.57
Cu	0.083	0.117	0.059	0.113	0.121	0.065	0.099	0.051	0.132	0.066	0.120	0.083	0.194	0.164	0.075	0.075	0.161	0.198
Ni	0.32	0.41	0.24	0.41	0.28	0.39	0.28	0.24	0.33	0.43	0.52	0.55	0.48	0.84	0.54	0.46	0.54	0.47
Pb	0.16	0.13	0.17	0.13	0.12	0.16	0.16	0.17	0.12	0.17	0.15	0.16	0.20	0.23	0.26	0.17	0.11	0.08
Zn	0.061	0.061	0.059	0.064	0.063	0.057	0.062	0.059	0.061	0.060	0.074	0.067	0.083	0.114	0.116	0.063	0.064	0.071
Pt	0.15	0.15	0.19	0.19	0.08	0.08	0.08	0.08	0.20	0.10	0.41	0.28	0.65	0.93	0.19	0.11	0.25	0.89
Interval	L, 0-12	L, 12-24	L, 0-12	L, 12-26	B, 0-25	L, 0-2	B, 0-25	L, 0-5	L, 5-34	B, 0-7	B, 0-13	B, 0-12	B, 0-16	L, 0-3	B, 0-13	L, 0-18	L, 18-32	L, 32-50
Type	Crust	Crust	Crust	Crust	Crust	Crust	Crust	Crust	Crust	Crust	Nodule	Nodule	Nodule	Crust	Crust	Crust	Crust	Crust

	CD16-A4	CD16-B1	CD16-B2	CD16-B3	CD16-B4	CD16-B5	CD17-A1	CD17-A2	CD21-A	CD23-A	CD25-A1	CD25-A2	CD25-A3	CD29-A1	CD29-A2	CD29-A3	CD29-A4
Mn	18.49	24.50	25.52	25.79	17.12	19.10	26.60	17.82	21.07	20.04	22.01	22.94	24.29	24.65	25.35	14.97	18.81
Fe	20.42	18.03	15.66	15.32	14.90	12.71	14.26	13.09	16.32	17.34	18.58	15.00	14.36	16.43	14.01	12.91	13.13
Mn/Fe	0.91	1.36	1.63	1.68	1.15	1.50	1.87	1.36	1.29	1.16	1.18	1.53	1.69	1.50	1.81	1.16	1.43
Si	5.24	2.71	3.38	3.09	3.33	1.59	2.93	1.84	5.04	5.26	3.69	4.11	3.72	2.76	2.93	3.88	1.38
Al	1.44	0.34	0.62	0.84	1.02	0.35	0.83	0.51	1.11	1.05	0.58	1.03	1.21	0.52	0.93	1.13	0.33
LOI	10.31	11.78	11.25	10.97	8.85	8.87	10.98	8.72	10.43	11.13	11.66	11.08	10.88	11.29	10.34	7.15	8.53
Co	0.25	0.81	0.77	0.56	0.24	0.49	0.69	0.39	0.66	0.55	0.70	0.67	0.56	0.77	0.53	0.21	0.38
Cu	0.182	0.065	0.145	0.201	0.165	0.157	0.205	0.141	0.113	0.081	0.063	0.139	0.184	0.106	0.207	0.158	0.164
Ni	0.29	0.39	0.47	0.49	0.29	0.32	0.66	0.29	0.41	0.33	0.34	0.47	0.52	0.44	0.55	0.26	0.28
Pb	0.11	0.18	0.14	0.08	0.08	0.11	0.12	0.14	0.13	0.13	0.16	0.12	0.09	0.16	0.08	0.06	0.15
Zn	0.73	0.061	0.070	0.075	0.067	0.064	0.087	0.071	0.064	0.060	0.066	0.064	0.077	0.062	0.073	0.056	0.065
Pt	1.17	0.14	0.30	0.77	0.65	0.76	0.62	0.53	0.24	0.13	0.09	0.30	1.24	0.11	0.71	0.66	0.34
Interval	L, 50-60	L, 0-16	L, 16-32	L, 32-55	L, 55-70	L, 70-75	L, 0-23	L, 50-65	L, 10-20	B, 0-22	L, 0-15	L, 15-30	L, 40-50	L, 0-20	L, 20-35	L, 35-52	L, 52-83
Type	Crust	Crust	Crust	Crust	Crust	Crust	Nodule	Nodule	Crust	Crust	Crust	Crust	Crust	Crust	Crust	Crust	Crust

Atomic absorption spectroscopy. Samples dried at 105°C for 2 hours. Analyst: Shigeru Terashima.

Table 9. Statistics for 97 bulk crusts from Table 7

Element	N	MEAN	MEDIAN	SD[1]	MIN[2]	MAX[3]
Fe (Wt%)	97	13.73	13.80	1.49	10.40	17.60
Mn	97	19.20	19.20	1.78	15.20	24.30
Mn/Fe	97	1.40[4]	-	-	-	-
Si	97	3.27	3.09	1.09	1.22	6.45
Na	97	1.32	1.33	0.08	1.07	1.60
Mg	97	0.85	0.85	0.07	0.72	1.10
K	97	0.44	0.43	0.07	0.32	0.79
Ca	97	2.45	2.06	0.97	1.79	5.90
Ti	97	0.95	0.95	0.09	0.74	1.23
Al	97	0.63	0.59	0.26	0.22	1.53
P	97	0.47	0.34	0.35	0.25	1.73
H2O+	97	6.66	6.90	1.61	2.40	10.40
H2O-	97	20.87	20.90	2.57	15.00	27.00
CO2	97	0.49	0.44	0.15	0.14	0.95
LOI	39	33.51	33.40	2.51	29.60	39.90
Ba (ppm)	97	1452	1300	371	1000	3100
Co	97	5792	5800	1243	3300	10300
Cu	97	848	850	339	340	2300
Mo	97	380	370	81	200	660
Ni	97	3518	3500	722	2200	5900
Sr	97	1284	1300	97	1100	1600
V	97	509	500	57	410	710
Y	97	163	170	26	58	230
Ce	97	933	870	207	670	1900
As	97	207	200	27	140	280
Cd	97	2.49	2.4	0.49	1.6	4.2
Cr	95	6.4	6.3	3.5	1.5	18.0
Pb	97	1339	1300	207	930	2100
Zn	97	552	550	60	450	700
Pd	23	0.0025	0.0018	0.0020	0.0005	0.0082
Pt	25	0.174	0.140	0.091	0.015	0.350
Rh	25	0.0149	0.0120	0.0164	0.0027	0.0910
Depth[5]	95	2385	2285	240	1880	2803
Thickness	90	29	22	24	3	110

[1] Standard Deviation; [2] Minimum; [3] Maximum; [4] Ratio of the Fe and Mn means, not a mean of the summation of the ratios; [5] Water depth in meters.

Table 10. Mean concentrations of selected elements in various groups of bulk ferromanganese crusts, in weight percentages except Pt in ppm. Data from Table 7.

	Fe	Mn	Mn/Fe	Al	P	Co	Cu	Ni	Pt
All Bulk Crusts, n = 97 (Pt = 25)	13.7	19.2	1.40	0.63	0.47	0.58	0.08	0.35	0.17
Bulk Crusts ≤5 mm thick, n = 10 (Pt = 1)	14.1	19.7	1.40	0.69	0.37	0.68	0.07	0.36	0.08
Inner 5 mm of crusts, n = 24 (Pt = 1)	12.6	19.4	1.54	0.75	1.17	0.48	0.11	0.38	0.31
Bulk Crusts ≤20 mm thick, n = 47 (Pt = 7)	14.4	18.9	1.31	0.71	0.35	0.60	0.08	0.34	0.10
Bulk Crusts ≥20 mm thick, n = 56 (Pt = 18)	13.2	19.3	1.46	0.59	0.56	0.55	0.09	0.36	0.20
Bulk Crusts with Co ≥ 1%, n = 4 (Pt = 1)	11.4	22.9	2.01	0.41	0.28	1.04	0.05	0.52	0.17
Central Karin Ridge Bulk Crusts, n = 38 (Pt = 10)	14.5	18.3	1.26	0.76	0.39	0.59	0.07	0.32	0.15
Southern Karin Ridge Bulk Crusts, n = 7 (Pt = 2)	12.8	18.8	1.47	0.55	1.01	0.51	0.08	0.33	0.24
SOJIR Bulk Crusts, n = 48 (Pt = 13)	13.2	19.9	1.51	0.54	0.48	0.57	0.10	0.38	0.18
8 Bulk Crusts from Table 8	15.62	23.35	1.49	0.73	-	0.63	0.105	0.43	0.24
Central Pacific Average[1], n = 311 (Pt = 29)	15.7	23.0	1.46	-	0.91	0.79	0.12	0.47	0.24

[1] Hein et al. (1990a).

Table 11. Concentrations of Rare Earth Elements (ppm) in ferromanganese crusts.

SAMPLE	CD1-10A1	CD1-17E	CD2-8A	CD2-8B	CD2-8C	CD2-8D	CD2-8E	CD2-8F	CD2-38A	CD2-38B	CD2-38C	CD2-38D	CD2-38E	CD2-38H
La	206	300	323	278	231	245	293	323	332	233	189	256	256	285
Ce	856	316	772	919	958	1480	1700	1530	808	840	1050	1100	1500	1170
Pr	31.9	40.0	63.5	53.4	40.8	44.4	55.4	59.2	70.3	44.7	34.5	40.8	48.3	49.6
Nd	132	178	266	216	165	172	214	232	279	177	135	166	183	195
Sm	27.1	33.9	57.2	46.1	34.1	35.8	43.4	47.0	61.0	38.3	28.6	33.2	34.6	39.6
Eu	7.05	9.46	14.9	11.6	8.85	8.99	10.6	12.0	15.8	9.99	7.56	8.81	8.33	10.1
Gd	32.8	47.8	62.1	51.0	38.6	38.6	44.1	52.7	63.2	41.0	30.0	37.7	33.9	44.8
Tb	5.07	7.24	9.84	8.27	6.21	5.80	7.04	8.22	10.4	6.86	4.97	5.82	5.46	7.13
Dy	34.2	51.9	63.0	50.5	39.1	35.3	43.2	49.0	64.5	42.6	30.3	38.7	31.7	42.6
Ho	7.39	12.4	12.4	10.3	8.04	7.02	8.80	10.3	12.5	8.58	6.37	9.04	6.25	9.19
Er	21.9	36.2	34.8	29.6	22.1	19.4	24.7	28.9	34.6	24.5	17.9	26.7	16.8	25.9
Tm	3.81	6.24	5.80	4.97	4.05	3.28	4.36	4.98	5.54	4.28	3.22	4.40	3.02	4.12
Yb	21.9	35.5	33.2	29.5	23.3	19.7	25.7	29.5	32.3	25.5	18.8	27.4	17.5	25.4
Lu	3.07	5.19	4.46	3.97	3.29	2.71	3.54	3.92	4.33	3.60	2.73	4.22	2.25	3.56
ΣREE	1390	1080	1722	1712	1582	2118	2478	2391	1793	1500	1559	1759	2147	1912
Ce*	1.07	0.20	0.57	0.79	1.02	1.48	1.40	1.15	0.56	0.86	1.35	1.10	1.41	1.02
Interval	B[1] 0-36	B 0-45	L 0-12.5	L 12.5-32.5	L 32.5-52.5	L 52.5-72.5	L 72.5-92.5	B 0-90	L 0-10	L 10-35	L 35-50	L 50-65	L 65-90	B 0-90

SAMPLE	JOD4-3-IIA	CD6-1-IIC	CD6-3A	CD6-23A	CD7-3A	JTD9-2A	JTD9-2B	CD13-8A	CD13-8B	CD13-8C	CD13-8D	CD13-8E	CD13-13A	CD14-1
La	251	218	281	285	332	322	303	316	286	322	250	288	290	257
Ce	897	1430	901	906	902	1010	862	845	1470	1830	1170	1660	819	960
Pr	54.3	40.7	54.5	56.5	72.7	73.5	66.5	65.1	56.4	57.5	48.4	51.3	55.7	50.6
Nd	209	159	218	231	285	293	262	260	232	210	188	190	227	204
Sm	45.1	32.9	45.9	48.0	63.9	63.3	56.0	57.1	46.8	41.3	37.8	36.2	45.9	42.3
Eu	11.6	8.19	12.1	12.8	16.2	17.1	14.5	15.2	12.2	10.4	9.83	9.59	11.9	10.6
Gd	47.0	36.4	52.7	54.3	69.0	68.9	62.4	62.3	56.5	47.0	42.5	39.4	52.3	48.1
Tb	7.69	5.60	8.29	8.82	10.7	11.0	9.73	9.95	8.19	7.26	6.64	6.12	8.48	7.33
Dy	45.8	35.6	52.1	54.0	62.5	65.6	55.9	58.1	49.2	45.1	40.4	36.3	52.3	45.1
Ho	8.90	7.23	11.0	11.3	12.6	12.5	11.6	11.9	9.95	9.46	8.17	8.04	11.2	9.64
Er	24.4	20.8	30.7	31.0	33.4	32.6	29.6	32.4	27.2	28.1	22.1	24.0	30.5	27.8
Tm	4.19	3.40	5.01	4.82	5.38	5.1	4.79	5.33	4.16	4.80	3.56	3.96	4.76	4.28
Yb	24.0	21.1	30.0	29.4	31.1	30.0	29.4	30.8	25.4	28.7	22.1	25.5	30.0	26.4
Lu	3.16	2.92	4.21	3.91	4.22	3.97	3.86	4.16	3.61	4.19	3.16	3.70	4.48	3.71
ΣREE	1633	2022	1706	1737	1901	2009	1771	1773	2288	2646	1853	2382	1644	1697
Ce*	0.82	1.59	0.77	0.75	0.62	0.70	0.65	0.62	1.22	1.40	1.12	1.42	0.68	0.89
Interval	B 0-13	B 0-50	B 0-40	B 0-15	B 0-25	L 0-7	L 7-35	L 0-10	L 10-33	L 33-50	B 0-50	L 45-50	B 0-12	B 0-35

Table 11. continued

SAMPLE	CD21-6A	CD21-7A	CD21-7B	CD21-7C	CD21-7D	CD24-1A	CD24-1B	CD29-2B	CD29-2C	CD29-2D	CD29-2E	CD30-10B	CD30-10C	CD30-10D
La	308	266	319	260	360	328	448	282	212	209	288	228	201	246
Ce	984	1060	926	1210	1540	1090	2350	901	1020	952	1620	776	1080	1720
Pr	70.0	51.2	62.4	49.7	60.3	61.1	64.1	53.4	38.4	34.5	51.0	40.5	35.1	41.9
Nd	278	200	245	194	227	251	242	217	154	141	199	169	141	165
Sm	61.7	39.4	50.8	37.4	40.7	52.3	39.6	44.1	31.1	26.8	37.9	35.2	28.8	32.6
Eu	15.9	9.94	13.5	9.59	10.2	12.5	9.26	10.8	7.93	6.78	8.99	7.97	6.67	7.40
Gd	65.3	44.1	56.0	38.4	44.8	53.9	45.7	48.7	32.6	30.6	38.7	35.0	29.5	32.5
Tb	10.6	6.83	9.38	6.24	6.85	8.96	7.33	7.95	5.41	5.16	6.29	6.08	4.97	5.33
Dy	62.0	41.4	57.3	37.6	42.7	54.5	46.4	50.3	35.3	31.3	40.1	41.1	33.2	36.8
Ho	12.0	8.56	11.8	7.43	9.16	10.5	10.4	10.4	7.35	6.11	8.04	8.84	7.20	8.05
Er	31.3	23.9	31.5	21.5	27.6	29.6	29.5	29.9	23.0	19.2	24.6	26.2	21.8	24.8
Tm	5.00	3.83	5.01	3.31	4.03	4.53	4.46	4.64	3.15	2.95	3.67	4.04	3.35	4.06
Yb	28.8	23.4	31.7	20.1	28.0	28.1	28.6	28.2	21.4	18.1	24.9	25.5	21.8	26.4
Lu	4.06	3.40	4.44	3.03	4.23	4.37	4.44	4.24	3.32	3.15	3.84	3.25	2.81	3.50
ΣREE	1937	1782	1824	1898	2406	1989	3330	1693	1595	1487	2355	1407	1617	2354
Ce*	0.72	0.95	0.69	1.12	1.07	0.80	1.38	0.77	1.18	1.15	1.39	0.84	1.33	1.75
Interval	B 0-6	B 0-79	L 0-28	L 28-65	L 65-80	L 0-22	L 22-50	L 0-9	L 9-49	L 49-76	L 76-105	L 0-25	L 25-39	L 39-70

By inductively coupled plasma-atomic emission spectrometry on air dried samples. Analyst: K. Stewart.
[1] B = Bulk, L = Layer.
* Ce anomaly from chondrite normalized data = Ce/(La+Pr)

Table 12. Correlation coefficient matrix for 97 bulk crusts listed in Tables 7 and 9; n = 97, except for LOI = 39, water depth and Cr = 95, Pd = 23, Pt and Rh = 25, crust thickness = 90; the zero correlation for 97 points at the 99% confidence level is |0.260|.

	Fe	Mn	Mn/Fe	Si	Na	Mg	K	Ca	Ti	Al	P	H_2O^+	H_2O^-	CO_2	LOI	Ba	Co
Mn	-0.526																
Mn/Fe	-0.891	0.840															
Si	0.697	-0.768	-0.831														
Na	0.011	0.225	0.106	0.168													
Mg	-0.008	0.532	0.286	-0.009	0.538												
K	0.044	-0.257	-0.161	0.573	0.406	0.360											
Ca	-0.551	0.088	0.405	-0.459	-0.354	-0.339	-0.191										
Ti	0.427	-0.201	-0.342	0.525	0.306	0.359	0.431	-0.409									
Al	0.498	-0.715	-0.679	0.935	0.160	0.051	0.727	-0.302	0.556								
P	-0.478	-0.019	0.301	-0.389	-0.390	-0.405	-0.201	0.987	-0.431	-0.256							
H_2O^+	0.139	-0.083	-0.109	0.051	0.097	-0.059	-0.126	-0.120	0.183	0.057	-0.127						
H_2O^-	-0.529	0.062	0.342	-0.407	-0.205	-0.400	-0.252	0.062	-0.451	-0.410	0.076	-0.154					
CO_2	-0.346	-0.071	0.191	-0.262	-0.316	-0.282	-0.136	0.836	-0.355	-0.133	0.833	-0.143	-0.063				
LOI	-0.550	0.288	0.477	-0.498	0.027	-0.047	-0.157	-0.092	-0.257	-0.489	-0.086	-0.055	0.950	-0.287			
Ba	-0.376	0.182	0.355	-0.352	-0.328	-0.169	-0.031	0.582	-0.113	-0.170	0.524	0.083	-0.035	0.386	-0.128		
Co	-0.202	0.569	0.404	-0.234	0.439	0.640	0.041	-0.327	0.082	-0.266	-0.360	-0.215	0.050	-0.240	0.250	-0.415	
Cu	-0.351	0.177	0.330	-0.110	-0.005	0.184	0.347	0.193	0.269	0.122	0.110	0.092	-0.098	0.020	-0.103	0.427	-0.228
Mo	-0.481	0.765	0.687	-0.817	-0.142	0.043	-0.468	0.339	-0.534	-0.781	0.264	-0.090	0.189	0.161	0.240	0.468	0.150
Ni	-0.705	0.847	0.876	-0.610	0.293	0.610	0.039	0.109	-0.104	-0.472	0.013	-0.089	0.182	-0.043	0.366	0.168	0.610
Sr	-0.179	0.518	0.382	-0.622	-0.226	-0.055	-0.466	0.495	-0.334	-0.595	0.447	-0.007	-0.161	0.324	-0.089	0.570	-0.111
V	0.213	0.255	-0.014	-0.304	-0.311	-0.141	-0.490	0.129	-0.326	-0.371	0.133	0.033	-0.186	0.094	-0.148	0.320	-0.147
Y	0.290	-0.249	-0.291	0.097	-0.052	-0.240	-0.230	0.050	-0.027	-0.031	0.114	0.112	-0.028	0.190	-0.198	-0.158	-0.099
Ce	-0.214	0.132	0.235	-0.415	-0.374	-0.315	-0.242	0.544	-0.119	-0.296	0.494	0.093	-0.039	0.367	-0.141	0.738	-0.387
As	0.605	0.065	-0.365	0.169	0.096	0.196	-0.229	-0.573	-0.056	-0.059	-0.523	0.027	-0.208	-0.394	-0.091	-0.444	0.319
Cd	-0.522	0.799	0.743	-0.484	0.341	0.691	0.084	-0.017	-0.068	-0.378	-0.110	-0.152	0.064	-0.064	0.338	0.033	0.697
Cr	0.295	-0.384	-0.398	0.600	0.212	0.165	0.594	-0.207	0.402	0.636	-0.175	-0.215	-0.240	-0.113	-0.297	-0.155	0.087
Pb	0.138	0.313	0.067	-0.248	-0.133	0.100	-0.325	0.027	-0.222	-0.310	0.019	-0.016	-0.146	0.018	-0.114	0.172	0.196
Zn	-0.456	0.558	0.599	-0.464	0.003	0.364	0.063	0.420	0.047	-0.266	0.316	0.064	-0.158	0.158	-0.024	0.679	-0.096
Pd	0.225	0.085	-0.108	0.087	0.319	0.463	0.141	-0.055	0.238	0.144	-0.109	-0.281	-0.570	0.123	-0.359	-0.059	-0.159
Pt	-0.475	0.340	0.479	-0.391	0.077	0.103	-0.005	0.547	-0.056	-0.191	0.492	-0.235	-0.188	0.582	0.127	0.541	-0.181
Rh	-0.290	-0.098	0.112	-0.028	0.024	-0.182	0.063	-0.018	0.067	0.009	-0.006	-0.227	0.406	-0.084	0.583	-0.050	0.114
Depth	-0.311	0.159	0.293	-0.351	-0.101	-0.082	-0.163	0.160	-0.165	-0.273	0.123	0.199	0.286	0.180	0.245	0.166	-0.107
Thick.	-0.553	0.122	0.414	-0.468	-0.200	-0.398	-0.197	0.712	-0.344	-0.347	0.689	-0.054	0.309	0.515	0.223	0.518	-0.352

	Cu	Mo	Ni	Sr	V	Y	Ce	As	Cd	Cr	Pb	Zn	Pd	Pt	Rh	Depth	
Mo	0.013																
Ni	0.355	0.499															
Sr	0.087	0.786	0.199														
V	-0.275	0.653	-0.119	0.742													
Y	-0.409	-0.159	-0.316	-0.024	0.023												
Ce	0.236	0.517	-0.068	0.679	0.482	-0.061											
As	-0.627	0.089	-0.199	0.070	0.505	0.213	-0.293										
Cd	0.176	0.436	0.860	0.167	-0.053	-0.315	-0.077	-0.004									
Cr	-0.089	-0.465	-0.212	-0.342	-0.256	0.028	-0.193	0.011	-0.089								
Pb	-0.437	0.553	0.000	0.528	0.761	-0.009	0.417	0.515	0.193	-0.005							
Zn	0.621	0.510	0.560	0.549	0.200	-0.405	0.523	-0.405	0.462	-0.179	0.169						
Pd	0.224	-0.034	-0.041	0.090	-0.045	-0.093	0.036	-0.177	-0.019	0.315	-0.348	0.216					
Pt	0.473	0.305	0.412	0.432	-0.031	0.148	0.521	-0.579	0.268	-0.288	-0.472	0.605	0.331				
Rh	0.088	-0.143	0.118	-0.301	-0.407	0.058	-0.116	-0.279	0.096	0.043	-0.170	-0.233	-0.215	0.048			
Depth	0.276	0.185	0.226	0.109	-0.026	-0.061	0.202	-0.240	0.097	-0.471	-0.201	0.192	0.013	-0.048	-0.155		
Thick.	0.293	0.342	0.159	0.406	0.015	0.070	0.445	-0.559	-0.120	-0.230	-0.218	0.366	0.016	0.642	0.118	0.263	

Table 13. Correlation coefficient matrix for 47 bulk crusts listed in Table 7 with thicknesses ≤ 20mm; n = 47, except for LOI = 15, Pd = 6, Pt and Rh = 7; the zero correlation for 47 points at the 99% confidence level is |0.370|.

	Fe	Mn	Mn/Fe	Si	Na	Mg	K	Ca	Ti	Al	P	H_2O^+	H_2O^-	CO_2	LOI	Ba	Co
Mn	-0.650																
Mn/Fe	-0.878	0.925															
Si	0.532	-0.866	-0.771														
Na	-0.233	0.177	0.216	0.010													
Mg	-0.371	0.636	0.599	-0.310	0.278												
K	-0.165	-0.221	-0.031	0.582	0.351	0.268											
Ca	-0.548	0.567	0.626	-0.414	0.111	0.620	0.159										
Ti	0.225	-0.380	-0.300	0.496	-0.138	0.109	0.388	-0.006									
Al	0.243	-0.688	-0.515	0.909	0.061	-0.066	0.776	-0.142	0.615								
P	0.101	0.004	-0.072	-0.019	-0.048	0.154	-0.005	0.531	-0.154	-0.015							
H_2O^+	0.166	-0.189	-0.172	-0.028	-0.191	-0.227	-0.284	-0.114	0.187	-0.037	-0.151						
H_2O^-	-0.378	0.019	0.158	-0.265	0.036	-0.467	-0.266	-0.053	-0.350	-0.292	-0.032	-0.024					
CO_2	0.158	-0.156	-0.183	0.148	-0.035	0.095	0.027	0.268	0.056	0.178	0.265	-0.169	-0.180				
LOI	-0.457	0.562	0.485	-0.648	0.043	0.164	-0.357	0.210	-0.392	-0.581	0.018	0.573	0.916	-0.588			
Ba	-0.242	0.082	0.211	0.067	-0.083	0.233	0.387	0.351	0.344	0.293	-0.084	0.255	-0.199	-0.146	0.205		
Co	-0.495	0.666	0.619	-0.530	0.224	0.514	-0.069	0.409	-0.283	-0.400	0.155	-0.490	0.037	0.178	0.204	-0.308	
Cu	-0.436	0.189	0.377	0.014	0.044	0.358	0.454	0.278	0.470	0.291	-0.326	0.104	-0.242	-0.225	-0.138	0.662	-0.152
Mo	-0.471	0.870	0.744	-0.837	0.118	0.385	-0.360	0.454	-0.613	-0.766	0.112	-0.135	0.124	-0.150	0.692	0.087	0.547
Ni	-0.814	0.872	0.939	-0.654	0.225	0.726	0.067	0.683	-0.149	-0.381	0.076	-0.217	0.039	-0.155	0.409	0.246	0.644
Sr	-0.068	0.659	0.425	-0.674	-0.032	0.299	-0.466	0.289	-0.434	-0.682	0.170	0.037	-0.156	-0.120	0.550	0.172	0.306
V	0.144	0.418	0.156	-0.492	-0.188	0.111	-0.500	0.143	-0.497	-0.574	0.371	-0.011	-0.071	-0.007	0.571	0.017	0.205
Y	0.695	-0.345	-0.568	0.149	-0.079	-0.369	-0.416	-0.321	-0.121	-0.115	0.302	0.136	-0.019	0.360	0.011	-0.474	-0.168
Ce	0.257	-0.109	-0.168	0.030	-0.289	-0.077	-0.026	0.013	0.305	0.048	-0.098	0.367	-0.241	-0.129	0.097	0.555	-0.323
As	0.406	0.168	-0.134	-0.263	-0.147	-0.026	-0.482	-0.094	-0.552	-0.484	0.392	-0.173	-0.035	0.169	0.468	-0.496	0.283
Cd	-0.675	0.858	0.863	-0.602	0.255	0.763	0.051	0.626	-0.219	-0.359	0.075	-0.347	-0.062	0.015	0.353	0.079	0.734
Cr	0.202	-0.341	-0.314	0.556	0.239	0.097	0.526	-0.036	0.261	0.595	0.182	-0.343	-0.212	0.131	-0.428	0.050	0.057
Pb	0.105	0.405	0.161	-0.445	-0.065	0.243	-0.387	0.212	-0.420	-0.487	0.362	-0.005	-0.070	0.063	0.678	-0.094	0.367
Zn	-0.493	0.555	0.619	-0.326	0.100	0.697	0.214	0.566	0.246	-0.065	-0.055	0.097	-0.247	-0.285	0.329	0.645	0.038
Pd	0.053	0.543	0.306	-0.184	0.515	0.718	0.119	0.894	-0.292	-0.114	0.233	0.473	-0.834	0.887	0.257	0.051	0.017
Pt	-0.335	-0.103	0.139	0.381	0.375	0.126	0.572	-0.173	0.066	0.429	-0.190	-0.377	-0.313	0.139	0.991	0.472	-0.152
Rh	-0.657	0.214	0.525	0.085	0.231	0.048	0.396	-0.063	0.345	0.259	-0.398	-0.487	-0.046	0.126	0.976	0.592	-0.022
Depth	-0.215	0.143	0.215	-0.245	0.031	0.139	-0.077	0.297	0.059	-0.157	0.023	0.182	0.154	0.129	-0.064	0.207	-0.081
Thick.	-0.060	-0.199	-0.078	0.153	0.158	-0.388	0.033	-0.056	0.059	0.096	-0.117	0.288	0.341	-0.167	0.231	0.257	-0.325

	Cu	Mo	Ni	Sr	V	Y	Ce	As	Cd	Cr	Pb	Zn	Pd	Pt	Rh	Depth	
Mo	-0.107																
Ni	0.414	0.646															
Sr	-0.096	0.807	0.371														
V	-0.418	0.697	0.128	0.789													
Y	-0.704	-0.139	-0.553	0.066	0.319												
Ce	0.183	0.040	-0.237	0.327	0.203	-0.123											
As	-0.775	0.427	-0.158	0.525	0.750	0.600	-0.046										
Cd	0.234	0.638	0.886	0.415	0.186	-0.395	-0.254	0.046									
Cr	-0.100	-0.313	-0.174	-0.271	-0.188	-0.003	-0.058	-0.053	-0.094								
Pb	-0.505	0.629	0.126	0.701	0.812	0.235	0.263	0.740	0.275	0.027							
Zn	0.723	0.332	0.693	0.300	0.006	-0.621	0.169	-0.406	0.543	-0.111	-0.006						
Pd	-0.044	0.511	0.313	0.354	0.557	0.192	-0.094	0.241	0.390	0.115	0.146	0.416					
Pt	0.415	-0.190	0.117	-0.479	-0.311	-0.361	-0.281	-0.322	0.320	0.255	-0.331	0.190	0.412				
Rh	0.597	-0.030	0.517	-0.341	-0.224	-0.557	-0.355	-0.597	0.638	-0.033	-0.475	0.513	0.333	0.875			
Depth	0.239	0.027	0.220	-0.007	-0.073	-0.188	0.118	-0.247	0.079	-0.497	-0.181	0.239	-0.127	-0.489	-0.214		
Thick.	0.028	-0.071	-0.125	-0.154	-0.222	0.065	0.133	-0.318	-0.284	-0.041	-0.202	-0.080	-0.521	0.404	0.580	0.075	

Table 14. Correlation coefficient matrix for 56 bulk crusts listed in Table 7 with thicknesses ≥20mm; n = 56, except for LOI = 25, Pd = 17, Pt and Rh = 18, water depth = 54; the zero correlation for 56 points at the 99% confidence level is |0.340|.

	Fe	Mn	Mn/Fe	Si	Na	Mg	K	Ca	Ti	Al	P	H_2O^+	H_2O^-	CO_2	LOI	Ba	Co
Mn	-0.429																
Mn/Fe	-0.879	0.793															
Si	0.738	-0.750	-0.866														
Na	0.132	0.233	0.038	0.257													
Mg	0.011	0.580	0.290	-0.052	0.633												
K	0.162	-0.297	-0.265	0.561	0.441	0.426											
Ca	-0.560	0.012	0.382	-0.465	-0.441	-0.420	-0.300										
Ti	0.578	-0.051	-0.377	0.537	0.505	0.516	0.495	-0.542									
Al	0.607	-0.763	-0.785	0.943	0.177	-0.043	0.662	-0.318	0.517								
P	-0.530	-0.073	0.316	-0.414	-0.471	-0.472	-0.290	0.993	-0.554	-0.272							
H_2O^+	0.202	-0.025	-0.132	0.182	0.256	0.102	0.108	-0.211	0.212	0.232	-0.214						
H_2O^-	-0.514	0.019	0.331	-0.347	-0.257	-0.283	-0.210	-0.056	-0.492	-0.394	-0.024	-0.278					
CO_2	-0.484	-0.082	0.283	-0.342	-0.398	-0.391	-0.207	0.932	-0.542	-0.203	0.930	-0.174	-0.134				
LOI	-0.534	0.202	0.480	-0.412	0.095	-0.008	-0.047	-0.219	-0.252	-0.447	-0.193	-0.174	0.955	-0.369			
Ba	-0.292	0.194	0.312	-0.460	-0.561	-0.212	-0.220	0.560	-0.270	-0.255	0.519	-0.018	-0.148	0.460	-0.353		
Co	-0.223	0.609	0.455	-0.264	0.491	0.705	0.088	-0.386	0.286	-0.348	-0.410	0.006	0.166	-0.388	0.343	-0.412	
Cu	-0.228	0.105	0.215	-0.151	-0.017	0.079	0.214	0.235	0.074	0.018	0.188	0.067	-0.090	0.192	-0.185	0.364	-0.303
Mo	-0.413	0.684	0.619	-0.797	-0.273	-0.061	-0.597	0.342	-0.480	-0.787	0.279	-0.122	0.114	0.241	0.007	0.582	0.007
Ni	-0.670	0.809	0.854	-0.640	0.270	0.639	0.036	0.026	-0.069	-0.562	-0.034	0.007	0.234	-0.020	0.412	0.094	0.687
Sr	-0.168	0.442	0.339	-0.578	-0.280	-0.154	-0.494	0.563	-0.285	-0.538	0.511	-0.094	-0.267	0.459	-0.343	0.680	-0.261
V	0.204	0.167	-0.052	-0.264	-0.348	-0.363	-0.548	0.225	-0.246	-0.297	0.204	0.049	-0.238	0.185	-0.404	0.535	-0.399
Y	0.094	-0.179	-0.140	0.187	0.014	-0.021	0.128	0.035	0.109	0.182	0.060	0.090	-0.109	0.028	-0.462	-0.133	0.017
Ce	-0.259	0.240	0.318	-0.487	-0.348	-0.334	-0.401	0.553	-0.280	-0.405	0.502	-0.067	-0.102	0.439	-0.344	0.743	-0.350
As	0.596	0.122	-0.345	0.216	0.217	0.195	-0.131	-0.657	0.238	0.030	-0.643	0.246	-0.141	-0.602	-0.079	-0.303	0.248
Cd	-0.561	0.768	0.770	-0.527	0.336	0.653	0.113	-0.058	0.037	-0.471	-0.129	0.034	0.175	-0.084	0.425	0.060	0.681
Cr	0.327	-0.378	-0.426	0.573	0.160	0.149	0.632	-0.240	0.503	0.596	-0.219	-0.071	-0.225	-0.221	-0.221	-0.204	0.053
Pb	0.003	0.369	0.185	-0.324	-0.176	-0.062	-0.371	0.136	-0.148	-0.365	0.101	-0.040	-0.108	0.072	-0.289	0.400	0.074
Zn	-0.381	0.549	0.555	-0.551	-0.083	0.219	-0.095	0.488	-0.114	-0.408	0.411	-0.018	-0.231	0.368	-0.246	0.741	-0.117
Pd	0.330	-0.011	-0.252	0.270	0.313	0.443	0.280	-0.087	0.318	0.315	-0.137	-0.367	-0.570	0.087	-0.566	-0.087	-0.186
Pt	-0.328	0.177	0.313	-0.318	-0.125	0.163	0.093	0.466	-0.083	-0.059	0.424	-0.416	-0.315	0.529	-0.090	0.448	-0.237
Rh	-0.194	-0.314	-0.064	0.135	-0.023	-0.203	0.197	-0.118	0.056	0.152	-0.084	-0.301	0.460	-0.179	0.626	-0.176	0.122
Depth	-0.281	0.083	0.244	-0.273	-0.074	-0.141	-0.155	0.100	-0.305	-0.253	0.093	0.147	0.280	0.190	0.302	0.069	-0.075
Thick.	-0.491	0.063	0.351	-0.451	-0.315	-0.351	-0.303	0.694	-0.496	-0.360	0.685	-0.248	0.140	0.599	0.006	0.439	-0.331

	Cu	Mo	Ni	Sr	V	Y	Ce	As	Cd	Cr	Pb	Zn	Pd	Pt	Rh	Depth	
Mo	0.096																
Ni	0.237	0.356															
Sr	0.254	0.784	0.075														
V	-0.082	0.701	-0.289	0.764													
Y	0.082	-0.295	-0.049	-0.181	-0.276												
Ce	0.272	0.711	-0.042	0.792	0.687	-0.136											
As	-0.488	0.061	-0.161	-0.054	0.341	-0.038	-0.256										
Cd	0.141	0.326	0.871	0.041	-0.234	-0.212	0.038	-0.111									
Cr	-0.042	-0.549	-0.239	-0.347	-0.323	0.102	-0.220	-0.038	-0.111								
Pb	-0.363	0.671	-0.009	0.539	0.723	-0.202	0.618	0.309	0.148	-0.096							
Zn	0.472	0.650	0.401	0.733	0.422	-0.234	0.704	-0.307	0.431	-0.210	0.411						
Pd	0.343	-0.162	-0.131	0.050	-0.129	-0.158	0.032	-0.250	-0.114	0.424	-0.414	0.195					
Pt	0.538	0.136	0.292	0.376	-0.025	0.059	0.464	-0.565	0.168	-0.067	-0.399	0.564	0.355				
Rh	-0.029	-0.347	-0.009	-0.460	-0.466	0.024	-0.230	-0.214	0.003	0.244	-0.084	-0.415	-0.252	-0.107			
Depth	0.288	0.194	0.187	0.115	0.024	-0.008	0.166	-0.116	0.124	-0.432	-0.159	0.103	0.035	-0.137	-0.238		
Thick.	0.422	0.340	0.105	0.509	0.154	-0.028	0.424	-0.476	-0.132	-0.255	-0.121	0.376	-0.002	0.531	-0.010	0.226	

Table 15. Correlation coefficient matrix for 5 layers within crust CD2-8 listed in Table 7; n = 5, except for Pd = 4; the zero correlation for 5 points at the 95% confidence level is |0.883|.

	Fe	Mn	Mn/Fe	Si	Na	Mg	K	Ca	Ti	Al	P	H_2O^+	H_2O^-	CO_2	Ba	Co
Mn	-0.947															
Mn/Fe	-0.987	0.984														
Si	0.320	-0.216	-0.258													
Na	-0.284	0.356	0.319	0.733												
Mg	-0.323	0.509	0.418	0.672	0.906											
K	-0.356	0.418	0.416	0.742	0.790	0.798										
Ca	-0.742	0.636	0.723	-0.465	-0.248	-0.158	0.192									
Ti	-0.558	0.269	0.434	-0.311	-0.040	-0.302	0.111	0.653								
Al	0.039	-0.034	0.001	0.782	0.475	0.433	0.848	0.134	0.131							
P	0.618	-0.589	-0.646	-0.298	-0.397	-0.437	-0.829	-0.700	-0.472	-0.738						
H_2O^+	0.964	-0.861	-0.919	0.324	-0.339	-0.277	-0.281	-0.618	-0.644	0.121	0.495					
H_2O^-	-0.359	0.331	0.326	-0.956	-0.597	-0.476	-0.716	0.344	0.113	-0.879	0.372	-0.357				
CO_2	0.106	-0.034	-0.118	-0.173	0.162	0.116	-0.458	-0.632	-0.388	-0.733	0.748	-0.047	0.377			
Ba	-0.159	-0.002	0.118	-0.302	-0.541	-0.535	0.022	0.763	0.585	0.331	-0.506	-0.050	0.052	-0.869		
Co	-0.194	0.271	0.190	-0.167	0.338	0.315	-0.252	-0.437	-0.265	-0.662	0.508	-0.326	0.397	0.949	-0.860	
Cu	-0.307	0.245	0.325	0.236	0.047	0.088	0.631	0.695	0.450	0.785	-0.893	-0.158	-0.405	-0.967	0.785	-0.840
Mo	-0.462	0.508	0.489	-0.814	-0.597	-0.316	-0.397	0.641	0.049	-0.523	-0.034	-0.320	0.839	-0.067	0.348	0.015
Ni	-0.788	0.877	0.848	0.277	0.720	0.823	0.781	0.404	0.151	0.356	-0.734	-0.710	-0.150	-0.121	-0.143	0.185
Sr	-0.165	0.028	0.132	-0.446	-0.663	-0.603	-0.114	0.779	0.507	0.174	-0.407	-0.039	0.218	-0.793	0.981	-0.794
V	0.417	-0.400	-0.404	-0.539	-0.946	-0.756	-0.664	0.157	-0.215	-0.323	0.355	0.533	0.437	-0.241	0.496	-0.431
Y	0.268	-0.267	-0.309	-0.636	-0.508	-0.505	-0.918	-0.383	-0.272	-0.950	0.909	0.160	0.717	0.767	-0.396	0.608
Ce	-0.058	-0.120	0.004	-0.379	-0.649	-0.667	-0.130	0.689	0.570	0.222	-0.359	0.027	0.118	-0.795	0.986	-0.831
As	0.660	-0.509	-0.623	-0.165	-0.358	-0.240	-0.692	-0.711	-0.769	-0.627	0.917	0.629	0.298	0.669	-0.550	0.444
Cd	-0.731	0.828	0.771	0.103	0.717	0.776	0.467	0.118	0.019	-0.070	-0.319	-0.742	0.104	0.380	-0.525	0.647
Cr	-0.119	-0.111	-0.006	0.155	0.422	0.008	0.096	-0.191	0.591	0.044	0.027	-0.359	-0.227	0.249	-0.191	0.273
Pb	-0.013	-0.101	-0.067	-0.926	-0.756	-0.775	-0.926	0.123	0.174	-0.889	0.613	-0.086	0.887	0.391	0.107	0.286
Zn	-0.201	0.171	0.235	0.318	0.051	0.118	0.645	0.611	0.331	0.828	-0.859	-0.038	-0.475	-0.972	0.748	-0.869
Pd	-0.886	0.940	0.938	0.309	0.726	0.976	0.812	0.888	0.154	0.377	-0.790	-0.716	-0.057	-0.292	0.072	0.020
Pt	0.057	-0.148	-0.058	0.119	-0.309	-0.286	0.299	0.549	0.360	0.664	-0.600	0.193	-0.350	-0.979	0.902	-0.990
Rh	-0.084	0.011	0.095	0.369	0.041	0.034	0.608	0.521	0.388	0.862	-0.796	0.041	-0.561	-0.974	0.761	-0.910

	Cu	Mo	Ni	Sr	V	Y	Ce	As	Cd	Cr	Pb	Zn	Pd	Pt
Mo	0.050													
Ni	0.362	0.082												
Sr	0.694	0.508	-0.189											
V	0.022	0.561	-0.680	0.620										
Y	-0.872	0.315	-0.581	-0.255	0.390									
Ce	0.679	0.348	-0.296	0.979	0.583	-0.259								
As	-0.810	0.063	-0.608	-0.428	0.440	0.796	-0.436							
Cd	-0.137	0.085	0.868	-0.528	-0.745	-0.139	-0.628	-0.266						
Cr	-0.169	-0.614	0.010	-0.314	-0.652	-0.014	-0.164	-0.322	0.164					
Pb	-0.504	0.587	-0.551	0.246	0.554	0.845	0.232	0.427	-0.260	-0.012				
Zn	0.990	0.006	0.325	0.658	0.059	-0.885	0.643	-0.736	-0.186	-0.244	-0.565			
Pd	0.501	0.467	0.971	0.059	-0.513	-0.610	-0.150	-0.620	0.769	-0.238	-0.682	0.461		
Pt	0.896	0.047	-0.086	0.834	0.379	-0.651	0.859	-0.548	-0.561	-0.248	-0.280	0.909	0.087	
Rh	0.969	-0.141	0.199	0.648	0.046	-0.873	0.674	-0.729	-0.303	-0.107	-0.560	0.979	0.303	0.937

Table 16. Correlation coefficient matrix for 5 layers within crust CD2-38 listed in Table 7; the zero correlation for 5 points at the 95% confidence level is |0.883|.

	Fe	Mn	Mn/Fe	Si	Na	Mg	K	Ca	Ti	Al	P	H_2O^+	H_2O^-	CO_2	Ba	Co
Mn	0.325															
Mn/Fe	-0.345	0.774														
Si	0.176	0.005	-0.125													
Na	0.166	0.811	0.686	0.550												
Mg	0.367	0.745	0.487	0.668	0.965											
K	-0.176	0.418	0.512	0.743	0.842	0.785										
Ca	-0.525	-0.937	-0.575	-0.302	-0.885	-0.897	-0.528									
Ti	-0.212	0.722	0.878	-0.335	0.489	0.336	0.151	-0.498								
Al	-0.411	-0.466	-0.209	0.734	0.110	0.122	0.607	0.292	-0.524							
P	-0.500	-0.946	-0.601	-0.288	-0.891	-0.894	-0.536	0.999	-0.517	0.293						
H_2O^+	0.764	0.825	0.313	0.225	0.688	0.776	0.236	-0.927	0.390	-0.471	-0.917					
H_2O^-	0.411	0.955	0.666	0.280	0.913	0.889	0.598	-0.988	0.533	-0.242	-0.992	0.861				
CO_2	-0.532	-0.949	-0.581	-0.248	-0.862	-0.866	-0.498	0.997	-0.496	0.329	0.997	-0.922	-0.989			
Ba	-0.702	-0.329	0.145	-0.790	-0.596	-0.784	-0.450	0.631	0.163	-0.179	0.609	-0.716	-0.544	0.591		
Co	0.574	0.900	0.518	0.221	0.795	0.834	0.351	-0.954	0.586	-0.440	-0.950	0.965	0.909	-0.942	-0.641	
Cu	-0.881	-0.263	0.310	-0.200	-0.152	-0.365	0.239	0.451	0.015	0.440	0.424	-0.743	-0.308	0.430	0.724	-0.622
Mo	0.375	0.905	0.652	-0.389	0.486	0.414	0.011	-0.761	0.719	-0.778	-0.770	0.738	0.766	-0.794	-0.067	0.771
Ni	-0.004	0.797	0.783	0.475	0.981	0.898	0.875	-0.820	0.540	0.149	-0.831	0.566	0.876	-0.802	-0.439	0.703
Sr	-0.339	-0.460	-0.215	-0.886	-0.848	-0.925	-0.846	0.701	0.016	-0.440	0.693	-0.580	-0.692	0.663	0.855	-0.595
V	0.559	0.452	0.090	-0.673	-0.120	-0.099	-0.609	-0.325	0.370	-0.977	-0.322	0.525	0.267	-0.368	0.083	0.443
Y	0.008	-0.844	-0.851	0.485	-0.462	-0.305	-0.080	0.608	-0.886	0.678	0.627	-0.493	-0.655	0.638	-0.204	-0.612
Ce	-0.541	-0.326	0.052	-0.896	-0.690	-0.836	-0.669	0.626	0.217	-0.396	0.609	-0.605	-0.579	0.588	0.952	-0.551
As	0.904	0.694	0.086	0.177	0.513	0.642	0.077	-0.828	0.173	-0.499	-0.812	0.962	0.745	-0.833	-0.717	0.859
Cd	0.247	0.917	0.741	0.379	0.975	0.934	0.707	-0.948	0.612	-0.114	-0.954	0.787	0.967	-0.933	-0.545	0.889
Cr	-0.316	-0.465	-0.249	0.757	0.104	0.175	0.445	0.271	-0.318	0.825	0.279	-0.318	-0.284	0.337	-0.341	-0.250
Pb	0.467	0.351	0.067	-0.546	-0.114	-0.062	-0.621	-0.249	0.492	-0.920	-0.243	0.505	0.157	-0.260	-0.018	0.483
Zn	-0.577	0.439	0.816	-0.538	0.201	-0.054	0.160	-0.131	0.672	-0.257	-0.163	-0.131	0.256	-0.169	0.654	0.034
Pd	-0.250	0.595	0.754	0.543	0.899	0.805	0.893	-0.613	0.549	0.326	-0.626	0.349	0.672	-0.576	-0.360	0.539
Pt	-0.613	-0.190	0.189	0.041	-0.008	-0.168	0.413	0.270	-0.238	0.571	0.250	-0.575	-0.132	0.243	0.454	-0.530
Rh	-0.674	-0.585	-0.156	0.030	-0.349	-0.458	0.169	0.631	-0.482	0.676	0.617	-0.839	-0.523	0.615	0.528	-0.825

	Cu	Mo	Ni	Sr	V	Y	Ce	As	Cd	Cr	Pb	Zn	Pd	Pt
Mo	-0.290													
Ni	0.035	0.476												
Sr	0.292	-0.075	-0.774											
V	-0.508	0.766	-0.179	0.377										
Y	-0.025	-0.923	-0.518	-0.056	-0.597									
Ce	0.483	0.009	-0.573	0.956	0.292	-0.229								
As	-0.812	0.671	0.372	-0.496	0.599	-0.355	-0.588							
Cd	-0.239	0.662	0.950	-0.744	0.097	-0.621	-0.593	0.617						
Cr	0.081	-0.772	0.083	-0.420	-0.866	0.680	-0.413	-0.397	-0.084					
Pb	-0.654	0.609	-0.200	0.349	0.875	-0.491	0.264	0.514	0.089	-0.544				
Zn	0.661	0.503	0.363	0.282	0.150	-0.765	0.528	-0.271	0.271	-0.481	-0.022			
Pd	0.146	0.233	0.934	-0.719	-0.409	-0.369	-0.496	0.111	0.828	0.362	-0.286	0.325		
Pt	0.898	-0.284	0.147	0.015	-0.551	0.093	0.162	-0.583	-0.127	0.061	-0.834	0.493	0.151	
Rh	0.868	-0.626	-0.211	0.214	-0.661	0.430	0.286	-0.799	-0.493	0.266	-0.838	0.234	-0.110	0.906

Table 17. Correlation coefficient matrix of selected elements from Table 7 and REEs from Table 11 for 14 bulk crusts. The zero correlation for 14 points at 95% confidence level is |0.531|.

	La	Ce	Pr	Nd	Sm	Eu	Gd	Tb	Dy	Ho	Er	Tm	Yb	Lu	REE*	Ce*
Ce	-0.120															
Pr	0.775	0.127														
Nd	0.828	0.013	0.989													
Sm	0.758	0.022	0.985	0.987												
Eu	0.786	-0.054	0.972	0.987	0.994											
Gd	0.865	-0.159	0.934	0.973	0.963	0.979										
Tb	0.841	-0.146	0.945	0.979	0.972	0.989	0.993									
Dy	0.859	-0.342	0.837	0.905	0.886	0.926	0.970	0.967								
Ho	0.869	-0.504	0.653	0.754	0.708	0.767	0.867	0.847	0.949							
Er	0.821	-0.575	0.504	0.620	0.566	0.631	0.760	0.729	0.869	0.979						
Tm	0.780	-0.593	0.396	0.511	0.461	0.532	0.668	0.632	0.794	0.926	0.969					
Yb	0.809	-0.552	0.418	0.535	0.467	0.537	0.677	0.644	0.800	0.943	0.985	0.980				
Lu	0.739	-0.625	0.315	0.441	0.362	0.434	0.589	0.554	0.729	0.900	0.951	0.940	0.972			
REE*	0.269	0.912	0.506	0.413	0.409	0.343	0.255	0.264	0.067	-0.122	-0.232	-0.284	-0.235	-0.341		
Ce*	-0.572	0.873	-0.288	-0.402	-0.358	-0.434	-0.547	-0.531	-0.689	-0.815	-0.845	-0.840	-0.818	-0.840	0.613	
Fe	0.490	-0.010	0.770	0.772	0.776	0.788	0.715	0.760	0.676	0.474	0.311	0.232	0.213	0.158	0.274	-0.281
Mn	-0.195	0.082	-0.429	-0.434	-0.501	-0.533	-0.451	-0.503	-0.462	-0.329	-0.252	-0.208	-0.171	-0.021	-0.080	0.179
Mn/Fe	-0.446	0.047	-0.736	-0.737	-0.766	-0.789	-0.701	-0.756	-0.677	-0.480	-0.333	-0.265	-0.234	-0.126	-0.227	0.292
Si	0.433	-0.426	0.567	0.608	0.648	0.698	0.667	0.697	0.718	0.622	0.549	0.539	0.472	0.347	-0.158	-0.583
Ca	-0.432	0.165	-0.660	-0.684	-0.663	-0.680	-0.661	-0.670	-0.659	-0.551	-0.475	-0.394	-0.425	-0.355	-0.102	0.395
Al	0.175	-0.430	0.264	0.273	0.330	0.372	0.332	0.353	0.374	0.309	0.276	0.352	0.237	0.115	-0.295	-0.473
P	-0.409	0.134	-0.638	-0.656	-0.629	-0.640	-0.623	-0.626	-0.610	-0.504	-0.428	-0.350	-0.384	-0.325	-0.118	0.362
H_2O^-	-0.077	0.028	-0.058	-0.051	-0.039	-0.040	-0.028	-0.045	-0.019	0.027	0.113	0.099	0.127	0.010	0.009	0.043
Ba	0.083	-0.154	-0.443	-0.403	-0.476	-0.440	-0.317	-0.374	-0.235	-0.022	0.100	0.259	0.215	0.264	-0.241	-0.140
Co	-0.175	-0.659	-0.411	-0.303	-0.324	-0.278	-0.162	-0.184	0.003	0.215	0.354	0.320	0.365	0.452	-0.715	-0.441
Cu	-0.008	0.168	-0.034	-0.113	-0.122	-0.163	-0.186	-0.208	-0.291	-0.305	-0.290	-0.190	-0.244	-0.288	0.111	0.094
Ni	-0.194	-0.297	-0.640	-0.594	-0.661	-0.649	-0.516	-0.572	-0.423	-0.166	0.006	0.111	0.119	0.229	-0.470	-0.136
Pt	-0.173	0.068	-0.432	-0.450	-0.494	-0.507	-0.440	-0.503	-0.488	-0.369	-0.297	-0.211	-0.234	-0.165	-0.095	0.130
Depth	-0.055	0.612	0.058	-0.030	-0.018	-0.076	-0.162	-0.132	-0.265	-0.376	-0.404	-0.342	-0.379	-0.441	0.547	0.504
Thick.	-0.005	0.502	-0.306	-0.353	-0.421	-0.452	-0.409	-0.450	-0.487	-0.389	-0.316	-0.246	-0.221	-0.206	0.362	0.422

	Fe	Mn	Mn/Fe	Si	Ca	Al	P	H_2O^-	Ba	Co	Cu	Ni	Pt	Depth
Mn	-0.474													
Mn/Fe	-0.906	0.792												
Si	0.648	-0.819	-0.844											
Ca	-0.586	0.307	0.559	-0.587										
Al	0.337	-0.683	-0.586	0.856	-0.322									
P	-0.556	0.211	0.494	-0.512	0.993	-0.269								
H_2O^-	-0.395	-0.314	0.109	0.155	-0.282	0.181	-0.253							
Ba	-0.435	0.616	0.583	-0.413	0.413	-0.202	0.364	-0.231						
Co	-0.443	0.141	0.392	-0.065	-0.078	-0.135	-0.058	0.402	0.069					
Cu	-0.266	0.259	0.243	-0.148	0.152	0.264	0.094	0.073	0.279	-0.387				
Ni	-0.756	0.767	0.861	-0.583	0.322	-0.343	0.267	0.114	0.718	0.538	0.306			
Pt	-0.326	0.543	0.449	-0.468	0.434	-0.177	0.371	-0.305	0.546	-0.144	0.456	0.460		
Depth	-0.093	0.166	0.137	-0.324	0.257	-0.212	0.232	0.019	0.114	-0.478	0.437	0.018	-0.141	
Thick.	-0.480	0.460	0.510	-0.635	0.571	-0.422	0.523	0.001	0.533	-0.318	0.491	0.402	0.606	0.447

Table 18. Correlation coefficient matrix of selected elements from Table 7 and REEs from Table 11 for 5 layers from crust CD2-8; use in conjunction with Table 15.

	La	Ce	Pr	Nd	Sm	Eu	Gd	Tb	Dy	Ho	Er	Tm	Yb	Lu	REE*	Ce*
Ce	-0.174															
Pr	0.998	-0.215														
Nd	0.979	-0.368	0.986													
Sm	0.956	-0.442	0.968	0.995												
Eu	0.922	-0.526	0.936	0.980	0.993											
Gd	0.890	-0.589	0.911	0.964	0.984	0.994										
Tb	0.879	-0.616	0.901	0.956	0.975	0.983	0.994									
Dy	0.868	-0.640	0.887	0.950	0.969	0.985	0.992	0.996								
Ho	0.859	-0.650	0.879	0.941	0.959	0.973	0.984	0.996	0.997							
Er	0.859	-0.641	0.882	0.940	0.958	0.967	0.983	0.997	0.993	0.998						
Tm	0.836	-0.650	0.854	0.916	0.928	0.939	0.952	0.978	0.979	0.991	0.990					
Yb	0.848	-0.625	0.869	0.922	0.935	0.939	0.955	0.982	0.976	0.989	0.993	0.997				
Lu	0.830	-0.635	0.849	0.905	0.916	0.922	0.937	0.969	0.966	0.982	0.984	0.998	0.997			
REE*	0.162	0.944	0.121	-0.040	-0.121	-0.217	-0.291	-0.321	-0.349	-0.363	-0.353	-0.371	-0.342	-0.358		
Ce*	-0.499	0.930	-0.536	-0.658	-0.711	-0.764	-0.816	-0.848	-0.857	-0.872	-0.871	-0.879	-0.867	-0.871	0.764	
Fe	0.224	-0.044	0.237	0.251	0.293	0.315	0.300	0.198	0.203	0.137	0.127	0.001	0.008	-0.049	0.035	-0.014
Mn	-0.243	-0.150	-0.260	-0.231	-0.260	-0.246	-0.236	-0.140	-0.120	-0.063	-0.070	0.069	0.037	0.105	-0.238	-0.122
Mn/Fe	-0.274	-0.020	-0.291	-0.287	-0.324	-0.328	-0.317	-0.218	-0.210	-0.148	-0.147	-0.013	-0.033	0.031	-0.118	-0.011
Si	-0.670	-0.413	-0.630	-0.531	-0.446	-0.370	-0.301	-0.323	-0.312	-0.325	-0.324	-0.373	-0.380	-0.395	-0.635	-0.090
Ca	-0.341	0.667	-0.386	-0.482	-0.560	-0.613	-0.655	-0.605	-0.607	-0.572	-0.572	-0.475	-0.481	-0.437	0.549	0.644
Al	-0.959	0.176	-0.948	-0.932	-0.895	-0.862	-0.826	-0.839	-0.836	-0.840	-0.836	-0.854	-0.856	-0.858	-0.144	0.505
P	0.888	-0.310	0.901	0.916	0.929	0.924	0.906	0.857	0.852	0.819	0.815	0.741	0.752	0.713	-0.010	-0.536
H_2O^-	0.740	0.146	0.704	0.648	0.576	0.527	0.466	0.497	0.500	0.516	0.507	0.573	0.564	0.589	0.391	-0.162
Ba	-0.366	0.973	-0.409	-0.547	-0.617	-0.686	-0.745	-0.763	-0.777	-0.782	-0.778	-0.767	-0.753	-0.751	0.851	0.973
Co	0.607	-0.800	0.637	0.726	0.755	0.780	0.824	0.876	0.875	0.904	0.909	0.938	0.934	0.946	-0.599	-0.954
Cu	-0.857	0.632	-0.883	-0.943	-0.970	-0.983	-0.997	-0.992	-0.989	-0.982	-0.983	-0.948	-0.954	-0.934	0.344	0.844
Ni	-0.572	-0.339	-0.567	-0.493	-0.480	-0.433	-0.387	-0.301	-0.279	-0.228	-0.232	-0.121	-0.152	-0.094	-0.536	-0.159
Pt	-0.643	0.828	-0.675	-0.770	-0.805	-0.836	-0.878	-0.916	-0.917	-0.937	-0.940	-0.954	-0.949	-0.954	0.613	0.975

	Fe	Mn	Mn/Fe	Si	Ca	Al	P	H_2O^-	Ba	Co	Cu	Ni
Mn	-0.947											
Mn/Fe	-0.987	0.984										
Si	0.320	-0.216	-0.258									
Ca	-0.742	0.636	0.723	-0.465								
Al	0.039	-0.034	0.001	0.782	0.134							
P	0.618	-0.589	-0.646	-0.298	-0.700	-0.738						
H_2O^-	-0.359	0.331	0.326	-0.956	0.344	-0.879	0.372					
Ba	-0.159	-0.002	0.118	-0.302	0.763	0.331	-0.506	0.052				
Co	-0.194	0.271	0.190	-0.167	-0.437	-0.662	0.508	0.397	-0.860			
Cu	-0.307	0.245	0.325	0.236	0.695	0.785	-0.893	-0.405	0.785	-0.840		
Ni	-0.788	0.877	0.848	0.277	0.404	0.356	-0.734	-0.150	-0.143	0.185	0.362	
Pt	0.057	-0.148	-0.058	0.119	0.549	0.664	-0.600	-0.350	0.902	-0.990	0.896	-0.086

Table 19. Correlation coefficient matrix of selected elements from Table 7 and REEs from Table 11 for 5 layers from crust CD2-38; use in conjunction with Table 16.

	La	Ce	Pr	Nd	Sm	Eu	Gd	Tb	Dy	Ho	Er	Tm	Yb	Lu	REE*	Ce*
Ce	-0.234															
Pr	0.946	-0.326														
Nd	0.955	-0.384	0.996													
Sm	0.906	-0.529	0.974	0.985												
Eu	0.883	-0.605	0.946	0.966	0.995											
Gd	0.901	-0.607	0.940	0.964	0.989	0.997										
Tb	0.870	-0.633	0.937	0.958	0.991	0.998	0.996									
Dy	0.866	-0.678	0.903	0.933	0.973	0.990	0.995	0.992								
Ho	0.844	-0.700	0.817	0.863	0.904	0.936	0.956	0.938	0.973							
Er	0.803	-0.722	0.751	0.805	0.850	0.890	0.918	0.895	0.943	0.994						
Tm	0.778	-0.760	0.738	0.793	0.846	0.888	0.915	0.897	0.944	0.990	0.997					
Yb	0.743	-0.746	0.669	0.729	0.781	0.829	0.863	0.838	0.899	0.971	0.991	0.993				
Lu	0.587	-0.735	0.460	0.534	0.593	0.658	0.704	0.669	0.755	0.880	0.928	0.928	0.965			
REE*	0.415	0.784	0.320	0.266	0.102	0.014	0.016	-0.022	-0.075	-0.127	-0.182	-0.232	-0.251	-0.356		
Ce*	-0.723	0.825	-0.759	-0.802	-0.872	-0.907	-0.922	-0.927	-0.952	-0.946	-0.939	-0.960	-0.931	-0.828	0.313	
Fe	0.717	-0.586	0.829	0.846	0.897	0.912	0.887	0.896	0.880	0.817	0.764	0.751	0.678	0.522	-0.059	-0.748
Mn	-0.200	-0.344	0.129	0.096	0.188	0.182	0.113	0.198	0.115	-0.072	-0.139	-0.096	-0.195	-0.341	-0.373	-0.139
Mn/Fe	-0.655	0.060	-0.404	-0.450	-0.396	-0.415	-0.466	-0.388	-0.462	-0.610	-0.644	-0.592	-0.643	-0.690	-0.307	0.351
Si	-0.004	-0.874	-0.031	0.044	0.177	0.267	0.299	0.304	0.390	0.499	0.570	0.611	0.655	0.757	-0.852	-0.625
Ca	0.039	0.644	-0.263	-0.257	-0.383	-0.404	-0.348	-0.424	-0.372	-0.226	-0.175	-0.221	-0.132	-0.002	0.564	0.429
Al	-0.390	-0.331	-0.569	-0.500	-0.430	-0.349	-0.295	-0.324	-0.212	-0.014	0.097	0.115	0.221	0.458	-0.622	-0.017
P	0.067	0.625	-0.237	-0.230	-0.355	-0.376	-0.318	-0.396	-0.342	-0.194	-0.144	-0.190	-0.101	0.027	0.564	0.401
H_2O^-	-0.190	-0.585	0.116	0.107	0.237	0.261	0.202	0.282	0.229	0.087	0.042	0.090	0.007	-0.099	-0.605	-0.301
Ba	-0.430	0.976	-0.521	-0.574	-0.698	-0.759	-0.762	-0.784	-0.817	-0.818	-0.824	-0.858	-0.831	-0.773	0.633	0.923
Co	0.176	-0.596	0.470	0.454	0.551	0.551	0.500	0.574	0.508	0.337	0.271	0.317	0.218	0.035	-0.381	-0.544
Cu	-0.872	0.559	-0.963	-0.973	-0.995	-0.989	-0.981	-0.990	-0.966	-0.884	-0.828	-0.831	-0.761	-0.565	-0.057	0.885
Ni	-0.509	-0.554	-0.265	-0.261	-0.119	-0.079	-0.117	-0.040	-0.062	-0.144	-0.145	-0.080	-0.117	-0.124	-0.803	-0.138
Pt	-0.857	0.257	-0.930	-0.914	-0.881	-0.838	-0.836	-0.845	-0.797	-0.683	-0.616	-0.623	-0.554	-0.332	-0.329	0.716

	Fe	Mn	Mn/Fe	Si	Ca	Al	P	H_2O^-	Ba	Co	Cu	Ni
Mn	0.325											
Mn/Fe	-0.345	0.774										
Si	0.176	0.005	-0.125									
Ca	-0.525	-0.937	-0.575	-0.302								
Al	-0.411	-0.466	-0.209	0.734	0.292							
P	-0.500	-0.946	-0.601	-0.288	0.999	0.293						
H_2O^-	0.411	0.955	0.666	0.280	-0.988	-0.242	-0.992					
Ba	-0.702	-0.329	0.145	-0.790	0.631	-0.179	0.609	-0.544				
Co	0.574	0.900	0.518	0.221	-0.954	-0.440	-0.950	0.909	-0.641			
Cu	-0.881	-0.263	0.310	-0.200	0.451	0.440	0.424	-0.308	0.724	-0.622		
Ni	-0.004	0.797	0.783	0.475	-0.820	0.149	-0.831	0.876	-0.439	0.703	0.035	
Pt	-0.613	-0.190	0.189	0.041	0.270	0.571	0.250	-0.132	0.454	-0.530	0.898	0.147

Table 20. Correlation coefficient matrix for the innermost 5mm of 23 crusts from Table 7, including selected elements and element ratios of the adjacent substrate rock from Table 4; n = 23, except for LOI, substrate Mn*, substrate Mn/Fe* = 21; the zero correlation for 23 points at the 95% confidence level is |0.412|. Elements and ratios with an * are from substrate rocks.

	Fe	Mn	Mn/Fe	Si	Na	Mg	K	Ca	Ti	Al	P	H_2O^+	H_2O^-	CO_2	LOI	Ba	Co	Cu	Mo	Ni	Sr
Mn	-0.057																				
Mn/Fe	-0.871	0.469																			
Si	0.760	-0.423	-0.736																		
Na	0.700	0.248	-0.457	0.611																	
Mg	-0.147	0.353	0.419	0.128	0.158																
K	0.109	-0.196	0.007	0.628	0.302	0.709															
Ca	-0.859	-0.378	0.559	-0.598	-0.831	-0.126	-0.153														
Ti	0.915	-0.011	-0.802	0.763	0.717	0.021	0.195	-0.863													
Al	0.621	-0.520	-0.660	0.962	0.473	0.167	0.694	-0.442	0.675												
P	-0.844	-0.413	0.536	-0.562	-0.816	-0.106	-0.115	0.998	-0.845	-0.406											
H_2O^+	0.400	0.503	0.001	0.320	0.532	0.633	0.466	-0.574	0.425	0.242	-0.563										
H_2O^-	0.787	0.486	-0.474	0.445	0.803	0.070	0.021	-0.942	0.762	0.253	-0.944	0.573									
CO_2	-0.517	-0.217	0.222	-0.586	-0.500	-0.715	-0.661	0.620	-0.580	-0.519	0.592	-0.747	-0.534								
LOI	0.526	0.390	-0.220	0.318	0.648	0.709	0.403	-0.795	0.552	0.205	-0.800	0.806	0.963	-0.845							
Ba	-0.801	0.195	0.821	-0.656	-0.705	0.162	-0.027	0.676	-0.822	-0.519	0.647	-0.136	-0.640	0.338	-0.477						
Co	0.655	0.402	-0.406	0.443	0.814	0.237	0.131	-0.849	0.712	0.268	-0.839	0.450	0.849	-0.564	0.705	-0.740					
Cu	0.187	0.019	-0.167	0.277	0.004	0.336	0.358	-0.222	0.335	0.385	-0.215	0.190	0.109	-0.439	0.226	-0.057	0.071				
Mo	-0.303	0.719	0.524	-0.719	-0.134	-0.163	-0.553	0.060	-0.433	-0.776	0.014	0.095	0.086	0.360	-0.135	0.488	-0.105	-0.315			
Ni	-0.474	0.480	0.690	-0.246	-0.026	0.894	0.461	0.111	-0.273	-0.197	0.119	0.398	-0.098	-0.426	0.487	0.344	0.124	0.221	0.072		
Sr	-0.519	0.299	0.482	-0.860	-0.573	-0.421	-0.715	0.513	-0.642	-0.827	0.472	-0.311	-0.358	0.652	-0.363	0.632	-0.562	-0.272	0.774	-0.146	
V	-0.205	0.640	0.397	-0.669	-0.141	-0.322	-0.631	0.037	-0.375	-0.750	-0.010	0.048	0.122	0.405	-0.165	0.439	-0.129	-0.381	0.969	-0.115	0.808
Y	-0.633	-0.518	0.260	-0.352	-0.628	-0.279	-0.102	0.836	-0.633	-0.214	0.841	-0.616	-0.726	0.635	-0.536	0.434	-0.706	-0.139	-0.135	-0.103	0.356
Ce	-0.440	0.319	0.481	-0.666	-0.383	-0.385	-0.524	0.369	-0.552	-0.615	0.323	-0.216	-0.304	0.631	-0.510	0.634	-0.500	-0.299	0.776	-0.185	0.836
As	0.805	0.460	-0.514	0.320	0.663	-0.026	-0.144	-0.859	0.710	0.117	-0.860	0.565	0.912	-0.484	0.795	-0.610	0.759	0.058	0.170	-0.209	-0.181
Cd	-0.424	0.580	0.726	-0.242	0.007	0.777	0.406	0.026	-0.298	-0.218	0.017	0.391	-0.004	-0.357	0.315	0.460	0.115	0.048	0.249	0.857	-0.060
Cr	0.177	-0.429	-0.171	0.670	0.147	0.435	0.839	-0.076	0.171	0.728	-0.042	0.319	-0.075	-0.452	0.101	-0.053	-0.019	0.234	-0.583	0.151	-0.654
Pb	-0.304	0.473	0.457	-0.615	-0.186	-0.316	-0.528	0.180	-0.485	-0.667	0.136	-0.032	-0.054	0.499	-0.342	0.505	-0.233	-0.588	0.865	-0.145	0.746
Zn	-0.754	0.433	0.944	-0.533	-0.347	0.573	0.243	0.451	-0.676	-0.431	0.435	0.168	-0.429	0.032	-0.141	0.798	-0.384	-0.051	0.406	0.729	0.326
Depth	-0.572	-0.014	0.603	-0.294	-0.502	0.613	0.358	0.523	-0.529	-0.191	0.536	0.099	-0.581	-0.257	0.226	0.561	-0.421	0.114	-0.056	0.652	0.075
Si*	0.717	0.211	-0.454	0.520	0.584	0.120	0.158	-0.737	0.660	0.384	-0.731	0.539	0.711	-0.614	0.534	-0.532	0.577	0.117	-0.094	-0.118	-0.409
Al*	0.682	0.259	-0.423	0.505	0.693	0.188	0.182	-0.750	0.671	0.349	-0.737	0.565	0.746	-0.640	0.635	-0.612	0.709	0.039	-0.114	0.008	-0.468
Fe*	-0.446	0.355	0.602	-0.385	-0.210	0.023	-0.073	0.232	-0.524	-0.421	0.202	0.042	-0.087	0.309	-0.242	0.587	-0.238	-0.503	0.536	0.157	0.355
Na*	0.622	0.197	-0.405	0.534	0.694	0.163	0.267	-0.719	0.637	0.403	-0.706	0.413	0.685	-0.622	0.528	-0.583	0.670	0.198	-0.206	0.018	-0.499
K*	0.517	0.094	-0.341	0.432	0.389	-0.012	0.111	-0.534	0.498	0.343	-0.538	0.341	0.466	-0.385	0.123	-0.358	0.314	0.158	-0.145	-0.187	-0.323
Mg*	0.454	0.164	-0.240	0.199	0.131	-0.022	-0.048	-0.388	0.299	0.139	-0.398	0.389	0.357	-0.279	0.155	-0.140	0.122	0.081	0.182	-0.242	-0.015
Ca*	-0.460	-0.409	0.143	-0.246	-0.371	-0.063	-0.030	0.583	-0.364	-0.106	0.598	-0.547	-0.636	0.377	-0.389	0.142	-0.368	0.108	-0.264	0.091	0.121
Ti*	0.614	0.293	-0.348	0.365	0.541	0.161	0.068	-0.640	0.549	0.190	-0.628	0.615	0.680	-0.524	0.603	-0.495	0.614	-0.170	0.036	-0.016	-0.304
P*	-0.501	-0.176	0.314	-0.307	-0.399	0.077	0.014	0.487	-0.397	-0.160	0.484	-0.439	-0.602	0.296	-0.493	0.355	-0.400	0.187	-0.129	0.197	0.161
Mn*	-0.203	-0.122	0.079	-0.167	-0.285	-0.219	-0.170	0.280	-0.160	-0.090	0.262	-0.307	-0.240	0.336	-0.316	0.197	-0.300	0.129	-0.036	-0.181	0.248
Mn/Fe*	0.014	-0.148	-0.118	0.088	-0.019	0.007	0.041	-0.058	0.146	0.177	-0.065	-0.155	-0.094	0.005	-0.159	-0.049	-0.036	0.362	-0.262	-0.034	-0.168
Mg/Al*	-0.487	-0.412	0.136	-0.423	-0.601	-0.567	-0.401	0.700	-0.560	-0.335	0.687	-0.702	-0.569	0.759	-0.559	0.379	-0.643	-0.232	0.069	-0.381	0.531

	V	Y	Ce	As	Cd	Cr	Pb	Zn	Depth	Si*	Al*	Fe*	Na*	K*	Mg*	Ca*	Ti*	P*	Mn*	Mn/Fe*
Y	-0.097																			
Ce	0.794	0.197																		
As	0.235	-0.722	-0.211																	
Cd	0.097	-0.179	-0.002	-0.167																
Cr	-0.613	-0.004	-0.503	-0.174	0.118															
Pb	0.899	0.029	0.875	0.029	0.135	-0.472														
Zn	0.268	0.146	0.430	-0.490	0.775	0.019	0.372													
Depth	-0.171	0.138	-0.029	-0.494	0.509	0.229	-0.110	0.663												
Si*	-0.086	-0.753	-0.352	0.669	-0.031	0.185	-0.174	-0.354	-0.216											
Al*	-0.119	-0.759	-0.448	0.678	0.017	0.159	-0.223	-0.351	-0.224	0.940										
Fe*	0.540	0.177	0.461	-0.204	0.455	-0.029	0.650	0.532	0.006	-0.154	-0.173									
Na*	-0.212	-0.674	-0.484	0.580	0.002	0.177	-0.356	-0.327	-0.194	0.837	0.892	-0.258								
K*	-0.114	-0.558	-0.251	0.391	-0.053	0.243	-0.170	-0.283	-0.194	0.835	0.728	-0.071	0.728							
Mg*	0.181	-0.522	0.095	0.447	-0.089	0.074	0.158	-0.138	-0.077	0.730	0.500	-0.006	0.308	0.608						
Ca*	-0.291	0.603	0.040	-0.562	-0.161	-0.121	-0.218	0.106	0.252	-0.813	-0.723	-0.394	-0.564	-0.725	-0.699					
Ti*	0.059	-0.680	-0.291	0.704	-0.035	0.138	-0.001	-0.287	-0.211	0.748	0.845	-0.015	0.603	0.432	0.437	-0.660				
P*	-0.162	0.443	0.178	-0.547	0.068	-0.083	-0.078	0.320	0.321	-0.783	-0.764	-0.220	-0.589	-0.597	-0.603	0.858	-0.707			
Mn*	0.012	0.533	0.416	-0.261	-0.176	-0.104	0.221	0.063	-0.070	-0.264	-0.408	0.014	-0.335	-0.023	-0.009	0.249	-0.435	0.321		
Mn/Fe*	-0.286	0.082	0.063	-0.128	-0.137	-0.046	-0.187	-0.063	-0.003	-0.323	-0.401	-0.416	-0.233	-0.183	-0.220	0.516	-0.487	0.564	0.634	
Mg/Al*	0.163	0.894	0.412	-0.523	-0.349	-0.286	0.266	-0.020	-0.100	-0.671	-0.740	0.213	-0.667	-0.486	-0.354	0.468	-0.677	0.343	0.622	0.172

Figure 1. Location of dredge sites on Karin Ridge and south Johnston Island ridge, central Pacific.

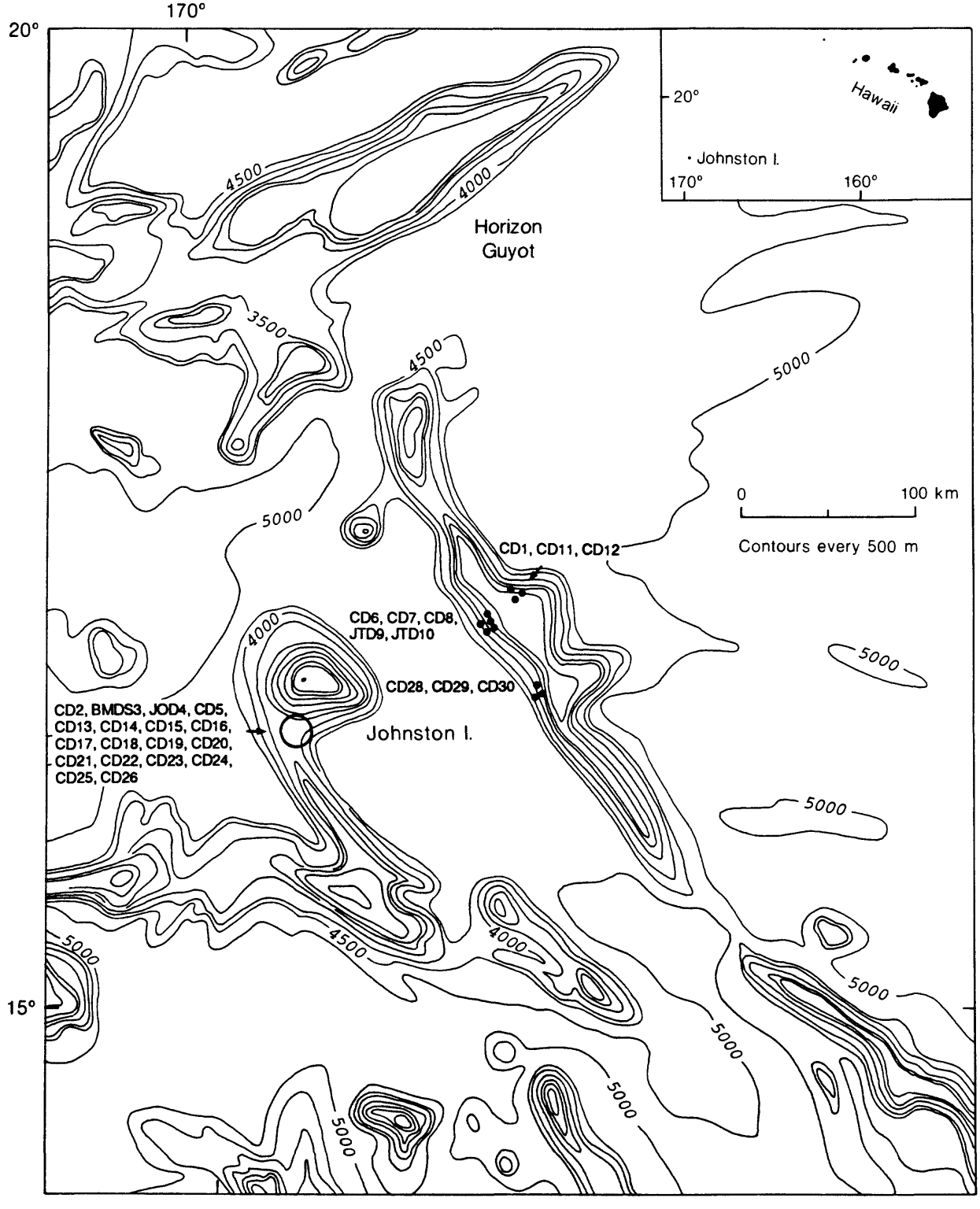

Figure 2. Chondrite-normalized REE plot. Shaded field represents complete data set for 42 samples (see Table 11). Chondrite composition for Figures 2-13 from Haskin et al. (1968).

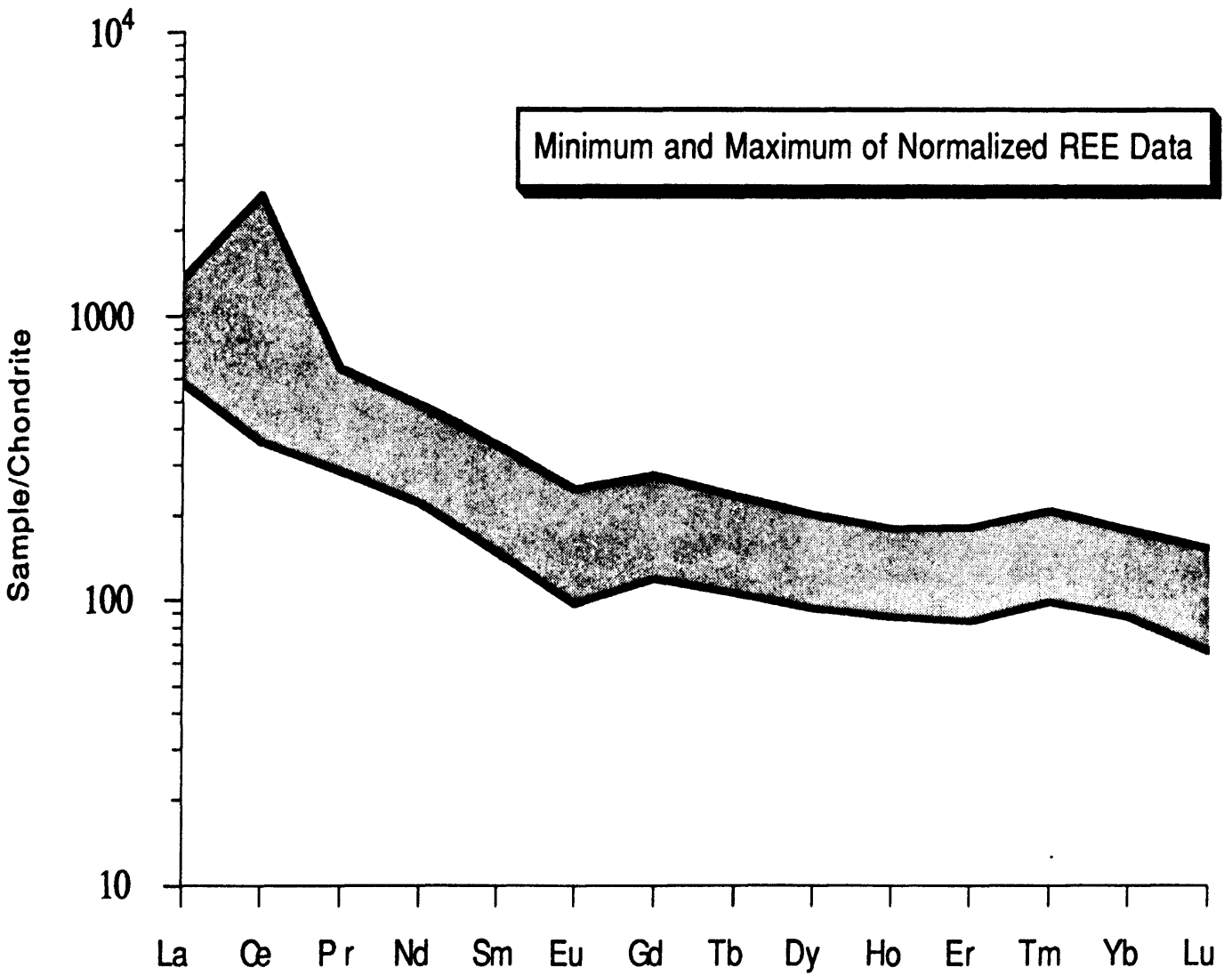

Figure 3. Chondrite-normalized REE plot of Central Karin Ridge bulk crusts. In Figures 3-13, B = Bulk and L = layer, followed by interval in millimeters.

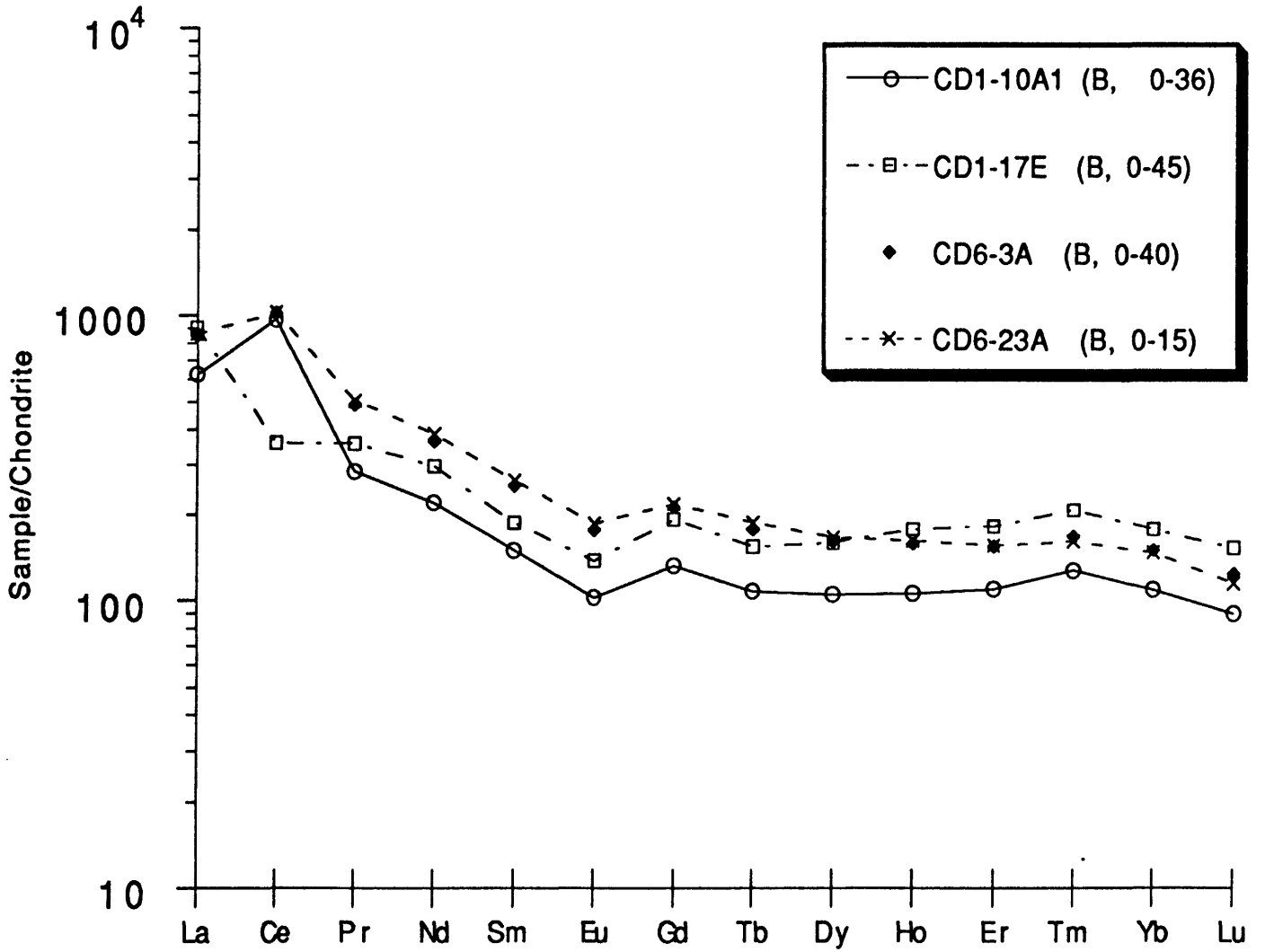

Figure 4. Chondrite-normalized REE plot of Central Karin Ridge crusts.

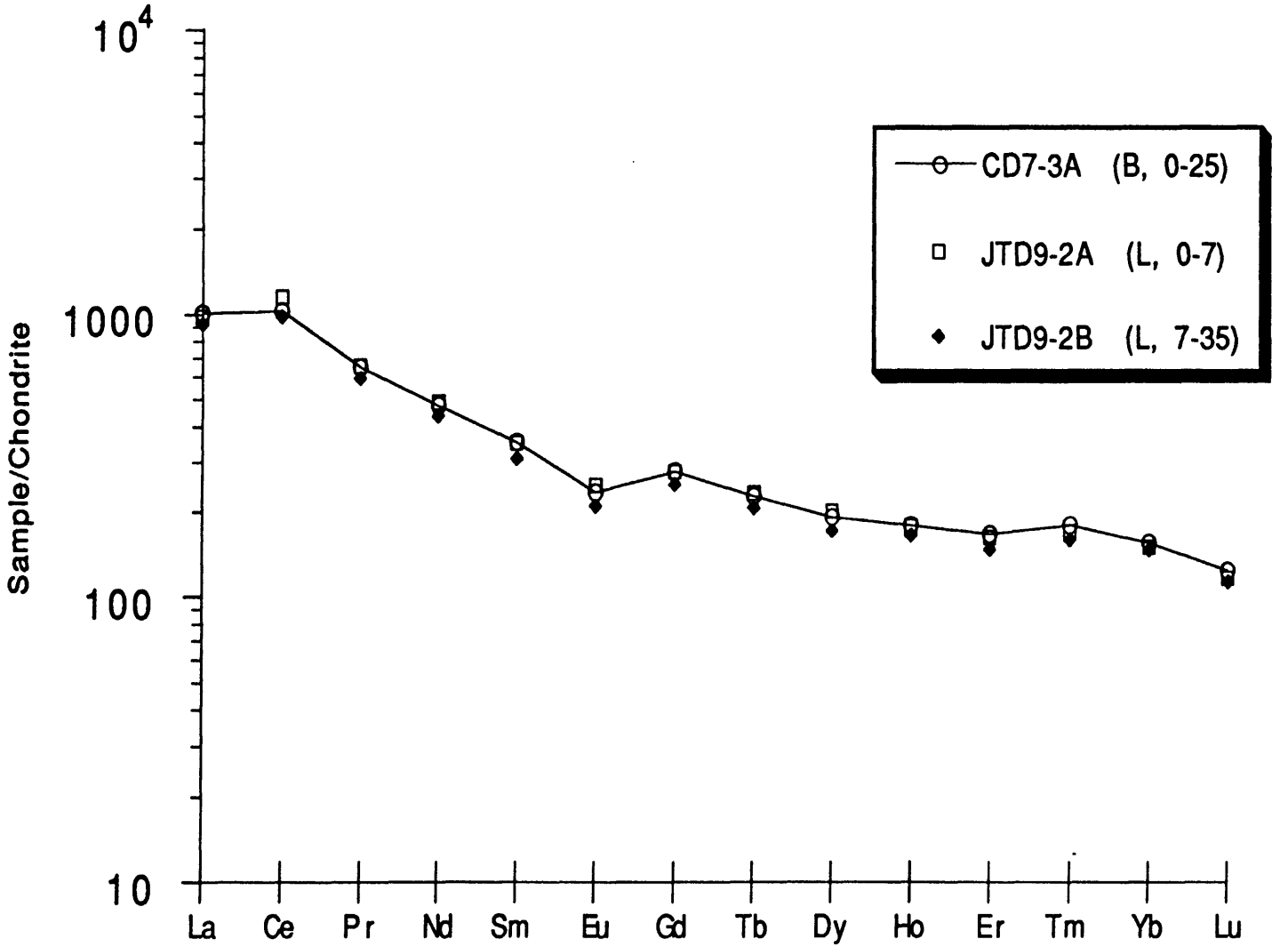

Figure 5. Chondrite-normalized REE plot of crust CD2-8 from SOJIR.

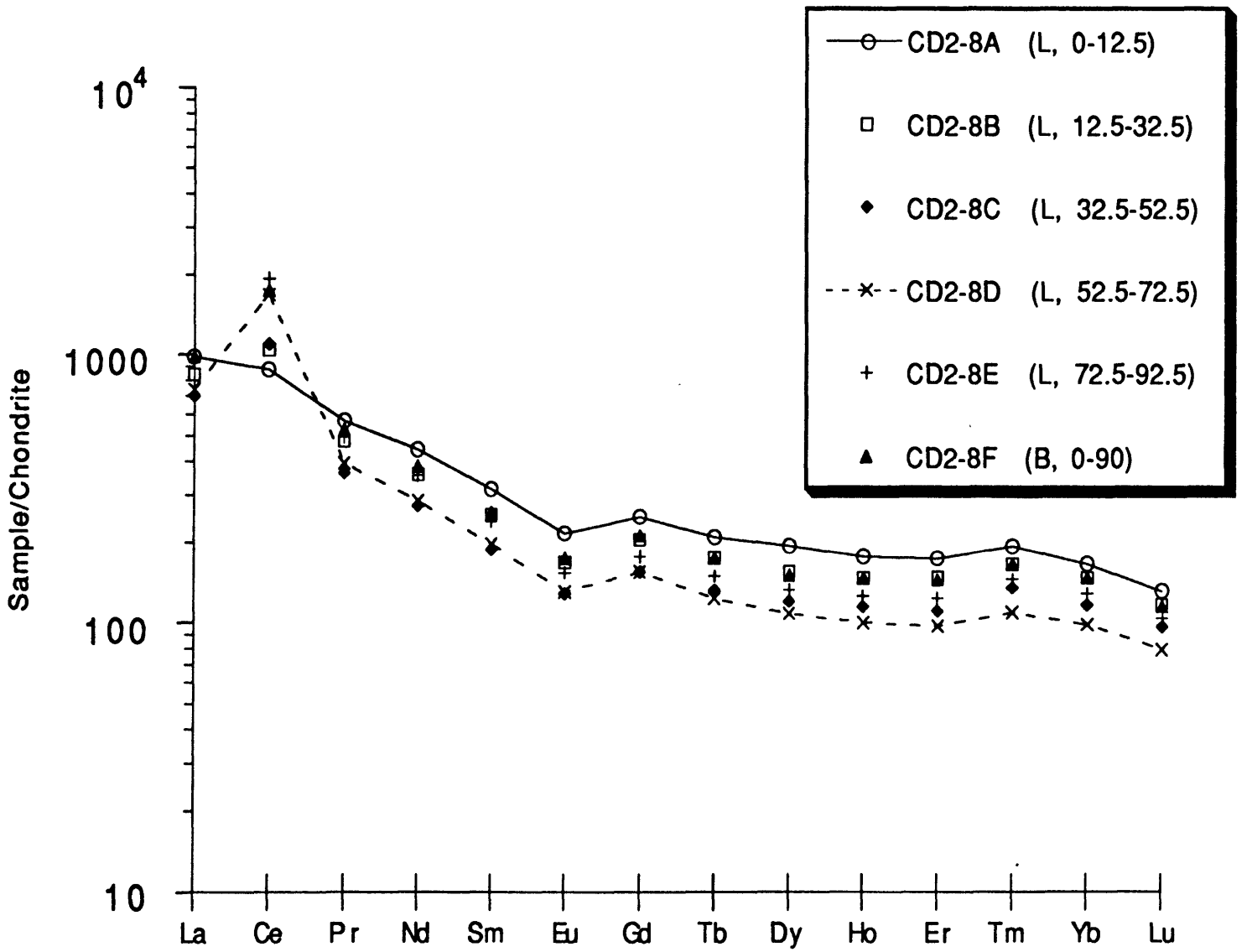

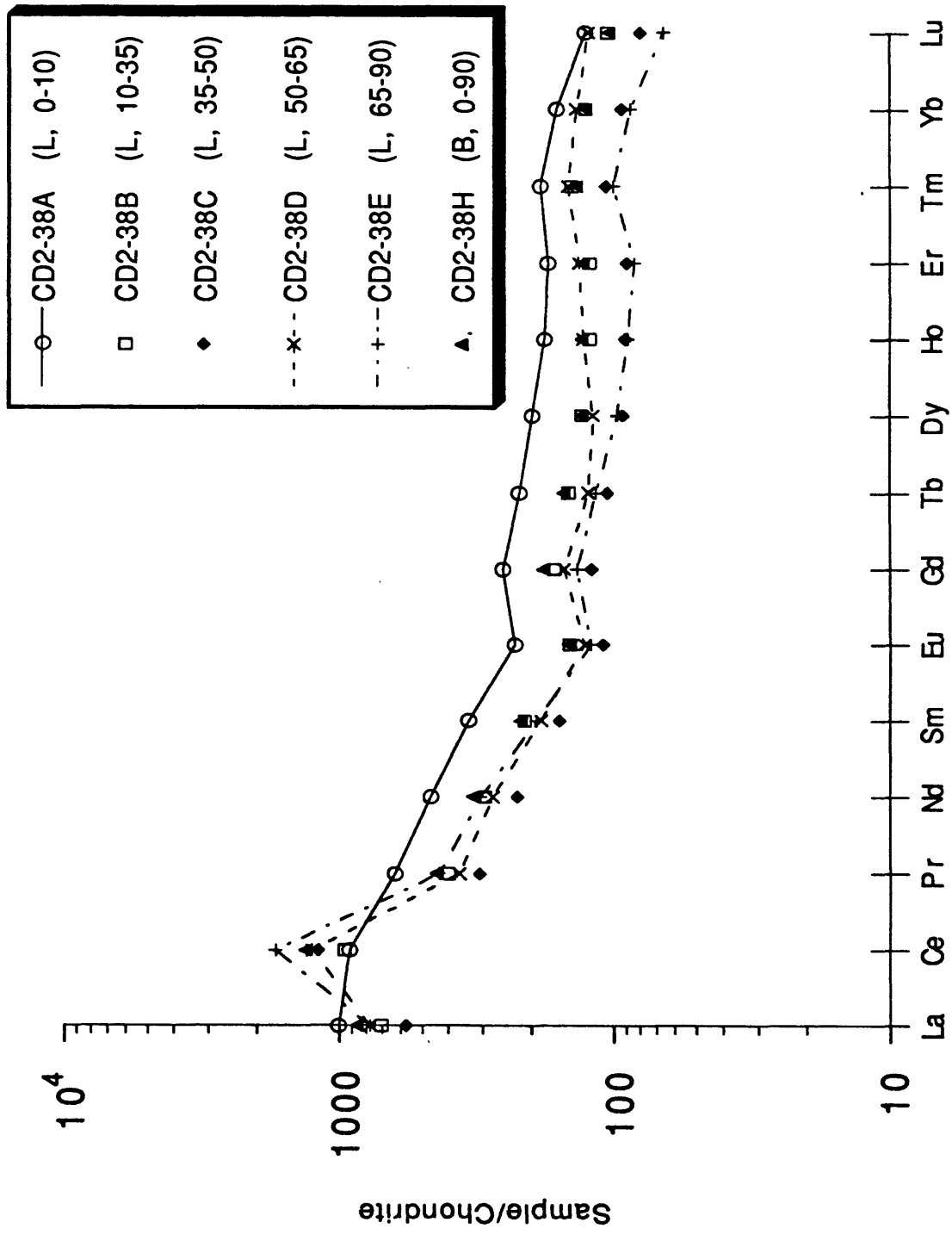

Figure 6. Chondrite-normalized REE plot of crust CD2-38 from SOJIR.

Figure 7. Chondrite-normalized REE plot of SOJIR bulk crusts.

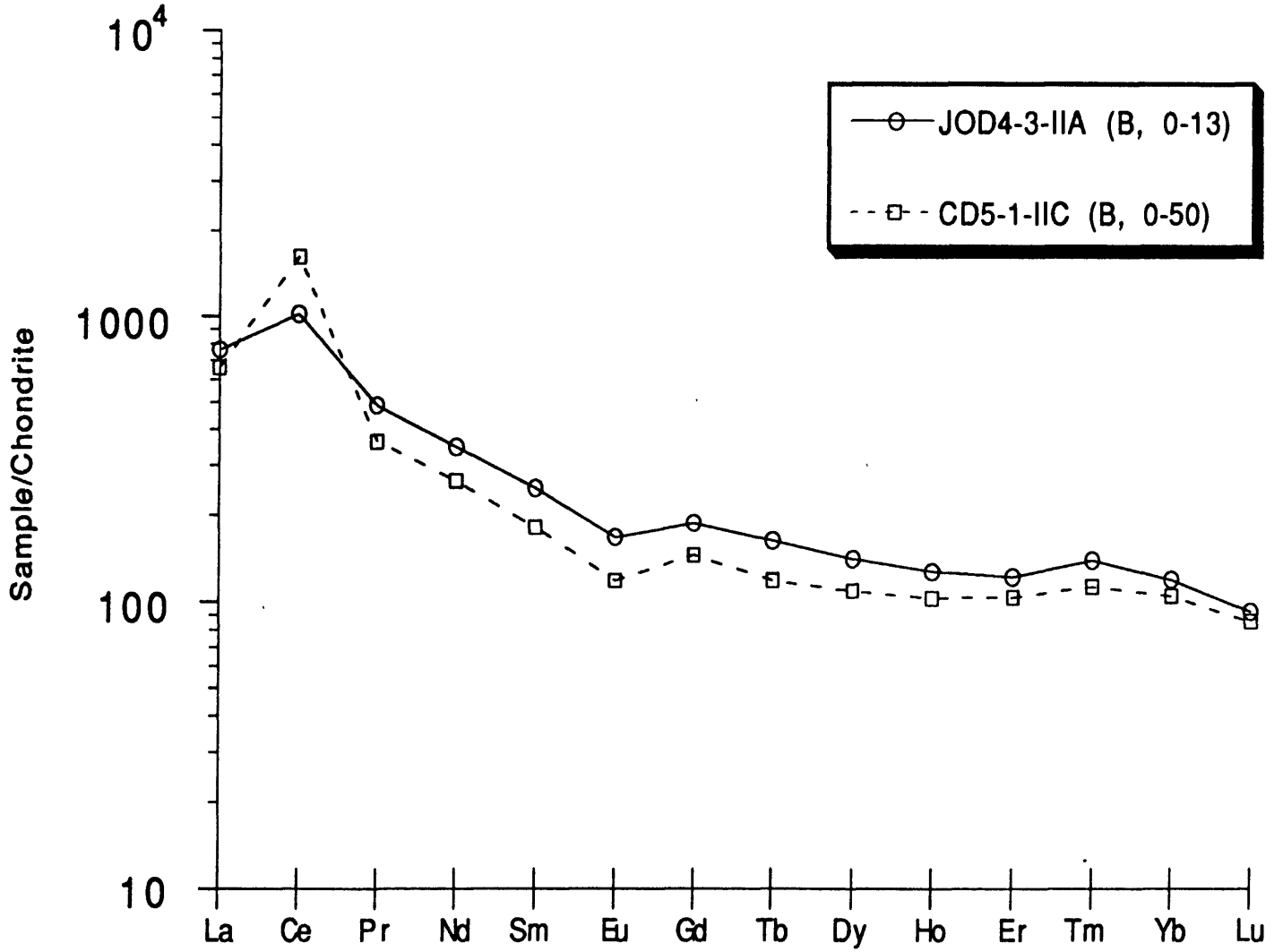

Figure 8. Chondrite-normalized REE plot of crust CD13-8 from SOJIR.

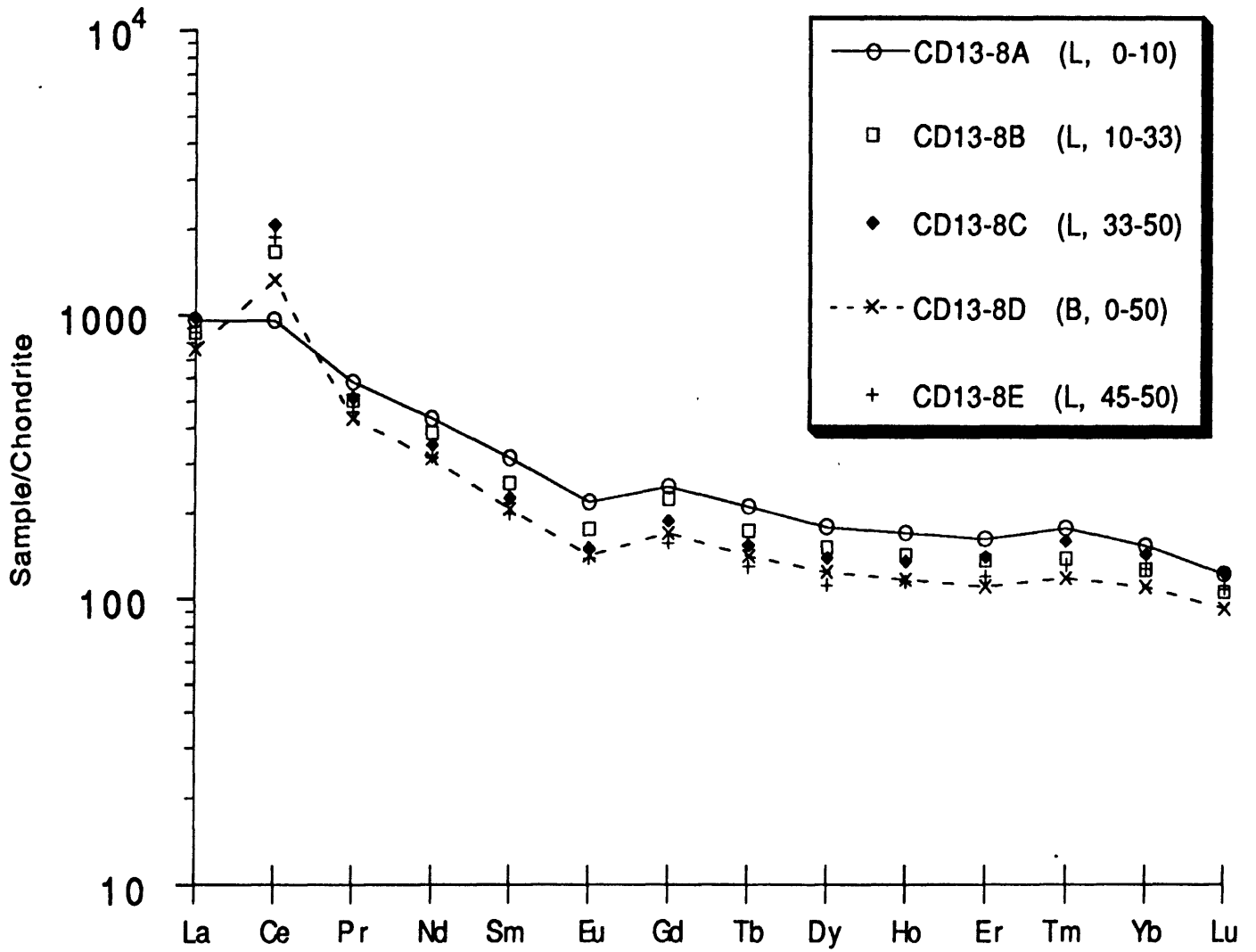

Figure 9. Chondrite-normalized REE plot of SOJIR bulk crusts.

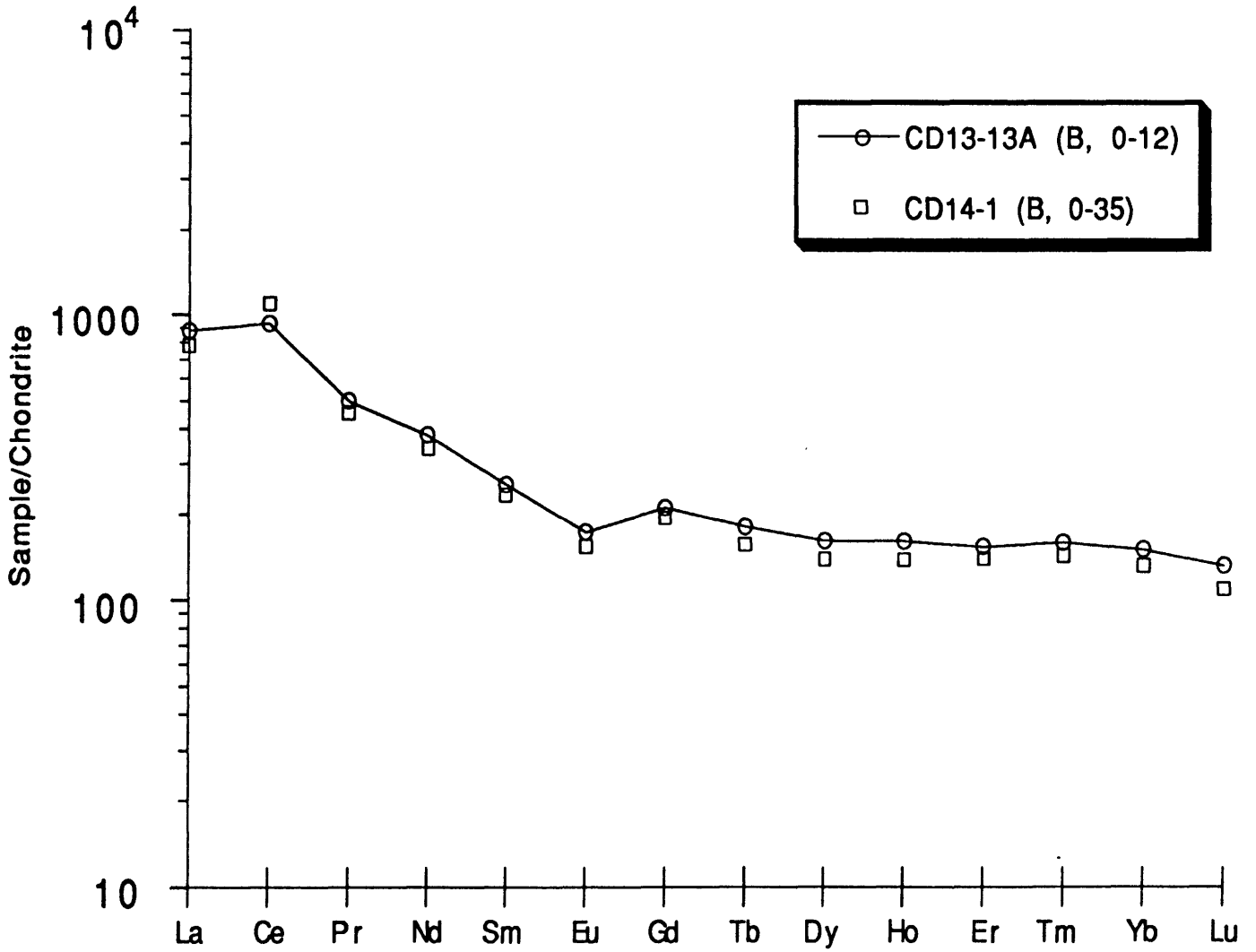

Figure 10. Chondrite-normalized REE plot of crust CD21-7 from SOJIR.

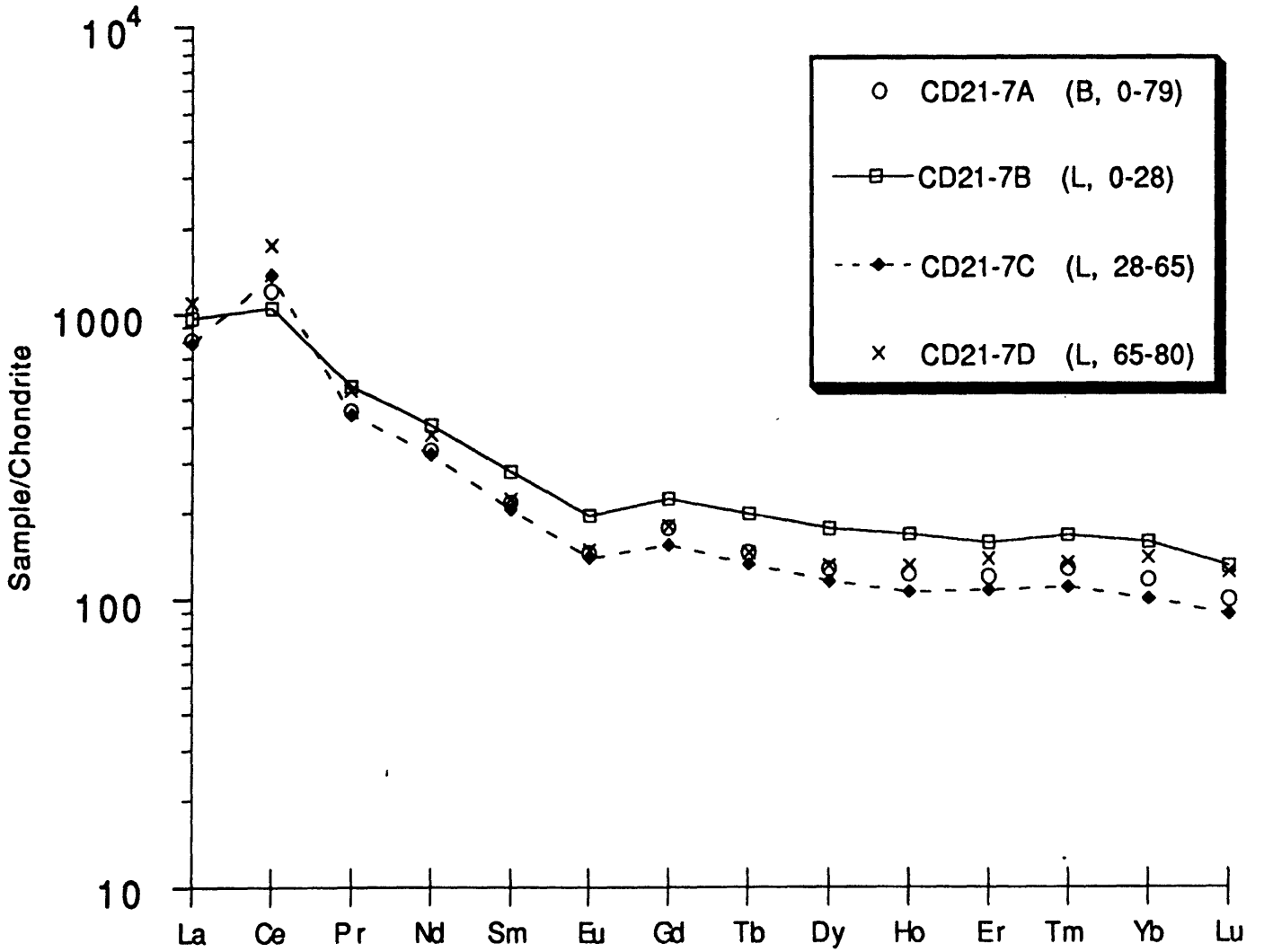

Figure 11. Chondrite-normalized REE plot of SOJIR crusts.

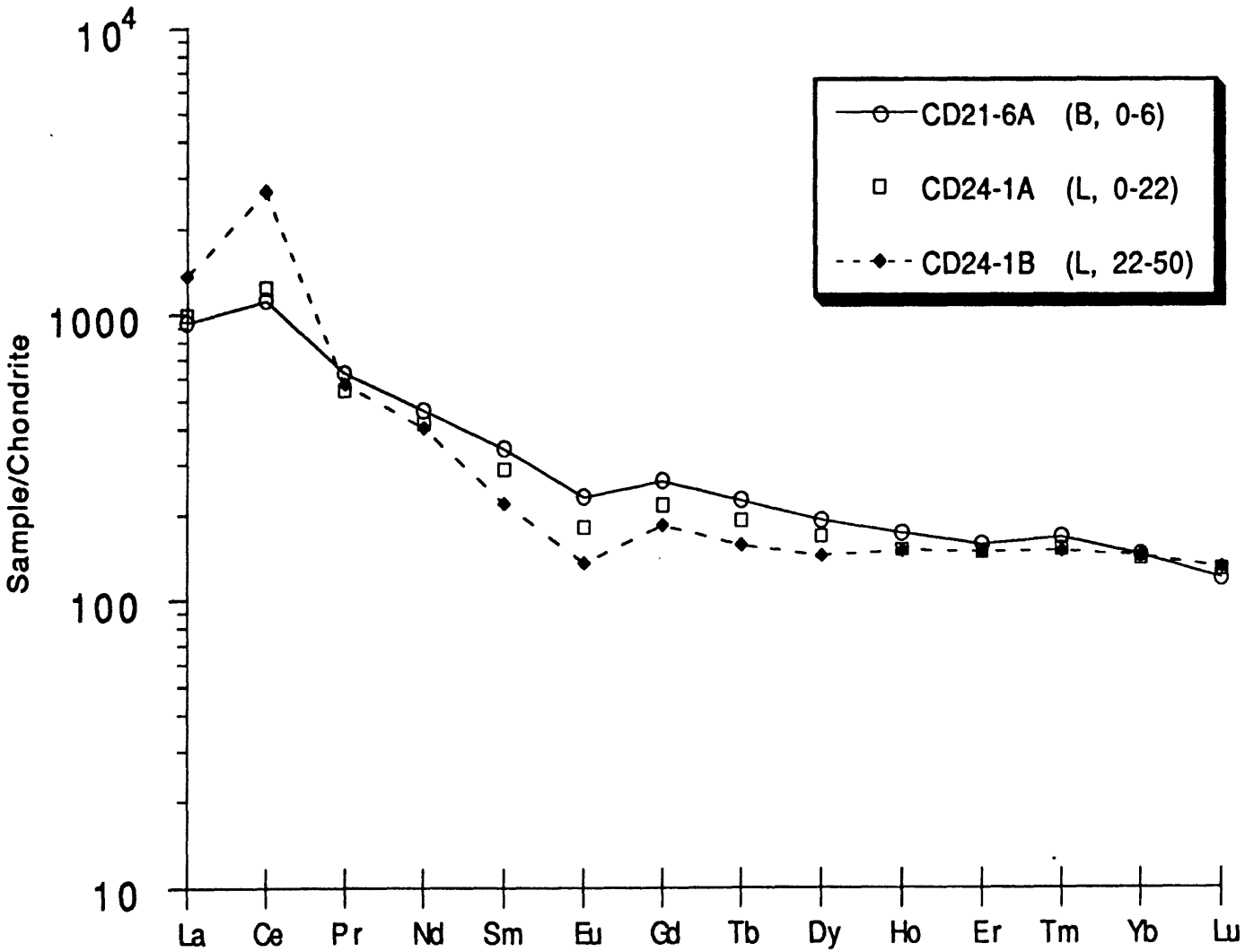

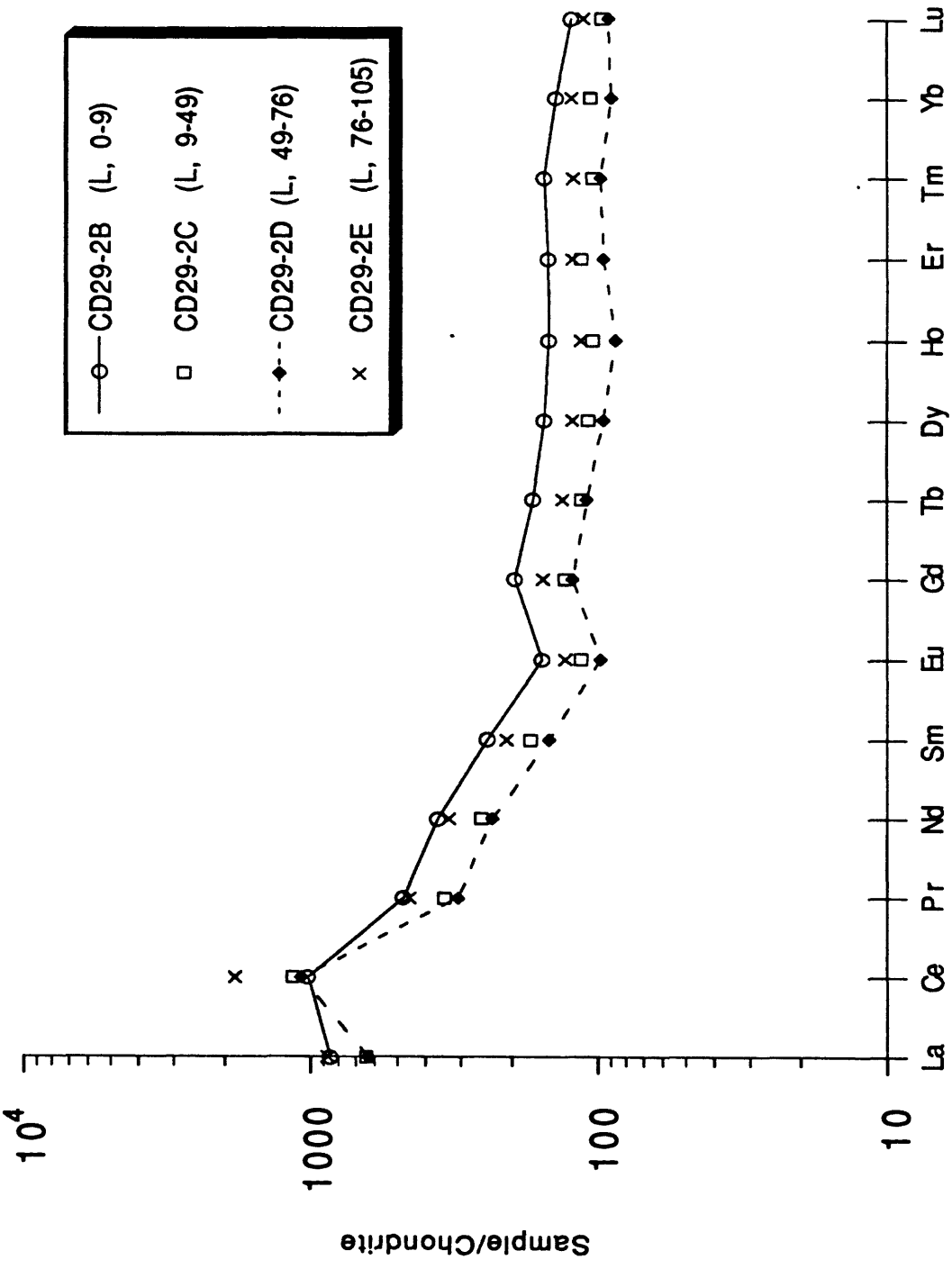

Figure 12. Chondrite-normalized REE plot of crust CD29-2 from Southern Karin Ridge.

Figure 13. Chondrite-normalized REE plot of crust CD30-10 from Southern Karin Ridge.

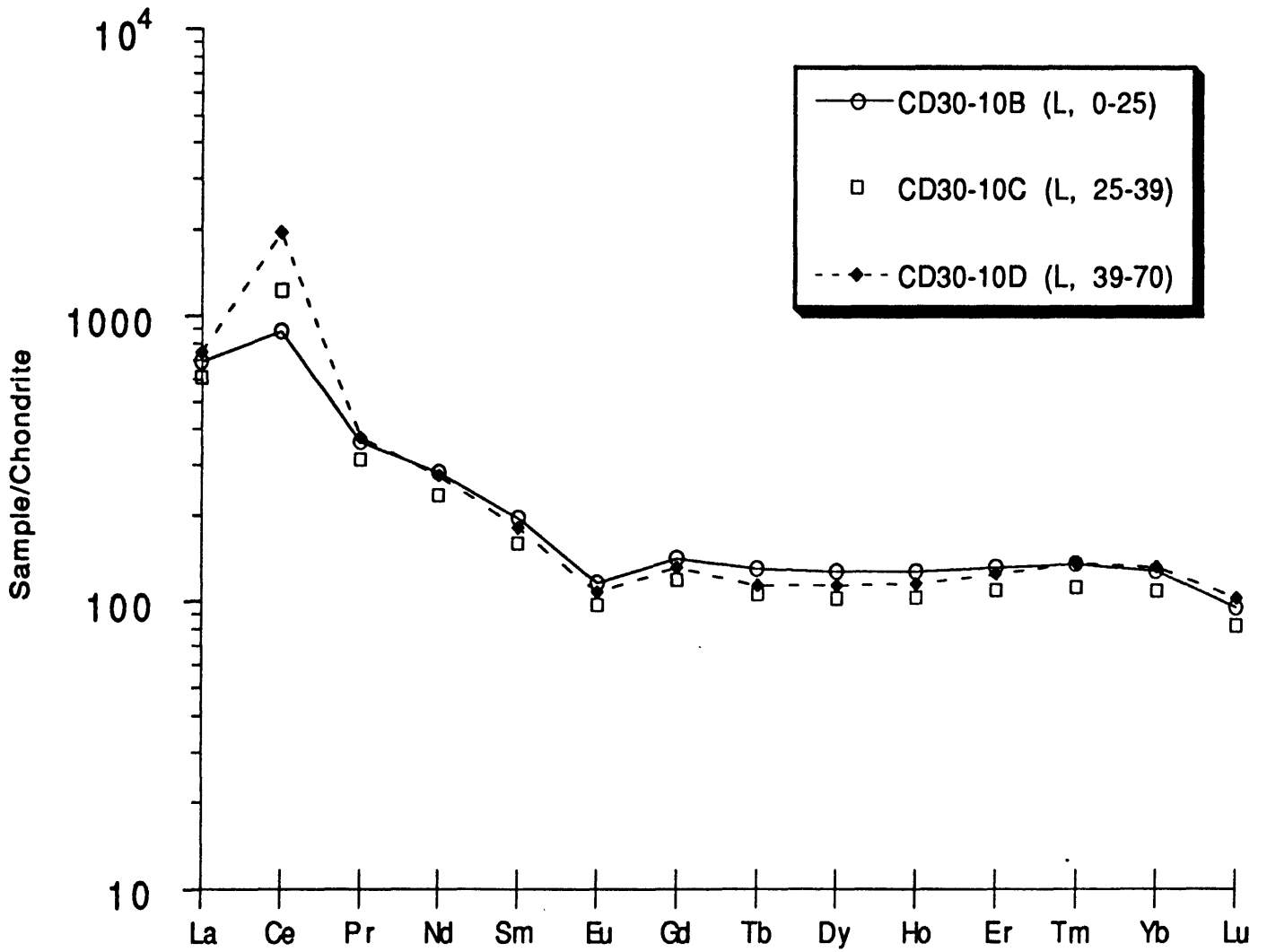

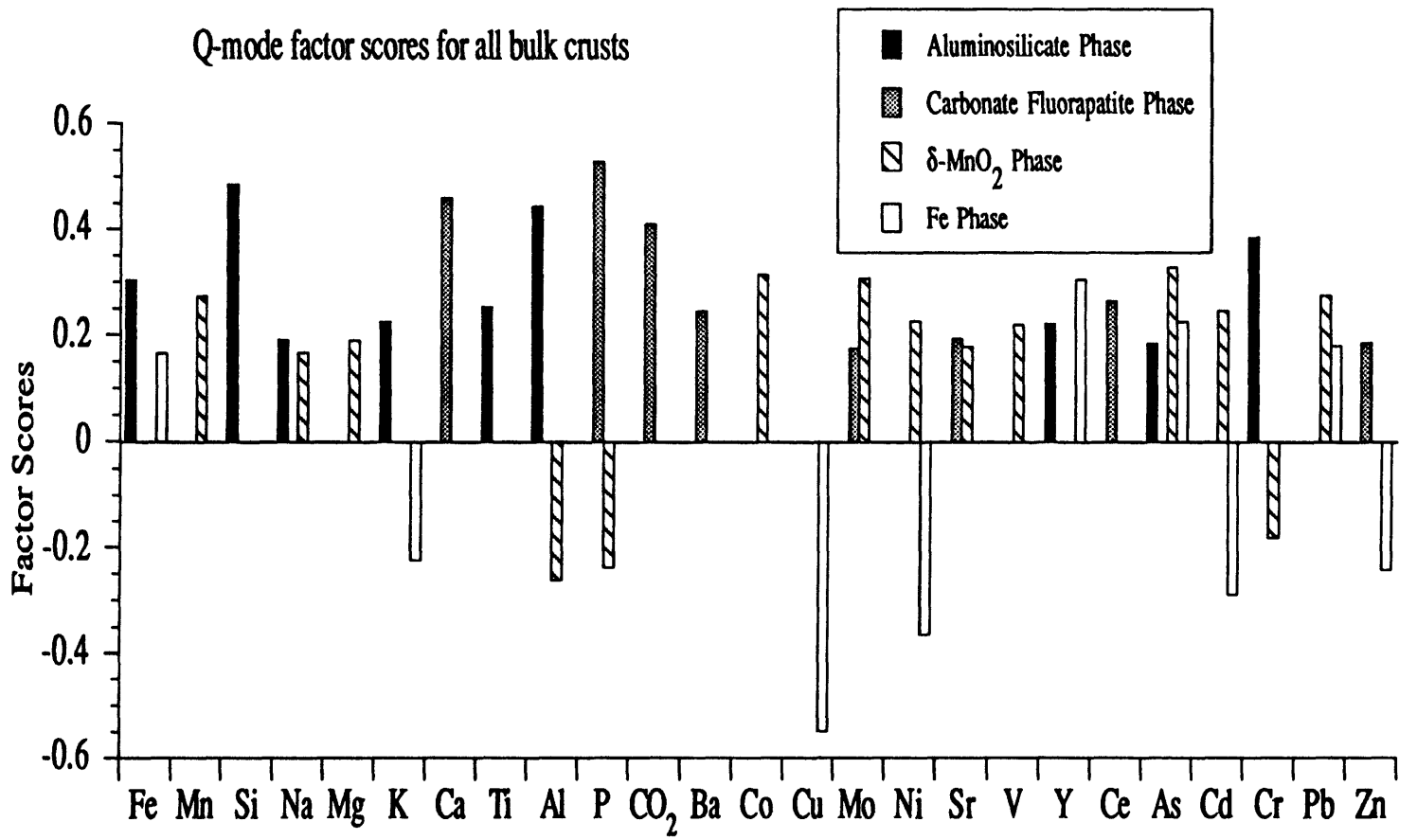

Figure 14. Q-mode factor sores for 95 bulk crusts. Factor scores between 0 and ⌊0.160⌋ are not included, because random noise makes it difficult to resolve the orientation of the factor to within 10° of an absolute direction in variable space. The four factors account for 99.2% of the data set.

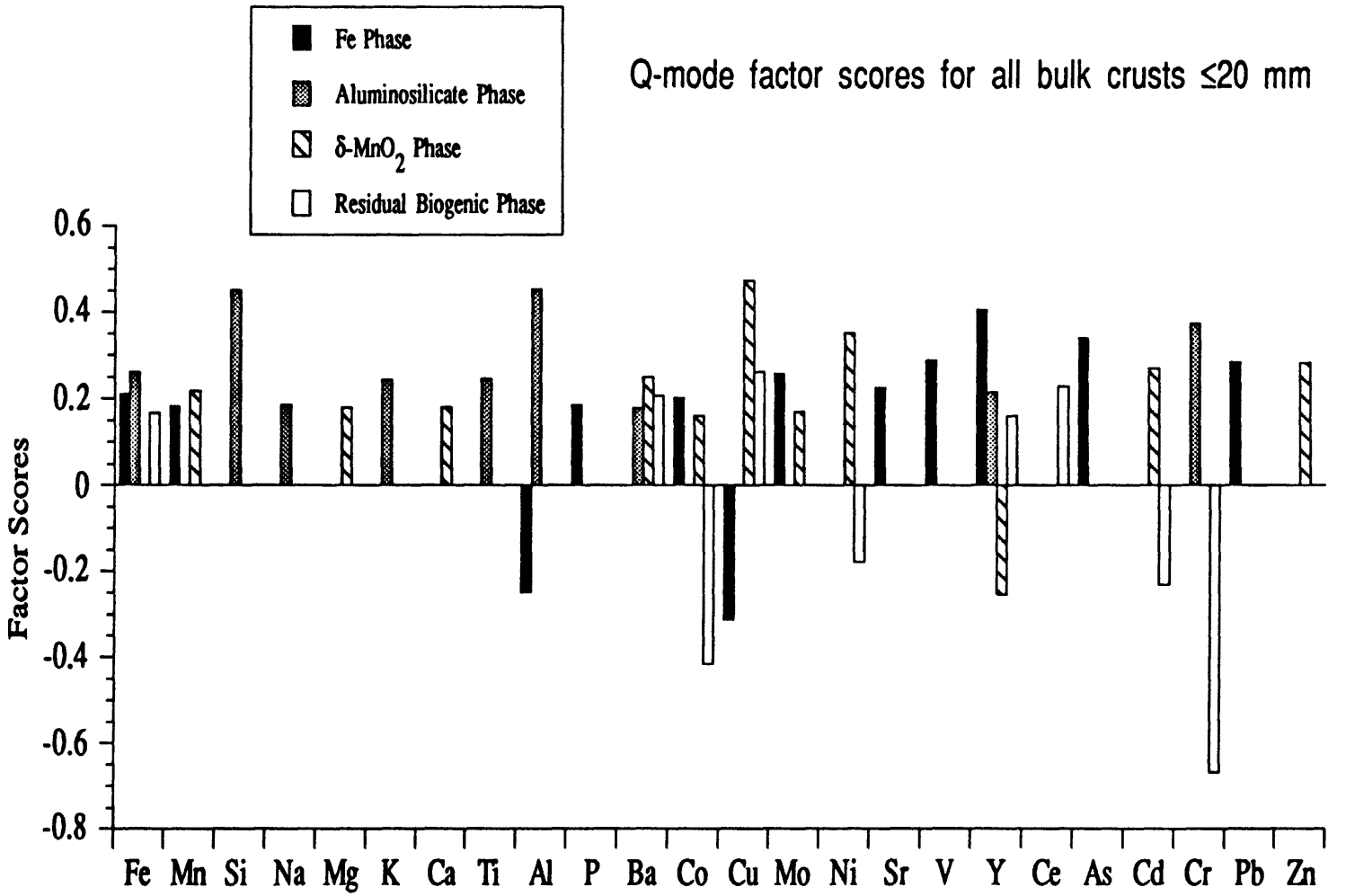

Figure 15. Q-mode factor scores for 47 bulk crusts ≤20 mm in thickness. Factor scores between 0 and |0.160| are not included, because random noise makes it difficult to resolve the orientation of the factor to within 10° of an absolute direction in variable space. The four factors account for 99.6% of the data set.

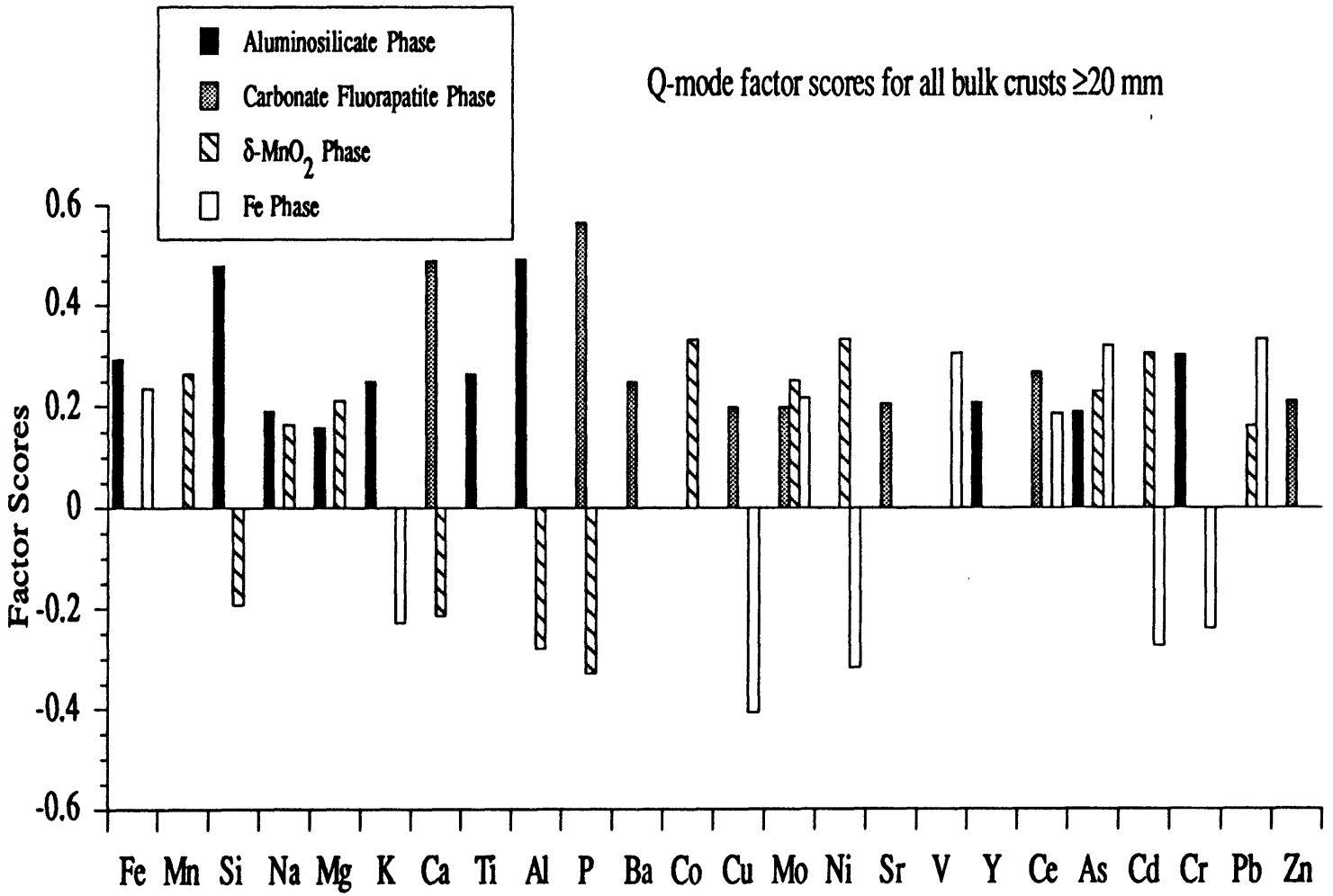

Figure 16. Q-mode factor scores for 54 bulk crusts ≥20 mm in thickness. Factor scores between 0 and |0.160| are not included, because random noise makes it difficult to resolve the orientation of the factor to within 10° of an absolute direction in variable space. The four factors account for 99.3% of the data set.

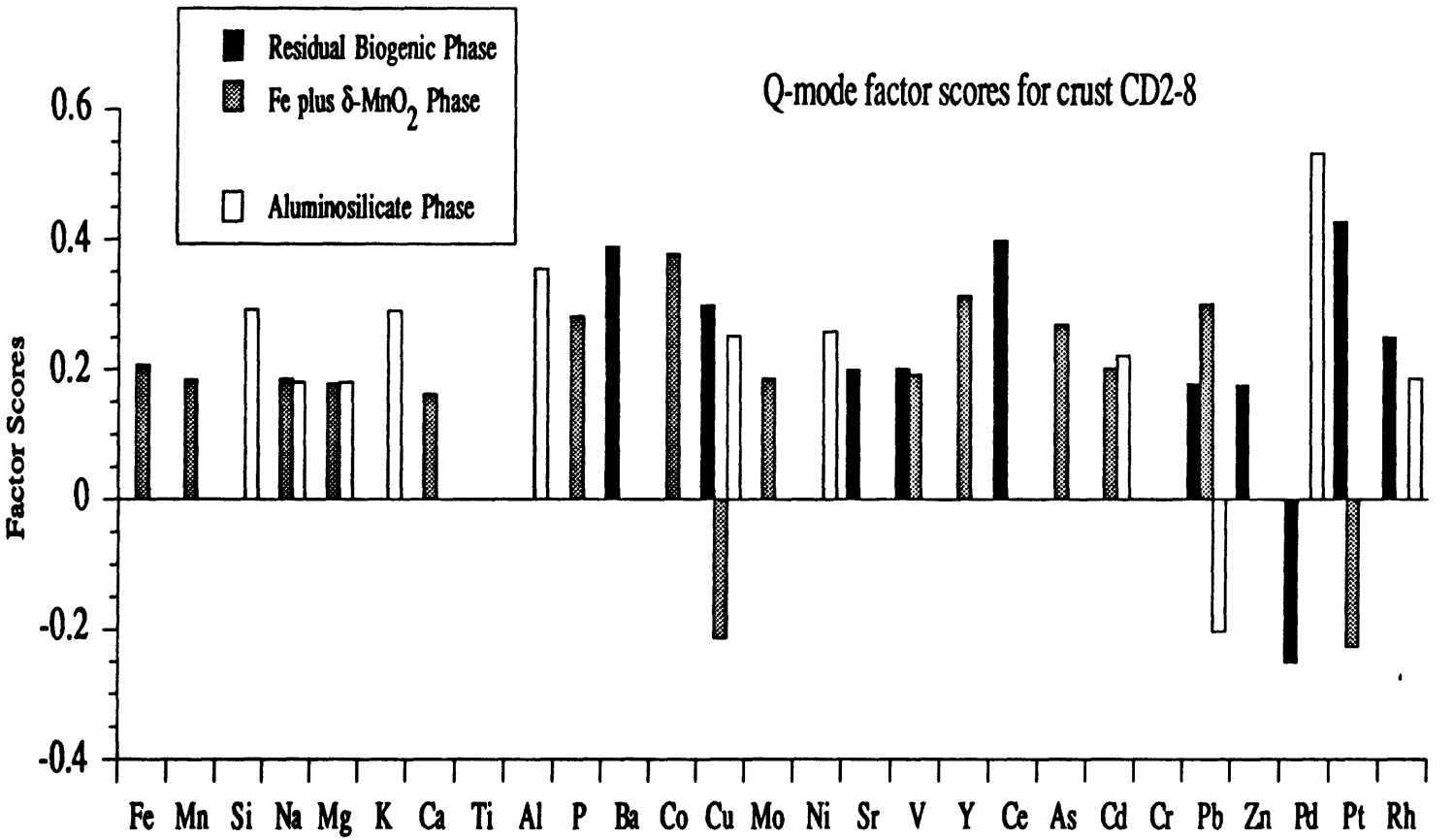

Figure 17. Q-mode factor scores for 5 layers of crust CD2-8. Factor scores between 0 and ⌇0.160⌇ are not included, because random noise makes it difficult to resolve the orientation of the factor to within 10° of an absolute direction in variable space. The three factors account for 99.1% of the data set.

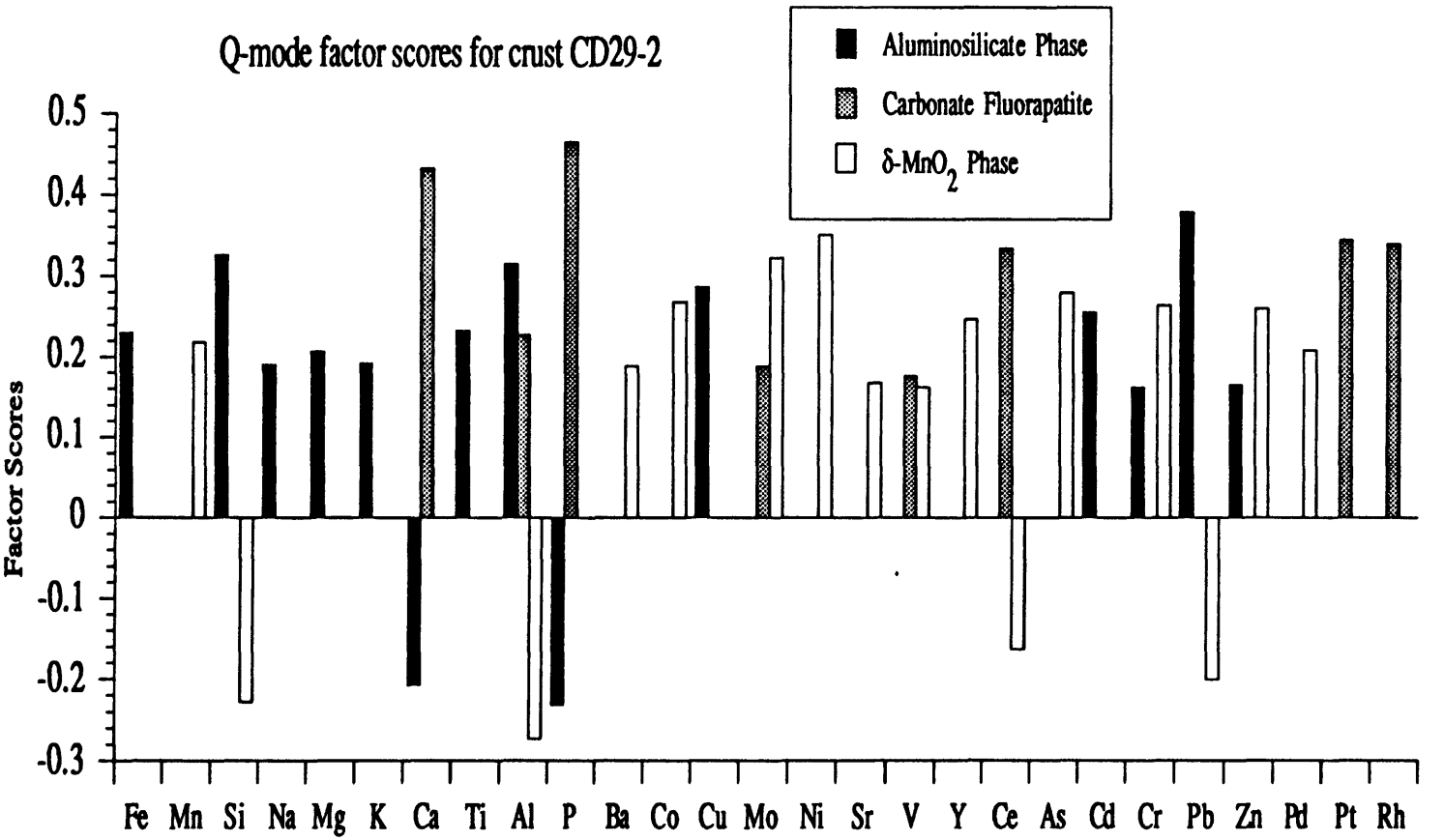

Figure 18. Q-mode factor scores for 4 layers of crust CD29-2. Factor scores between 0 and |0.160| are not included, because random noise makes it difficult to resolve the orientation of the factor to within 10° of an absolute direction in variable space. The three factors account for 99.5% of the data set.